NTIA-REPORT-79-31

Performance of a Very Long 8 GHz Microwave Link

J.E. Farrow
R.E. Skerjanec

U.S. DEPARTMENT OF COMMERCE
Juanita M. Kreps, Secretary

Henry Geller, Assistant Secretary
for Communications and Information

November 1979

TABLE OF CONTENTS

LIST OF FIGURES

LIST OF TABLES

PERFORMANCE OF A VERY LONG 8 GHz MICROWAVE LINK

J.E. Farrow and R.E. Skerjanec*

This paper discusses measurement of signals received over a 160-km (100-mile) line-of-sight microwave radio link operating at 8.4 GHz. Signals were recorded at both ends of the path at various times over a period of about 18 months. The effects of macro-scale meteorological conditions are discussed, particularly those which are peculiar to the central European location of the path. The data obtained from this measurement effort are presented both in terms of radio link availability and in terms of long-term propagation performance. The data were also analyzed to obtain distributions of fade duration for single receivers and for both receivers in a diversity configuration. The study supports the idea that it is possible to achieve reliable propagation at 8 GHz on a link as long as 160 km and with less than normal diversity spacing.

1. INTRODUCTION

From October 1977 through June 1979, the Institute for Telecommunication Sciences of the National Telecommunications and Information Administration conducted measurements on the Defense Communication System (DCS) 8-GHz radio link extending from Hohenstadt to Zugspitze in southern West Germany.

These measurements were made to analyze fading activity and propagation characteristics on this, the longest line-of-sight link in the Digital European Backbone (DEB) system.

The intermittent measurements included two autumnal periods during which anomalous propagation conditions are very common in central Europe. The interruption of measurements during the installation of the communication equipment precluded the collection of data during the summer of 1978. The warmer time of the year is expected to produce another period of disturbed propagation (Vigants, 1975; Barnett, 1972), and this supposition appears to be confirmed by the limited summertime data available.

*The authors are with the Institute for Telecommunication Sciences, National Telecommunications and Information Administration, U.S. Department of Commerce, Boulder, CO 80303.

2. PATH PHYSICAL PARAMETERS

Figure 1 is a map of the DEB Phase I system currently being installed in Europe. The Hohenstadt-to-Zugspitze path is seen in the upper 1/3 of the figure, and is 160 km long.

Figure 2 shows the path profile for this same link. Ray tracings are included in the figure for two different vertical refractive index gradients. The upper set of rays is drawn for a k of 4/3 and the lower rays for a k of 2/3. Note that clearance for the center-line rays is available for even the extreme value of refractive gradient corresponding to a k of 2/3.

The path passes over the rolling farm country and small lakes of Bavaria and then over the Alps in southern Germany. At about 135 km from Hohenstadt, the terrain rises steeply to the high Alps as shown in Figure 3, a photograph of the Zugspitze.

Figure 4 is a path profile showing terrain illuminated by the half-power beamwidth rays of the primary antenna (the lower antenna) at each end of the path. This figure indicates that for a k value of 4/3, the terrain is not strongly illuminated by the transmitter at the Hohenstadt end of the path. The antenna pattern at Hohenstadt will also discriminate against reflected energy transmitted from the Zugspitze even though the terrain is illuminated from that end. This would make ground reflections an unlikely cause of the very deep phase-interference fading observed on this and on other such paths (Thompson, et al., 1975).

The radio equipment was configured for dual space diversity at each terminal. At Hohenstadt the diversity spacing of the antennas was 25 m with the lower antenna 12 m above ground level. Figure 5 shows a photograph of the Hohenstadt tower with the test antennas installed. At the Zugspitze terminal the antennas were separated only 5.2 m vertically because of space limitations on the mountain top. Figure 6 is a photograph of the Zugspitze antennas. The antennas were staggered horizontally to permit them to fit more easily into the restricted space. Since 12 m between antennas is the recommended vertical spacing to avoid simultaneous

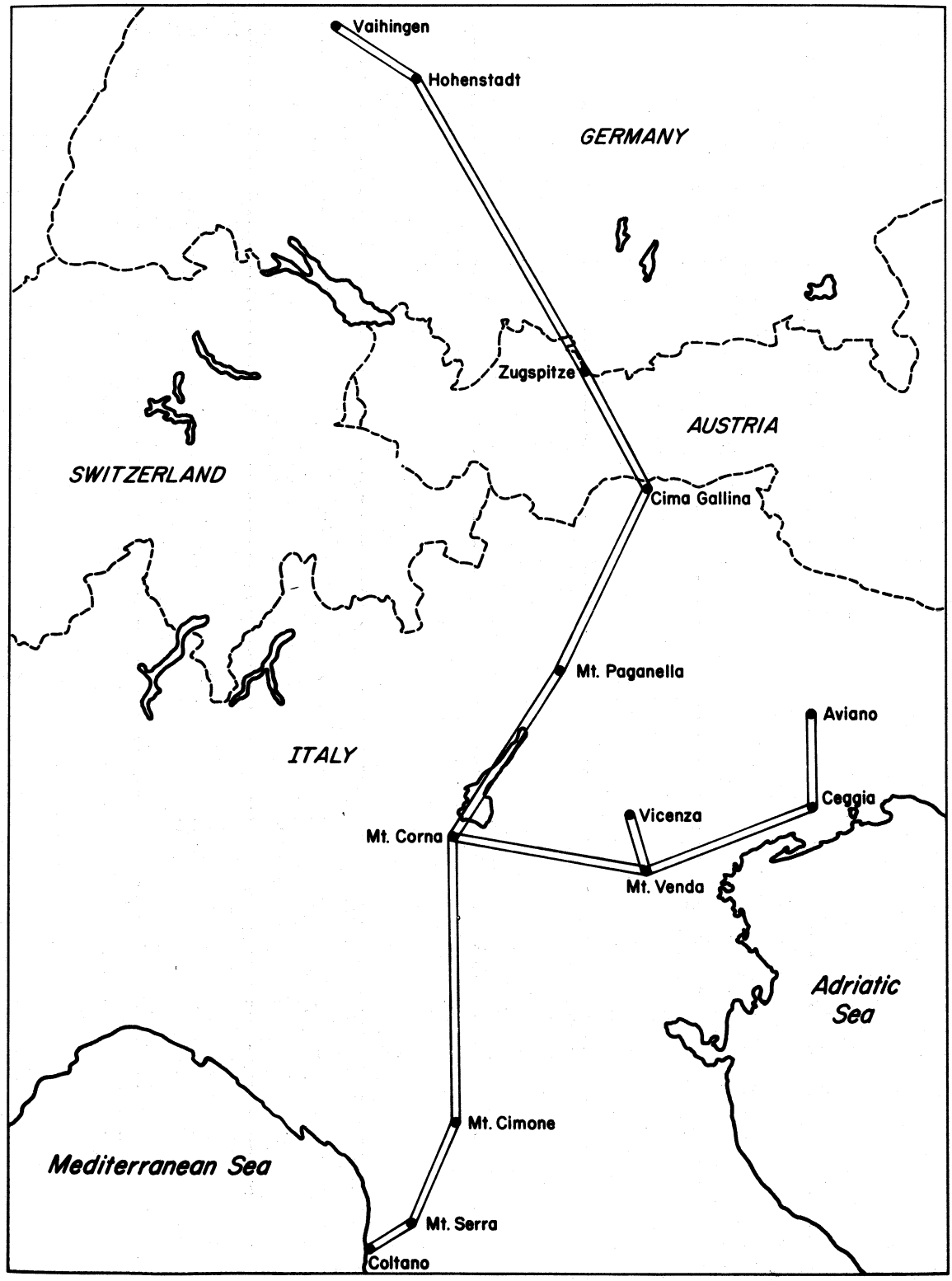

Figure 1. DEB Phase I system map.

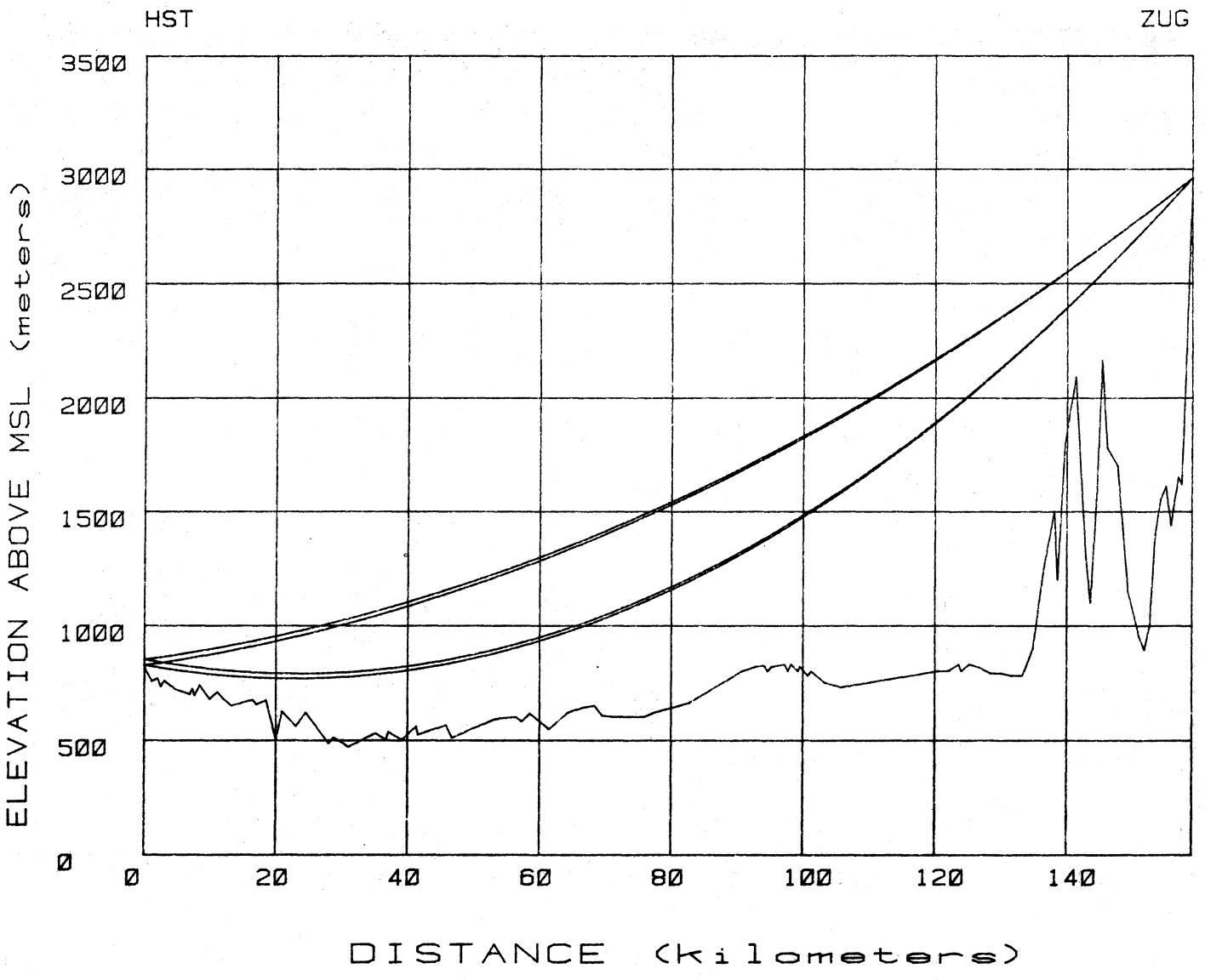

Figure 2. Hohenstadt to Zugspitze profile showing the ray trajectories for k values of 4/3 and 2/3.

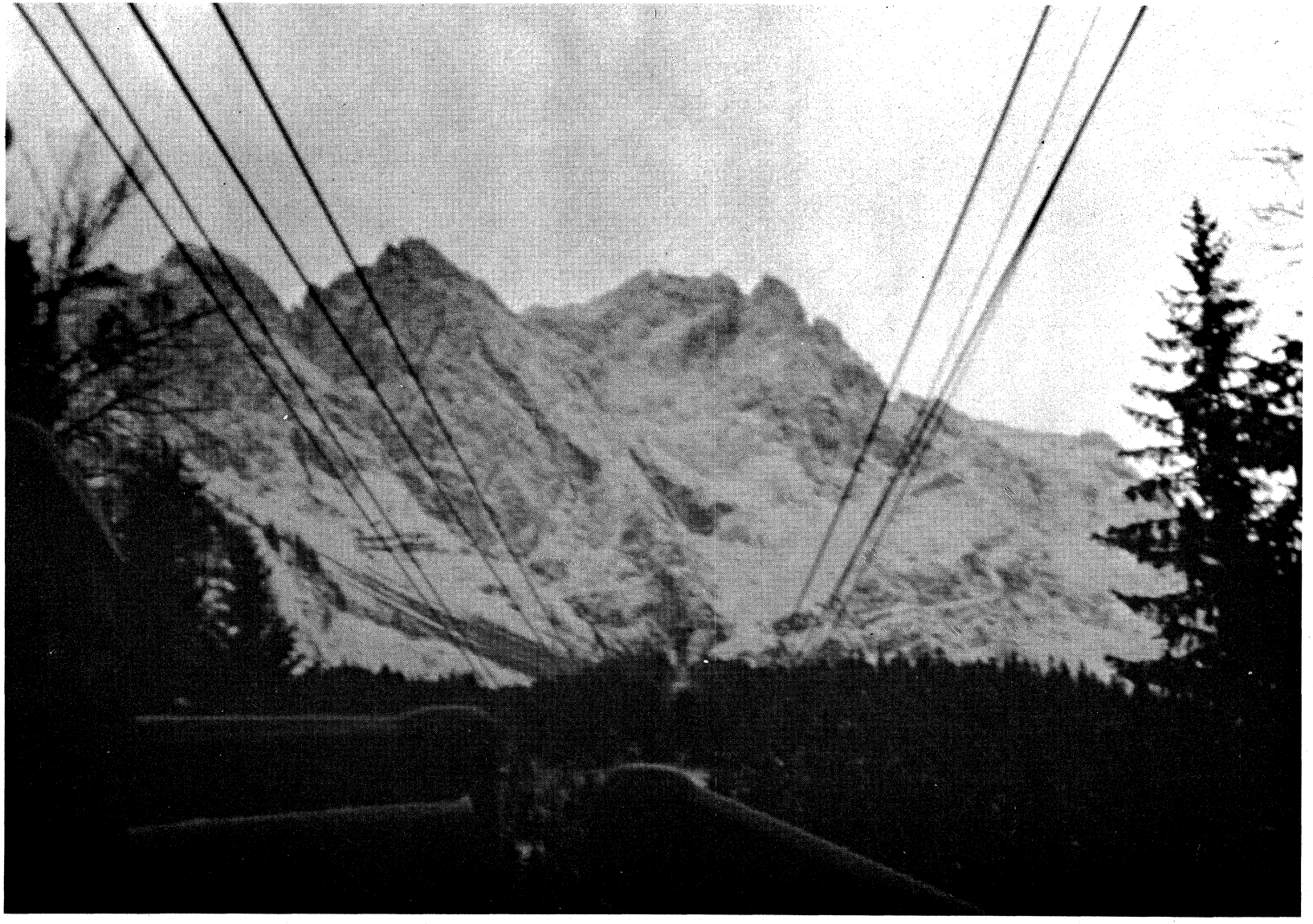

Figure 3. North face of the Zugspitze.

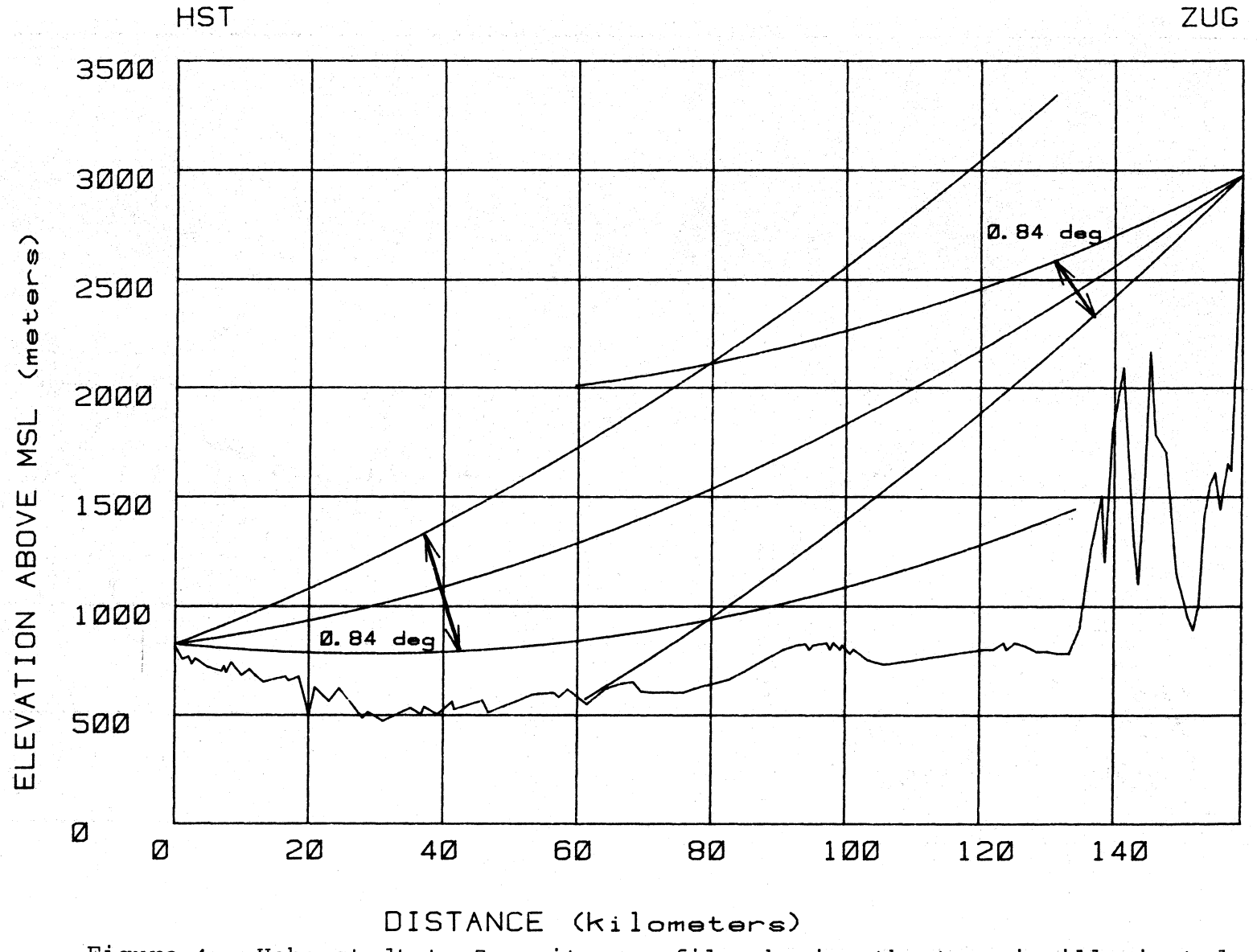

Figure 4. Hohenstadt to Zugspitze profile showing the terrain illuminated by the half-power antenna beams. The rays are drawn for a k value of 4/3.

Figure 5. Hohenstadt tower showing test antennas installed.

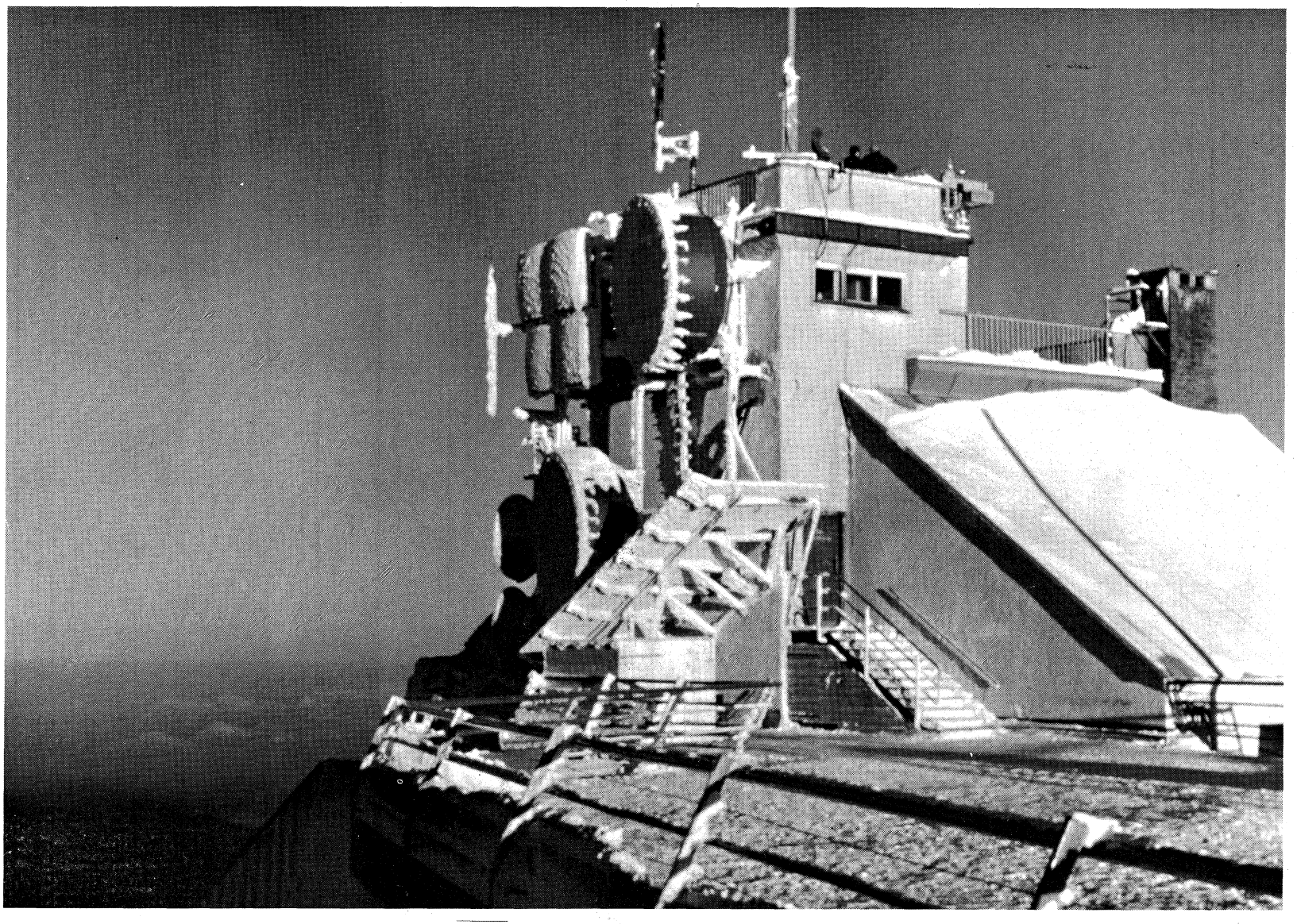

Figure 6. Zugspitze equipment building showing DEB antennas.

deep fading on two or more diversity branches (White, 1970), the degree of diversity protection available at this terminal was uncertain. The system design called for 10-ft (3-m) diameter antennas and 10 watts of transmitter power at each end of the path.

3. PATH PERFORMANCE ESTIMATES

There is no single recognized model to describe in detail the expected performance of microwave radio links longer than about 70 km. Development of such a model is underway at this time at ITS, under the sponsorship of the U.S. Army Communications Command and the U.S. Air Force Electronic Systems Division. Data for the model are being acquired on selected DEB links at 8 and 15 GHz (private communication, L. G. Hause).

The problem in selecting the equipment to be used for a long microwave link is the unknown depth to which the link will fade and hence the fade margin necessary to provide a given link availability. Furthermore, there is no well-developed model to indicate what diversity spacing is required to provide uncorrelated or independent signals for a protection channel (McGavin et al., 1970). The measurement program reported here will address both the problem of long-term variability and the question of diversity spacing.

4. DATA ACQUISITION

Two separate data acquisition techniques were used on this radio link. The measurements taken at the Zugspitze site, because of space limitations, were made by recording the combiner control voltage (which is approximately linear in volts versus received level in dBm) for each diversity receiver on an analog strip chart recorder. All analysis of the strip chart records was done by hand. This meant that the Zugspitze data could be analyzed only by inspection; no effort was made to extract long-term signal variability information in terms of continuous distributions of received signal level. The strip chart

recorder had a peak frequency response of 50 Hz so that rapid variations in signal level would be preserved. The charts were timed with rectangular wave timing signals with half periods of one minute and one hour. Some of the more recent charts have one channel that shows which diversity receiver was carrying traffic so that the activity of the diversity switch could be tracked and the adequacy of the diversity configuration evaluated.

The signal level information collected at Hohenstadt was put on strip chart also; but in addition, it was fed to a minicomputer-based data acquisition system. The system contained an analog-to-digital converter board (A/D) which sampled the combiner control voltage twenty times per second. The samples were sent to a histogram program which retained every tenth sample for binning into a 20-level histogram. The histogram bin interval was 3 dB so a signal level range of greater than 60 dB could be accommodated. These histograms were accumulated for a one hour period and then written into a permanent magnetic tape archive record. Each hourly histogram for each channel contained about 7200 samples which provided good resolution for level variations.

In order to take particular notice of deep fades, each A/D sample was also sent to a fade message program. This program was designed to measure the length of time that the received signal was below a predetermined threshold for any particular event and also to note the lowest value of signal observed during the fade. To do this the program compared two successive samples, and if the most recent one was below threshold and the previous sample was above, a fade message was opened with the start time equal to the clock time of the first sample below threshold.

To determine the lowest level during a fade, the first sample was retained and the next sample compared with it. (Each new sample was also compared with the threshold to see if it was above that level.) The lower value of the two was retained and compared with the next sample value, and again the lower value

retained. In this way, the lowest value occurring during any given interval would be the one which finally remained. After the start of a fade when one or more below-threshold samples were observed, any sample which was again above threshold would cause the fade event message to be closed at the time associated with the first above-threshold sample. The signal level value which was the lowest observed would also form part of the fade event message. Thus the message would give the start time, end time, and the lowest level of each fade below the threshold. The beginning and ending times were known to the nearest 50 milliseconds which was the sampling period of the A/D converter. Since both received signal level channels were being sampled and the data handled the same way, it was fairly straightforward to analyze the data to determine when either or both of the signals were below threshold. This permitted us to determine the distribution of fade lengths at the threshold and also simultaneous fades on the two diversity branches. Even though data were available from both ends of the path, the different methods of acquiring and analyzing the data have made the results somewhat difficult to compare directly but the results of both analyses will be presented later in this report.

5. METEOROLOGICAL ANALYSIS

Meteorological analyses for microwave propagation studies are usually done during periods of unusually bad propagation conditions or for periods during which interruptions of radio link traffic occur. The causes of interruptions have been thoroughly discussed in the literature (Dougherty 1968, White 1970). In general, the conditions that lead to poor propagation are limited in space and time and can be observed and identified only if extremely fine-grained meteorological data can be obtained. The exceptions to this statement are such phenomena as extremely heavy rains (which lead to flooding and hence considerable public notice) or fog conditions associated with strong stratification (which will again lead to public notice

by interfering with transportation system activity). From the viewpoint of the student of radio propagation, it is unfortunate that such catastrophic weather conditions are not only rare in time but even more so in the space which he may have under observation. For these reasons, the meteorological analysis which was done for this path dealt only with macro-scale phenomena such as could be determined from world-wide synoptic meteorological charts. Specifically, the type of weather condition which has been identified as causing propagation problems on this path and in fact over many paths in Central Europe is an autumn condition characterized by a static or slow-moving high pressure system (Samson, 1970). Such systems have been observed to cause problems with great numbers of military microwave links in Germany, particularly during October hence the name "Great October Blackout" which is often used by military personnel in Europe to refer to the phenomenon. Although this is not a phenomenon which affects the same links every year, the pattern is familiar enough to warrant comment.

6. DATA PRESENTATION

Recording was started at Hohenstadt in mid-October 1977 on a test system which used the DEB antennas and a temporary transmitter at the Zugspitze and two smaller, 6-foot (2-m) temporary antennas and two test receivers at Hohenstadt. This test system was operated until the end of April 1978 when the DEB radio transmitter at the Zugspitze was turned on. At that time, the temporary transmitter was moved to Hohenstadt and signals were recorded in both directions on the path for a short time until 1 June 1978 when the temporary antennas at Hohenstadt were removed to permit installation of the permanent DEB antennas.

On 23 September 1978, recording at both ends of the link resumed using the permanent DEB equipment. The major part of the data obtained at the Zugspitze was recorded between 23 September 1978 and 15 June 1979.

Table 6-1. System Gain Calculations

	Temporary Installation	Permanent Installation
Path Length	159 km	159 km
Frequency	8.3 GHz	8.25 GHz
Ant. size ZUG	10 ft (3 m)	10 ft (3 m)
HST	6 ft (1.8 m)	10 ft (3 m)
Ant. gain ZUG	45.9 dBi	45.5 dBi
HST	41.5 dBi	45.5 dBi
Line Loss ZUG	2.5 dB	2.7 dB
Lower HST	5.5 dB	2.0 dB
Upper HST	7.7 dB	3.0 dB
Free Space Loss	154.5 dB	154.5 dB
Atmospheric Absorption	2.6 dB	2.6 dB
Transmitter Power	+42.3 dBm	+37 dBm
Received Signal Level		
Lower Antenna	-35.4 dBm	-33.8 dBm
Upper Antenna	-37.6 dBm	-34.8 dBm

Table 6-1 gives the values of system gain for each of the arrangements mentioned. Note the similarity in received signal level for the two configurations. This similarity lends confidence to the expectation that the two sets of data can be amalgamated to present a longer term data base than either would provide alone.

6.1 Strip Chart Data from the Zugspitze

The strip charts recorded at the Zugspitze were analyzed primarily to determine the fraction of time that fading occurred. The fading periods were further segregated roughly by fade rate, fade depth, and the occurrence of simultaneous fades on both diversity branches. Primarily, two different types of fading were considered.

The first type is called scintillation which is the term used to describe rapid, shallow fading. The signal remained generally near the unfaded line-of-sight level with only occasional excursions to 20 dB below this level. An example of data obtained under the least disturbed conditions is shown in Figure 7 and an example of scintillation fading is shown in

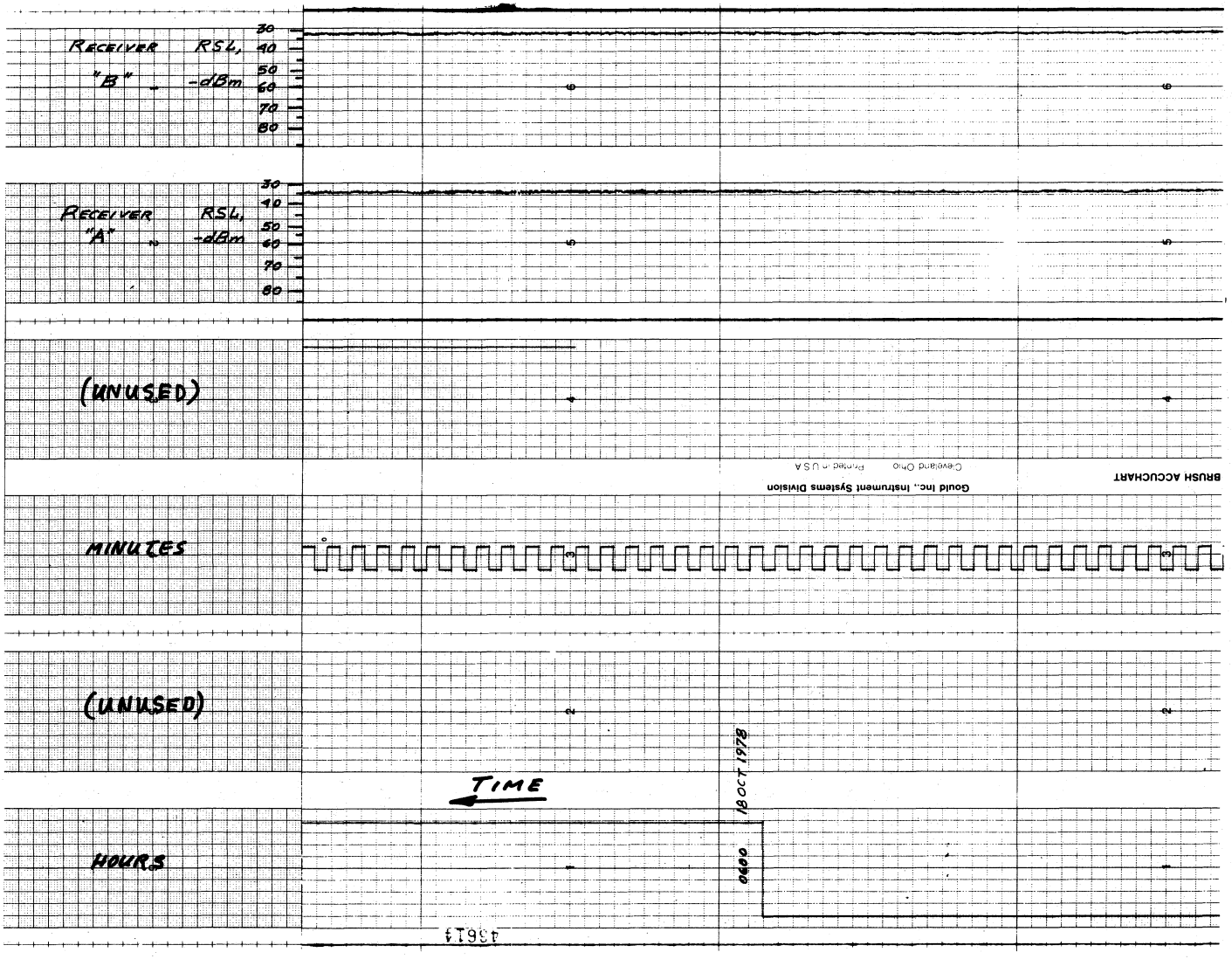

Figure 7. Recording of "free space" propagation conditions made at the Zugspitze.

Figure 8. On these and subsequent figures, the small rectangular timing signal has a period of 2 minutes, and the larger rectangular timing signal has a period of 2 hours. The scintillation fading results from the addition of a multitude of small received signal components of random phase and magnitude to the main, on-path signal. These components are caused by atmospheric turbulence and could arise from scattered or weakly reflected signals originating from antenna side lobes or the edges of the main beam.

A second type considered was well-developed phase interference fading which results from the addition of two or more signal components of very nearly equal amplitude. The delayed component would very likely arise from a strong reflection or be due to atmospheric multipath associated with atmospheric refractive index layering.

There is a wide variation in fade rates as can be seen from Figures 9, 10, and 11. Note that Figure 9 shows a period of very slow fading, apparently resulting from smooth changes in effective reflecting surface position. Figure 10 shows a more typical fade rate which could result from more than a single delayed component and which would in turn imply the existence of more than one atmospheric component. Figure 11 shows a very high fade rate, and again the character of signal suggests multiple delayed components which are changing fairly rapidly in time. Transitions between fading regimes could be fairly rapid as shown by the data in Figure 12. Note that in a period of an hour or so, the fading changed (reading right to left, in the direction of increasing time) from scintillation fading to interference fading to nearly undisturbed line-of-sight conditions.

Periods occurred when more than one fading mechanism seemed to be involved. An example of this sort of condition is illustrated in Figure 13 which shows a period of severely depressed median signal level with superimposed phase interference fading. Periods of this severity were fortunately rare and close inspection of the data shows that even in these severe conditions both signals were simultaneously below the -70 dBm

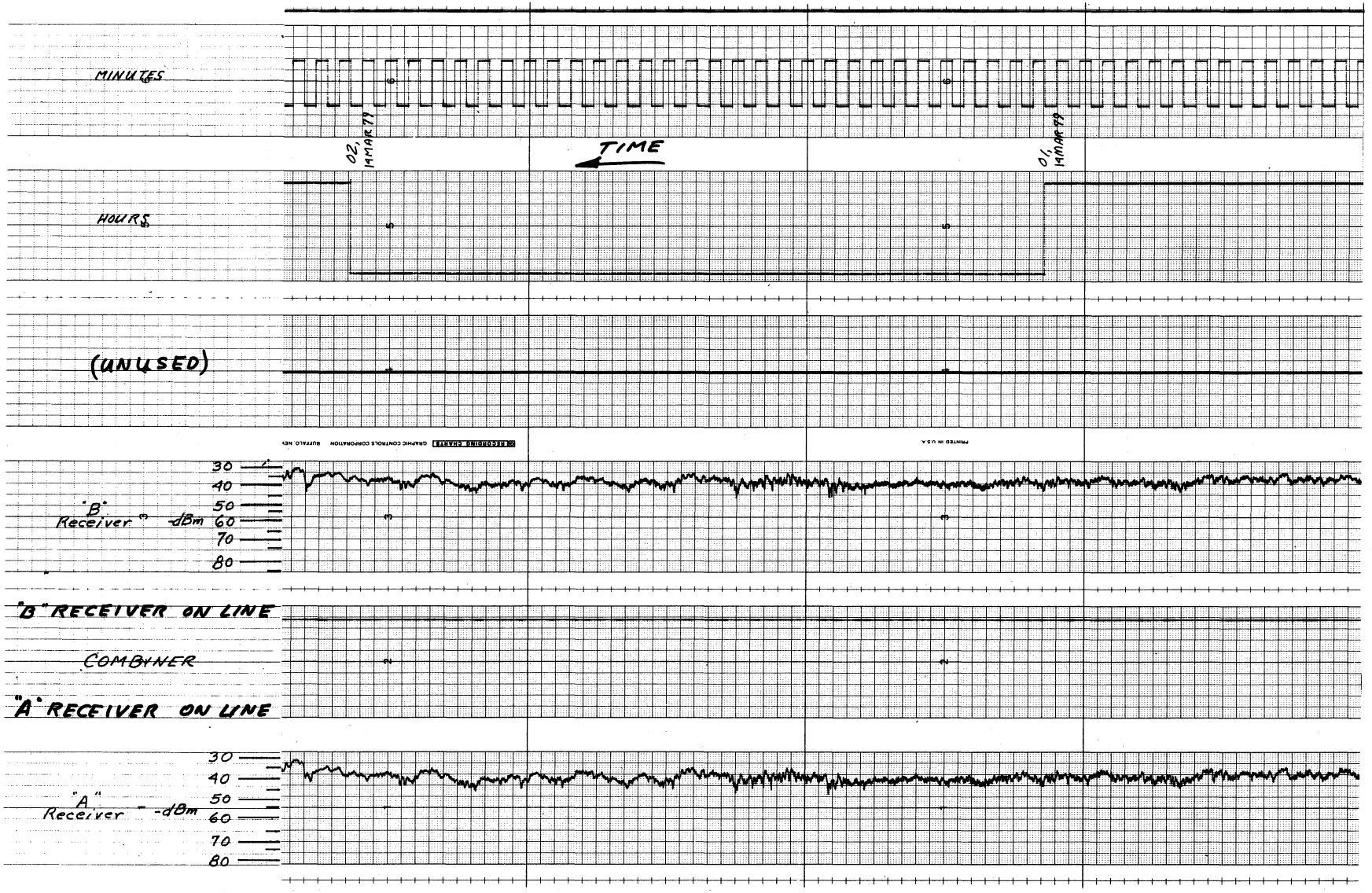

Figure 8. Zugspitze recording showing scintillation type propagation conditions.

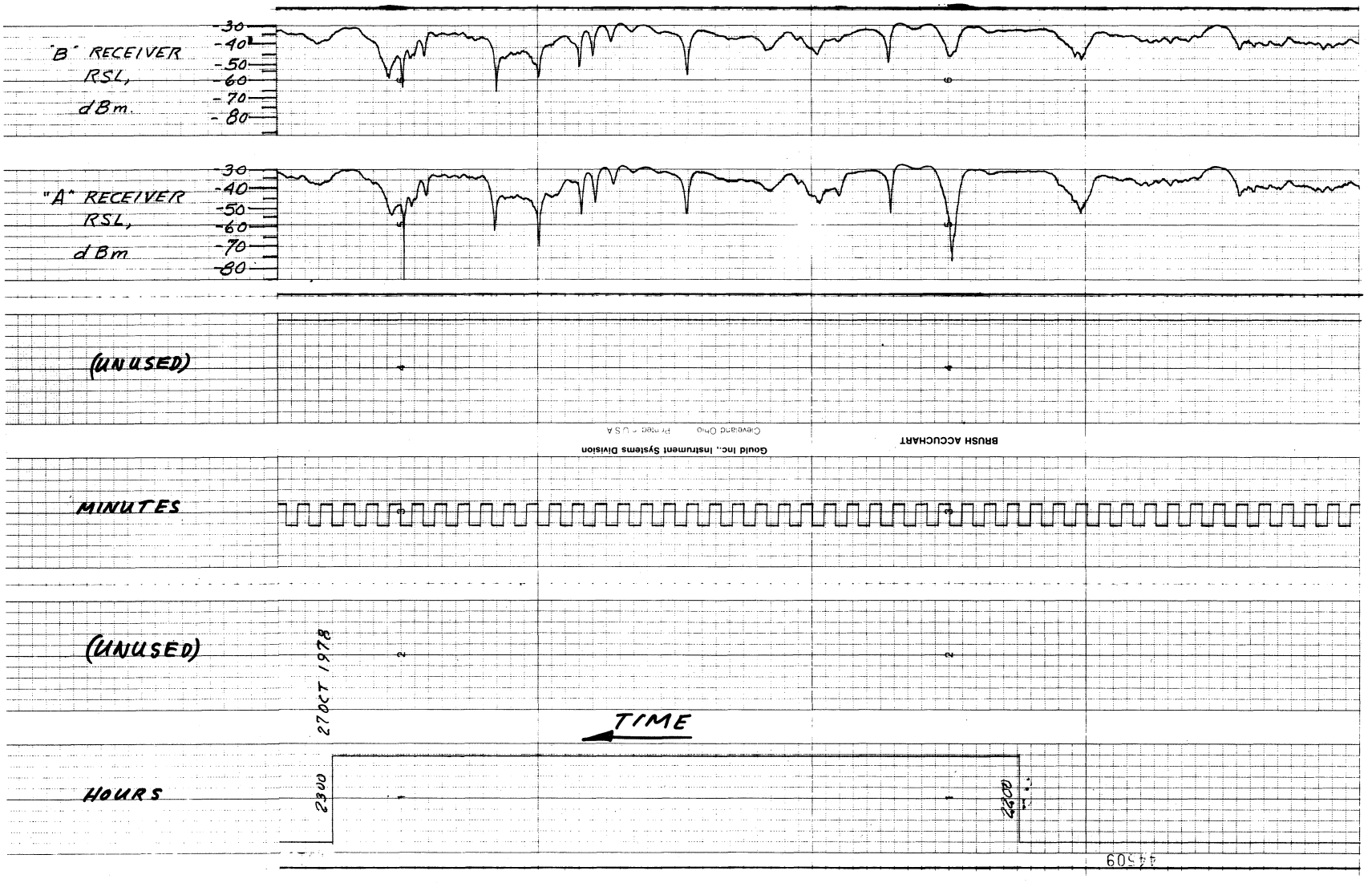

Figure 9. Zugspitze recording showing well-developed slow phase interference fading.

Figure 10. Zugspitze recording showing diversity switch activity caused by phase interference fading.

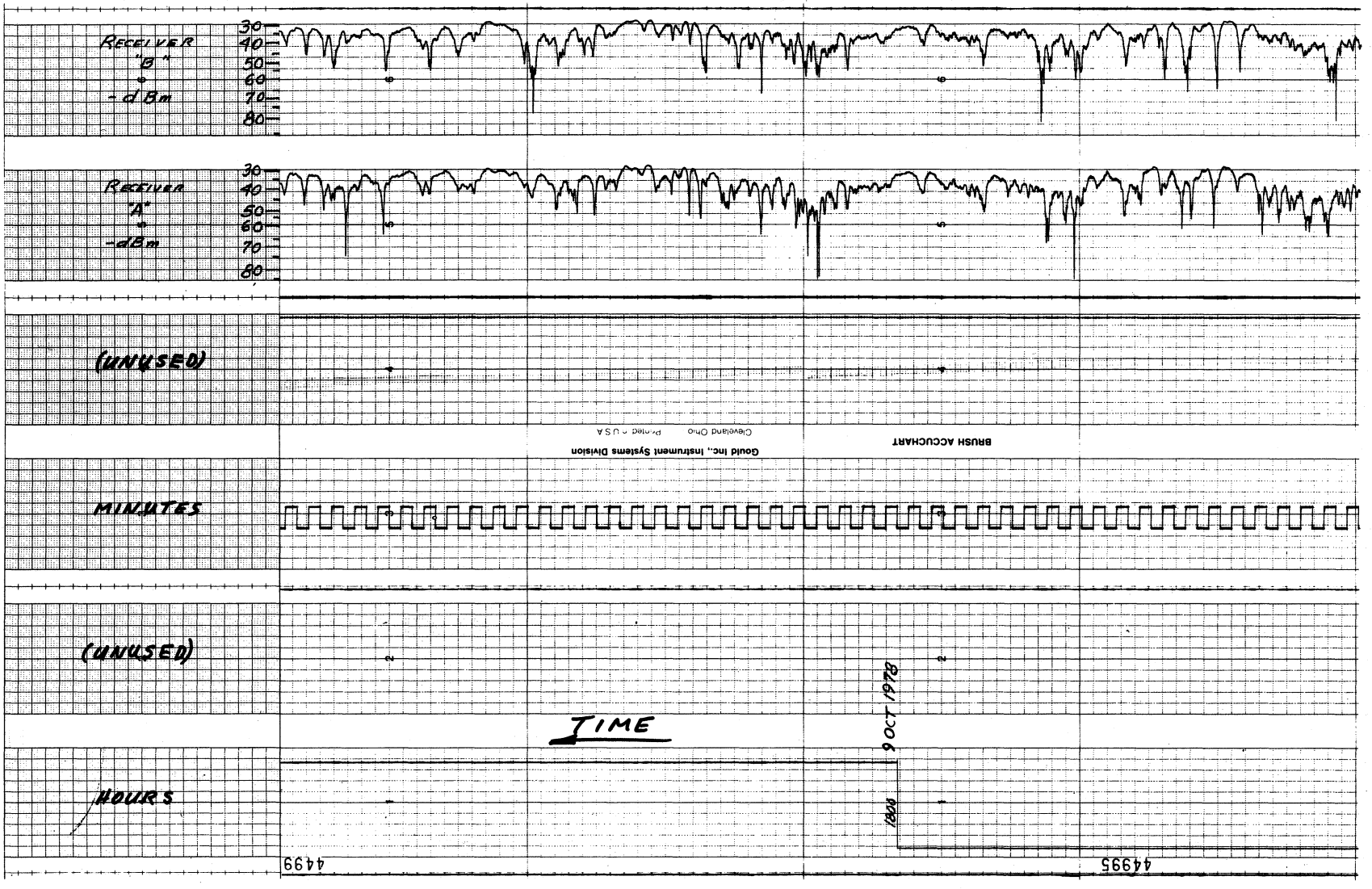

Figure 11. Zugspitze recording showing rapid phase interference fading.

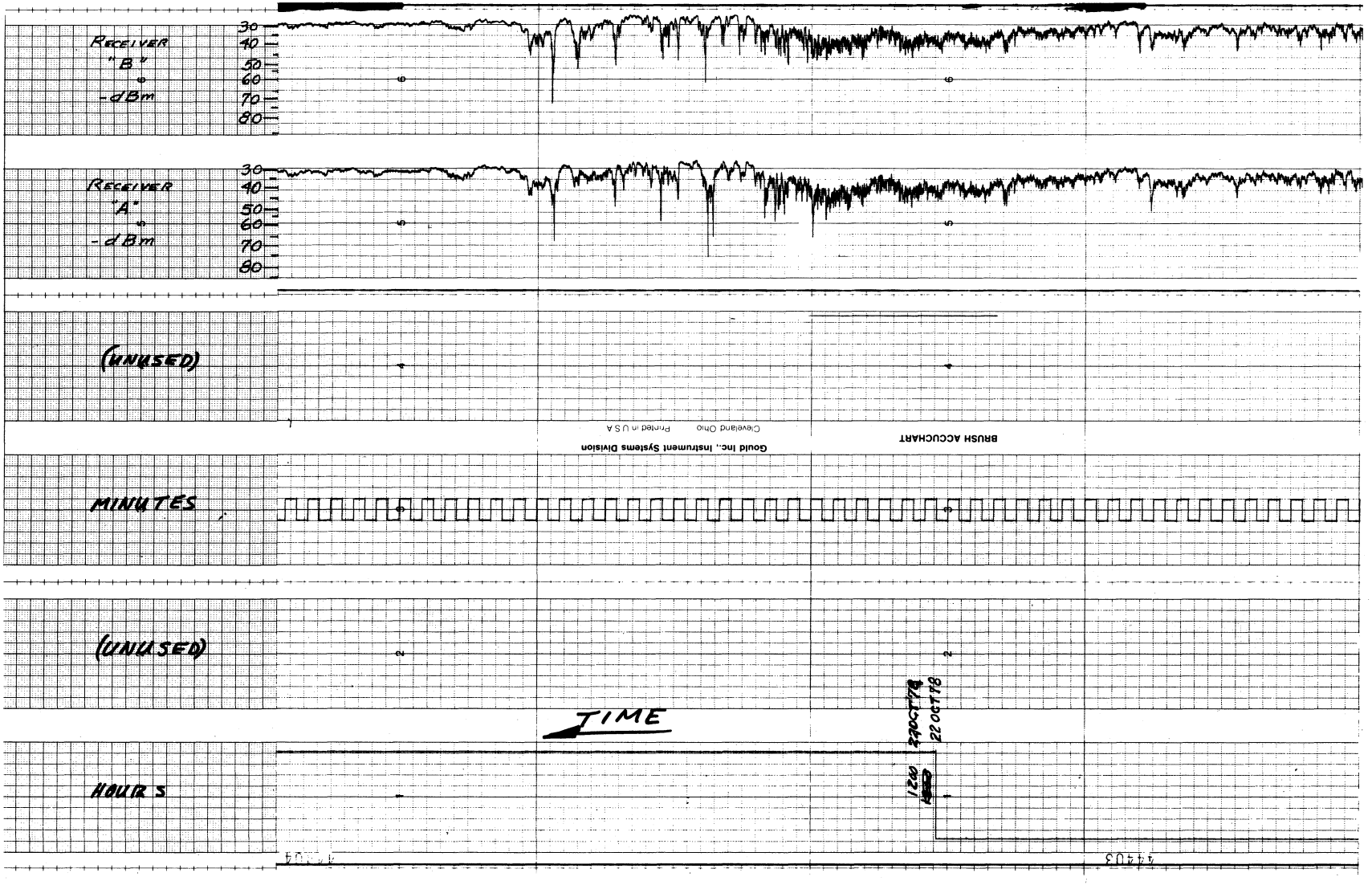

Figure 12. Zugspitze recording showing fast changes among various fading conditions.

Figure 13. Zugspitze recording showing depressed median signal accompanied by rapid phase interference fading.

level (corresponding to PCM threshold) for only a small fraction of the time.

6.1.1 Diversity Performance at the Zugspitze.

When the first charts from the Zugspitze were reviewed, it appeared that the correlation or similarity between the signals from the two diversity branches might be so high as to reduce severely the effectiveness of the diversity. The similarity of fading patterns was thought to be caused by the close antenna spacing at this site. Figure 14 shows an example of the data that caused the concern. Note that even fine details of the signal are seen in both channels. However, a careful analysis of later data showed that when deep fades occurred, they were more often offset in time, as was the case for the deep fade just before 2300 hours on 27 October 1979 (Figure 14).

The offset between the minimum values is one small chart division which is about 15 seconds. This is ample time for the diversity switch to operate and no interference with traffic should occur.

Figure 15 is an example of the data obtained after the switch combiner had been connected to show which receiver was supplying the baseband signal to the multiplex. Even though the signals are not so similar visually as on the previous figure, there is still a very high apparent correlation between the signals; but the deep fades are themselves uncorrelated, that is, they do not occur simultaneously on both channels.

From this, we have concluded that the diversity separation in the vertical direction is adequate to provide signals to the two receivers which are only infrequently subject to simultaneous deep fades.

Figure 14. Zugspitze recording showing lack of correlation between very deep fades.

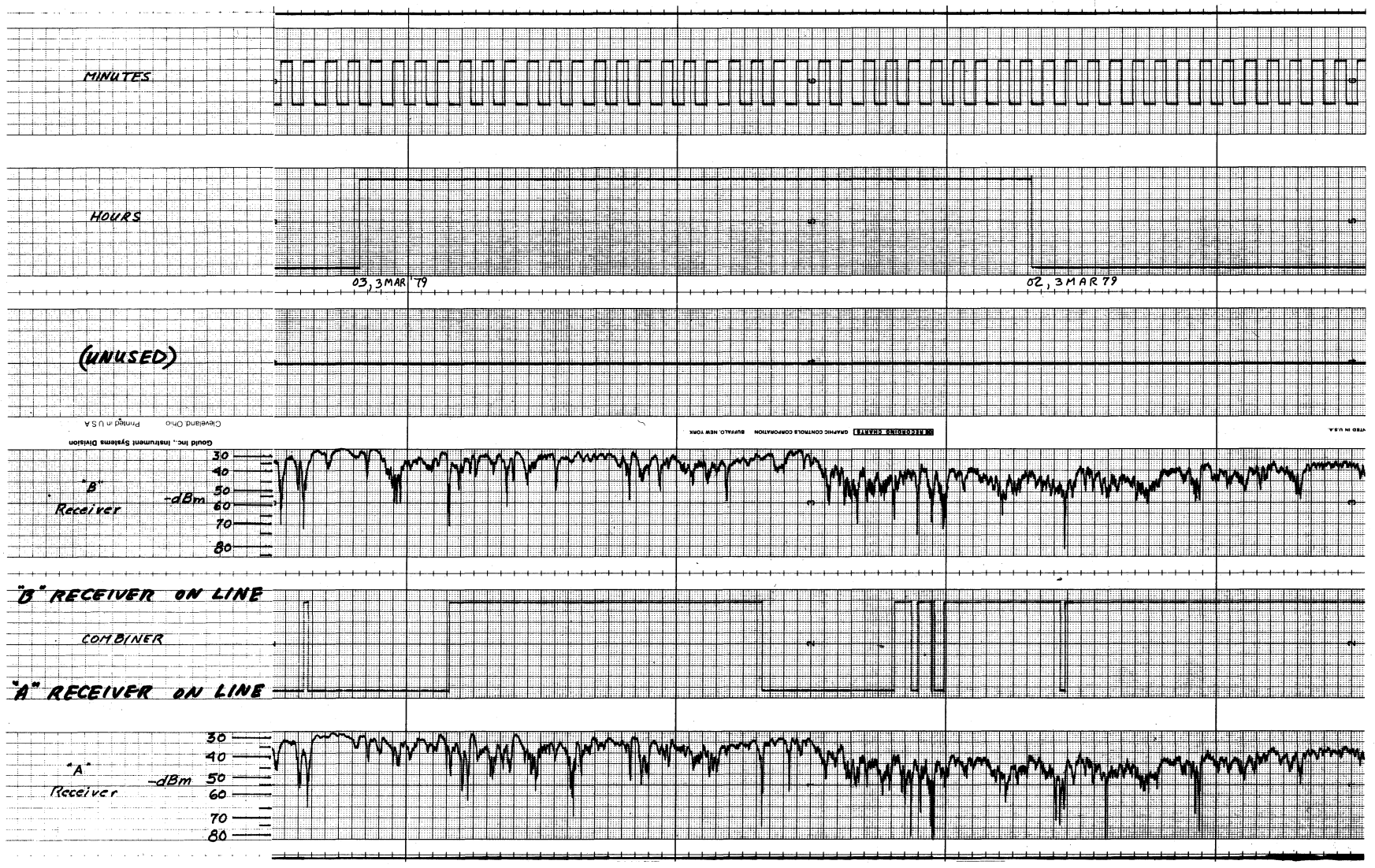

Figure 15. Zugspitze recording showing the degree of protection afforded by the diversity system.

Table 6.1-1. Zugspitze Fade Data
September 1978 to June 1979

Month/Year	Number of Hours of Data	No Fading	No Phase Interference Fading >20 dB	Coincident Fades Per Month	Coincident Fades Per Hour of Data
SEP 78	171	59.1%	78.4%	11	.064
OCT 78	744	38.7%	49.9%	61	.082
NOV 78	574	24.7%	32.9%	19	.033
DEC 78	336	84.5%	88.1%	0	0
JAN 79	240	77.9%	93.7%	0	0
FEB 79	360	70.3%	90.9%	1	.003
MAR 79	668	83.8%	94.7%	1	.001
APR 79	611	92.5%	95.6%	0	0
MAY 79	629	85.1%	91.6%	15	.024
JUN 79	336	63.4%	75.6%	12	.036

Table 6.1-1 summarizes the results of the analysis of the Zugspitze strip charts. The data are blocked off by month with the second column giving the total number of hours of data available. The next two columns show the fraction of the data when no fading occurred and when no fading in excess of 20 dB was present. The next two columns show the number of coincident fades (simultaneously observed on both channels) and the normalized coincident-fade rate per hour. This last column is simply the number of coincident fades divided by the number of hours of data. The only complete month of data was October; during all other months interruptions for installation, alignment, and testing led to the loss of considerable data.

Nevertheless, Table 6.1-1 shows an interesting fact about propagation over this link at least. The most damaging occurrences from the standpoint of traffic continuity are the simultaneous fades below PCM threshold. Although short, these fades will cause some disturbance. Note the increase of coincident fades per hour from September to October, the decrease during

November, and the absence of coincident fades in December. The fraction of time without deep fading decreases from September to November but recovers to a high level in December. This large percentage of the month without deep fading persists from December until May. The month of June again shows a significant decrease in the fraction of time which is free from deep fading.

The table shows another relationship which was suggested by Vigants (1975), namely, that the warmer time of the year will be a period of increased fading activity. The marked increase in fading in June 1979 suggests that this may be true for this link. The rate of simultaneous correlated fading has also increased during June so that the number of fades per hour is at the highest level since the autumn. Although the table does not show it, the periods of severe fading through September, October and November tended to last for a day or even several days at a time while the fading periods during June occurred generally at night and seldom lasted as long as 24 hours. This difference in the diurnal fading pattern is presumably a reflection of the different causes of the atmospheric layer conditions. The situations which produced the autumn fading were large, stagnant, high pressure systems which were not changed much from day to night or from day to day since they gave rise to very stable inversion-type conditions. The summer effects, on the other hand, resulted from layering caused by nighttime radiation cooling of the ground and lower levels of the atmosphere which would be broken up by solar heating during the morning. These latter effects could be modified by cloud cover but would generally represent typical atmospheric layering conditions.

6.2 Magnetic Tape Data from Hohenstadt

As described previously, the magnetic tapes contained hourly histograms for each receiver plus data messages giving the beginning and end times and depth of fade for each excursion of the signal below threshold. The item of greatest interest which resulted from the analysis was the measured

propagation reliability of the radio link during the period of investigation. Therefore, analysis began with a listing and review of the fade messages on each diversity channel separately. Figure 16 shows part of a typical printout of fade messages. The type numbers, 50 and 51, describe which of the diversity branches faded; type 50 refers to signal fades on the radio receiver connected to the lower antenna, and 51 refers to signal fades on the receiver connected to the upper antenna. The fade message printout is organized to show the site (number 1), the type (50 or 51) and the message length in computer words (8, which is used as a check of data integrity). The next two groups of data are the start and end times of the fade. The Julian date is given, followed by the hour, minute, second, and tens of milliseconds. This is followed by a value in millivolts corresponding to the lowest reading of signal level observed during the fade, and by a duration in days, hours, minutes, seconds, and tens of milliseconds. The occurrence of overlapping type 50 and 51 messages is shown along with the duration of the overlap.

Since the system was being installed and tested during most of the test period, it was necessary to edit the data rather carefully so that the apparent fades which were caused by equipment shutdown or testing would not contaminate the results.

The fade messages were analyzed initially by printing each message out and attempting to eliminate those which appeared to be the result of phenomena unrelated to propagation. After considerable study, the data were edited to eliminate all signal level excursions below the software threshold if that excursion lasted longer than one minute. This was longer by a considerable margin than the majority of observed fades, and a review of the strip chart data showed that virtually none of the valid data would be eliminated if this rule was followed.

The analysis of the fade message data began with the development of duration histograms for each received signal level separately and then for periods when coincident fading was observed on the two diversity channels. The time bin sizes

SITE	TYPE	LENGTH	START TIME	END TIME	LOWEST LEVEL		DURATION
1	51	8	136: 4:56:22:55	136: 4:56:23: 0	2620	DURATION:	0:00:0":00,45
1	51	8	136: 6:24:34:10	136: 6:24:34:30	2880	DURATION:	0:00:0":00,20
1	51	8	136: 6:24:56:60	136: 6:24:56:85	2700	DURATION:	0:00:0":00,25
1	51	8	136: 6:25: 6:75	136: 6:25: 6:85	3555	DURATION:	0:00:0":00,10
1	50	8	136: 6:25: 7: 0	136: 6:25: 7:10	2935	DURATION:	0:00:0":00,10
1	50	8	136: 6:25:21:70	136: 6:25:21:90	3100	DURATION:	0:00:0":00,20
1	51	8	136: 6:34:32:55	136: 6:34:32:70	3035	DURATION:	0:00:0":00,15
1	51	8	136: 6:41: 5:10	136: 6:41: 5:15	3685	DURATION:	0:00:0":00,05
1	51	8	136: 6:43:10: 0	136: 6:43:10:15	3290	DURATION:	0:00:0":00,15
1	51	8	136: 7:11:18:10	136: 7:11:19:50	3230	DURATION:	0:00:0":01,40
1	50	8	136: 7:11:53:30	136: 7:11:54:65	2985	DURATION:	0:00:0":01,35
1	51	8	136: 7:12:17:15	136: 7:12:17:60	1985	DURATION:	0:00:0":00,45
1	50	8	136: 7:19:47:15	136: 7:19:47:20	3205	DURATION:	0:00:0":00,05
1	50	8	136: 7:21:37:85	136: 7:21:38: 0	2760	DURATION:	0:00:0":00,15
1	50	8	136: 7:23: 8:75	136: 7:23: 9:15	2250	DURATION:	0:00:0":00,40
1	51	8	136: 7:30:54:15	136: 7:30:54:55	3525	DURATION:	0:00:0":00,40
1	50	8	136: 7:44:25:70	136: 7:44:37:35	1940	DURATION:	0:00:0":11,65
1	50	8	136: 7:44:57:70	136: 7:45:18:80	1955	DURATION:	0:00:0":21,10
1	50	8	136:12:37:24:45	136:12:37:43:60	105	DURATION:	0:00:0":19,15
1	50	8	138:23:10:50:85	138:23:10:51:65	2970	DURATION:	0:00:0":00,80

TYPE 50 START 101:08:23:51,90 DUR= ,750 TYPE 51 START 101:08:23:51,90 DUR= ,750 OVERLAP ,75

TOTAL DURATION (SECONDS) OF OVERLAP= ,75

2 OVERLAPPING MESSAGES EXCEED 1 MIN--NOT PRINTED

Figure 16. Sample computer printout of Hohenstadt fade data.

chosen were 0.1 s for periods up to 5 s, 0.5 s for periods from 10 to 30 s and 2 s for periods from 30 to 60 s. This selection provided good resolution for short fade durations and kept the number of histogram bins from being unmanageably large. These histograms were transformed into cumulative distributions and plotted against a logarithmic fade duration axis (on log-normal probability paper) as shown in Figure 17. Figure 18 shows the same data for both receivers plotted against the fade duration in decibels, where $T(dB) = 10 \log_{10} t(s)$ (on linear-normal probability paper). From Figure 17, a median value of fade duration to a level 30 dB below the normal unfaded received signal level can be read as 2.2 seconds for the lower antenna and 3.7 seconds for the upper antenna. Both of these results are consistent with the discussion in CCIR 1978, page 190 which indicates that for a 70 km path at this frequency, a median duration of 5.3 seconds could be expected and that as path length increases, the duration decreases but as the path clearance increases, so does the duration. These expectations are borne out by the data,but the large difference in median values for data from the two antennas is puzzling since the additional path clearance for the higher path is relatively small as can be seen from the profile in Figure 2. Table 6.2-1 shows the size of the data base for these curves.

Table 6.2-1. Hohenstadt Fade Data

	Hours of Data	Number of Fades	Fade Rate
Upper Antenna	4619	2225	.5
Lower Antenna	4605	1419	.3
Both Antennas	4605	98	.02

Note that the number of fades on the upper antenna was about half again as large as the number observed on the lower antenna. No explanation is offered for this phenomenon but the difference in path clearance might have some influence on the number of fades which occur.

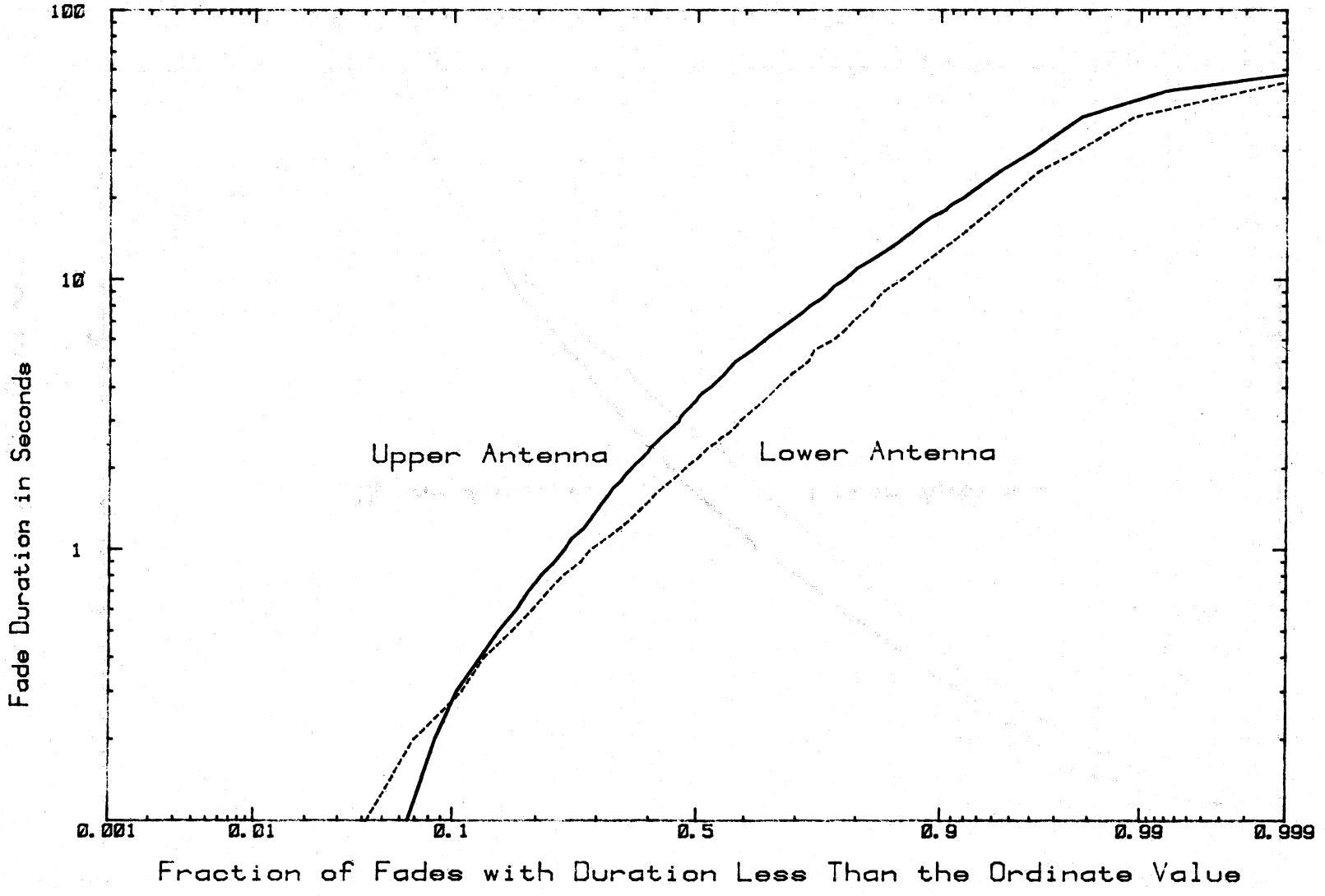

Figure 17. Distribution of single-channel fade durations in seconds, Hohenstadt data for fades 30 dB below free-space conditions.

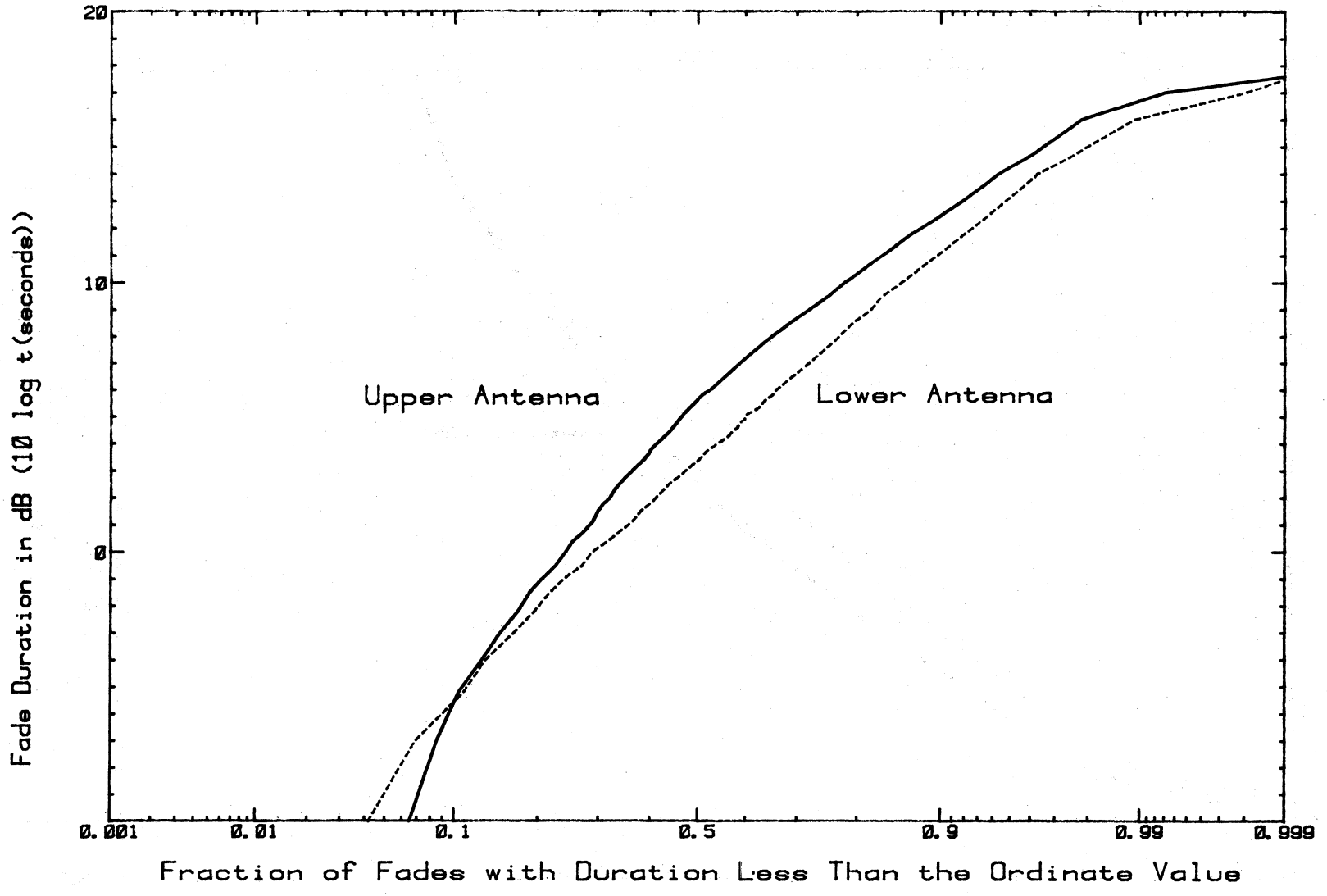

Figure 18. Distribution of single-channel fade durations in decibels, Hohenstadt data for fades 30 dB below free-space conditions.

From Figure 18, an approximate value for the standard deviation of the fade duration T, in dB can be read. The value of 6.2 dB compares favorably with the 5.6 dB value offered by CCIR 1978. The observation that the standard deviation of fade duration depends only slightly on path geometrical characteristics and the climatic conditions encountered seems to be supported by these data.

A similar analysis was performed for simultaneous fades below the -66 dBm threshold. The duration of these fades appears to be log-normally distributed with a median value of 2.5 s. The standard deviation of the log of the duration is 6.5 dB, which is interestingly close to the values measured for the data from each antenna separately. Plots of these simultaneous fade data are given in Figures 19 and 20 against logarithmic and dB scales. Table 6.2-2 describes the data base on which these figures are based. Note that the bulk of the fade data was collected during October 1977. Unfortunately, signal level distribution and fade information from Hohenstadt was not available for the September-November 1978 time period because of problems with the data acquisition equipment, but data were again being collected by late November.

Table 6.2-2. Simultaneous Fade Data by Month

Month Year	Number of Fades	Total Duration, Seconds
OCT 77	52	234.21
NOV 77	16	75.30
DEC 77	12	173.65
JAN 78	6	10.4
MAR 78	5	48.45
APR 78	0	0
MAY 78	3	54.1
⋮		
DEC 78	4	22.75
JAN 79	0	0
FEB 79	0	0
MAR 79	0	0
	98	618.86

Average Simultaneous Fade Duration, 6.3 s.

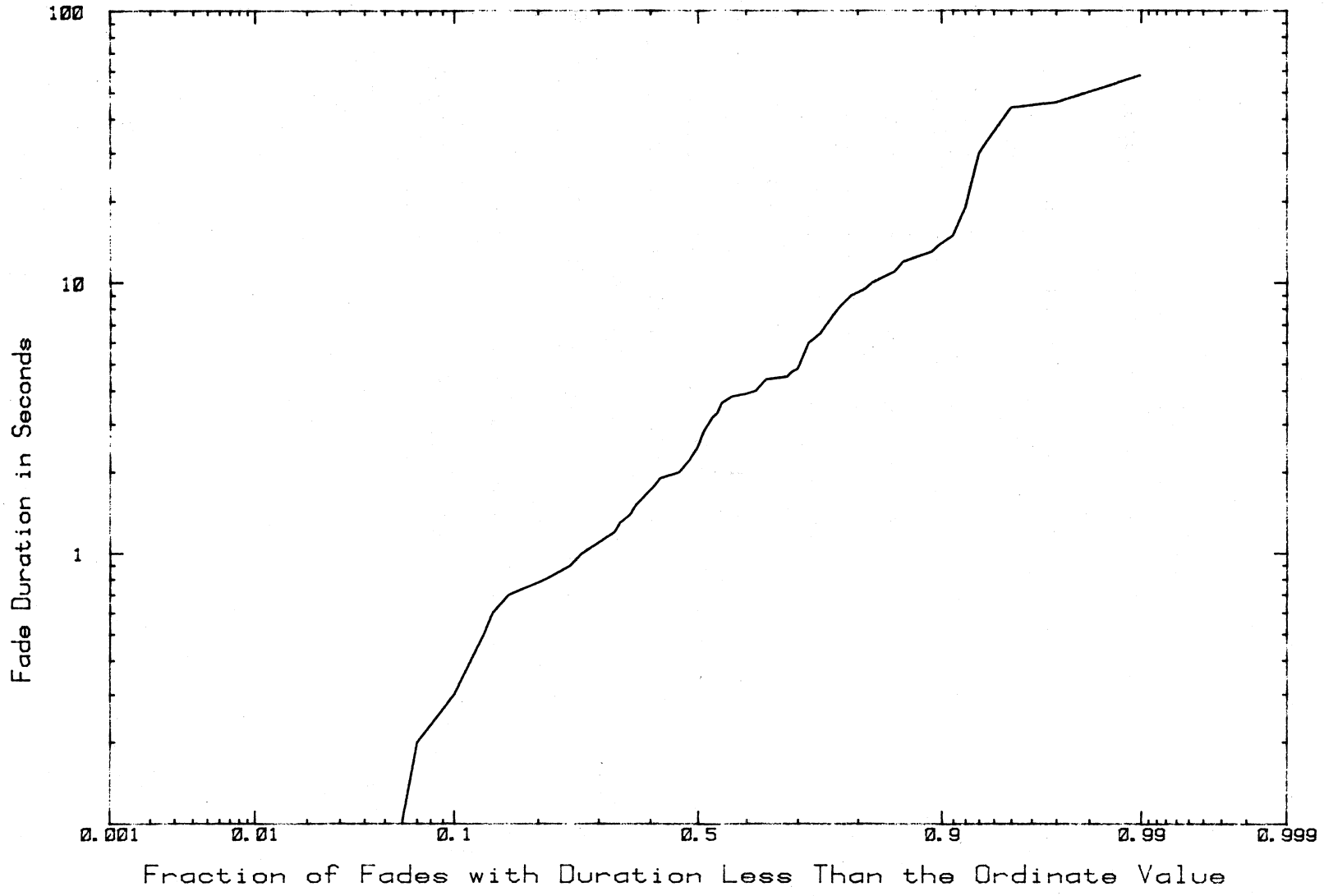

Figure 19. Distribution of simultaneous fade durations in seconds, Hohenstadt data for fades 30 dB below free-space conditions.

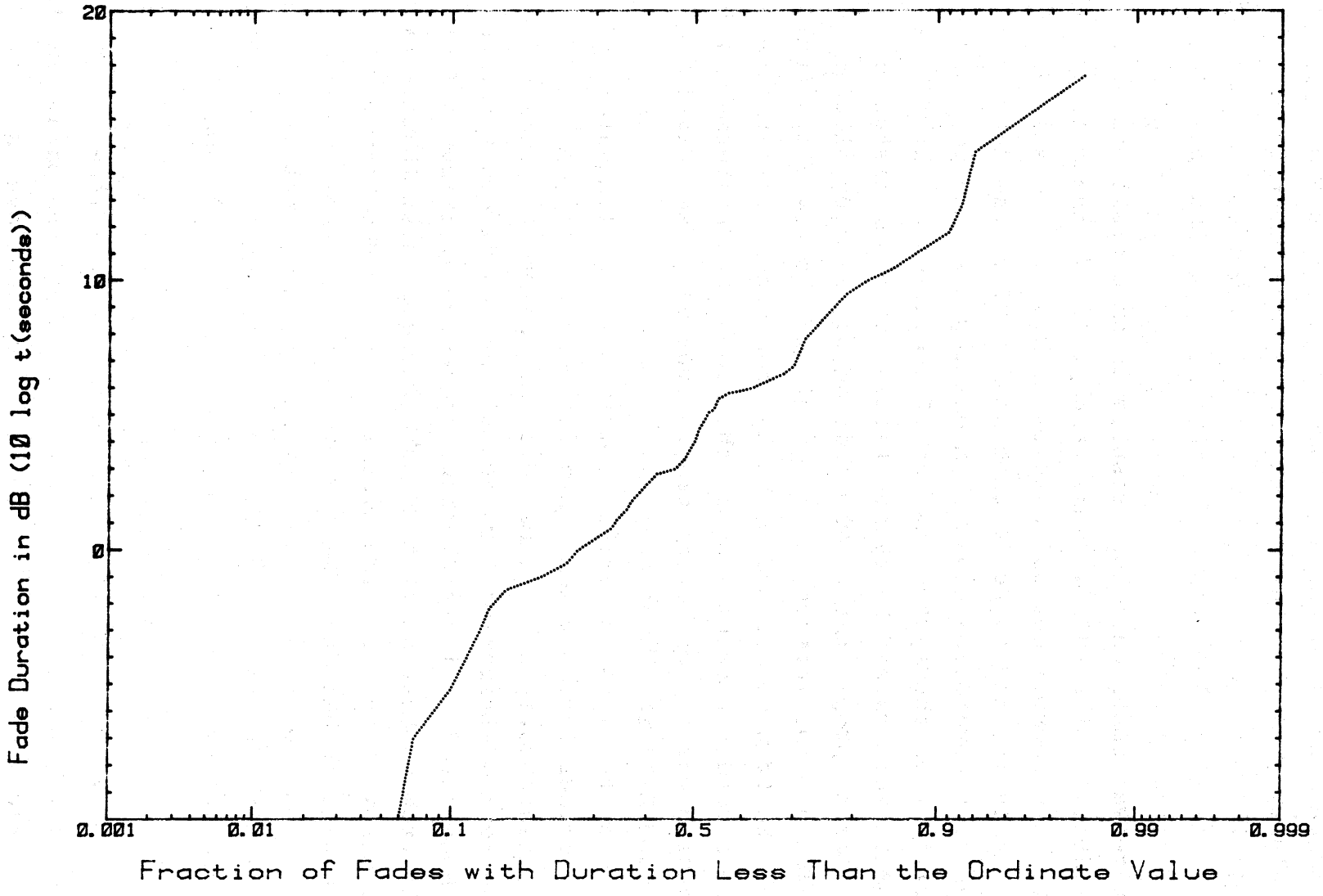

Figure 20. Distribution of simultaneous fade durations in decibels, Hohenstadt data for fades 30 dB below free-space conditions.

Current planning calls for data to be accumulated indefinitely on this link, and as further data become available, particularly during summer months, supplements to this report will be issued.

An interesting outcome of this study is that of the 4505 hours of data, a total of only 618 seconds of propagation outage was observed. This results in an overall propagation reliability of 0.99996. This value includes the effects of diversity improvement and assumes no bias in the sampling.

Analyzing the magnetic tape hourly histogram data at the Boulder Laboratories began with editing the data to eliminate periods when the system was out of operation. Most of these outages were caused by system testing or other disturbances not related by propagation. The editing was done by plotting the median and the interdecile range of each hourly distribution. These plots were grouped by weeks, and since this arrangement gave a good representation of the radio-link performance, this grouping was chosen for displaying the data (see Figures A-1 through A-53 in the Appendix).

From these plots, it was fairly easy to eliminate most of the periods during which contaminated data were collected. The remaining hourly histograms were then summed to obtain one long-term distribution for each of the two diversity branches at Hohenstadt. Figure 21 shows these two distributions of all data from Hohenstadt plotted on a Rayleigh distribution grid. The shape of the measured distributions at the high signal levels departs somewhat from the Rayleigh distribution, but it is a good representation of the long-term fade depth as was suggested by Hause and Wortendyke (1979). These are, of course, single receiver curves and hence do not include diversity improvement.

7. CONCLUSIONS AND RECOMMENDATIONS

The propagation performance of this radio link is of wide interest primarily because of the length of the path. Relatively little 8 GHz data for such long links and over such an extended period of time have been accumulated to this time,

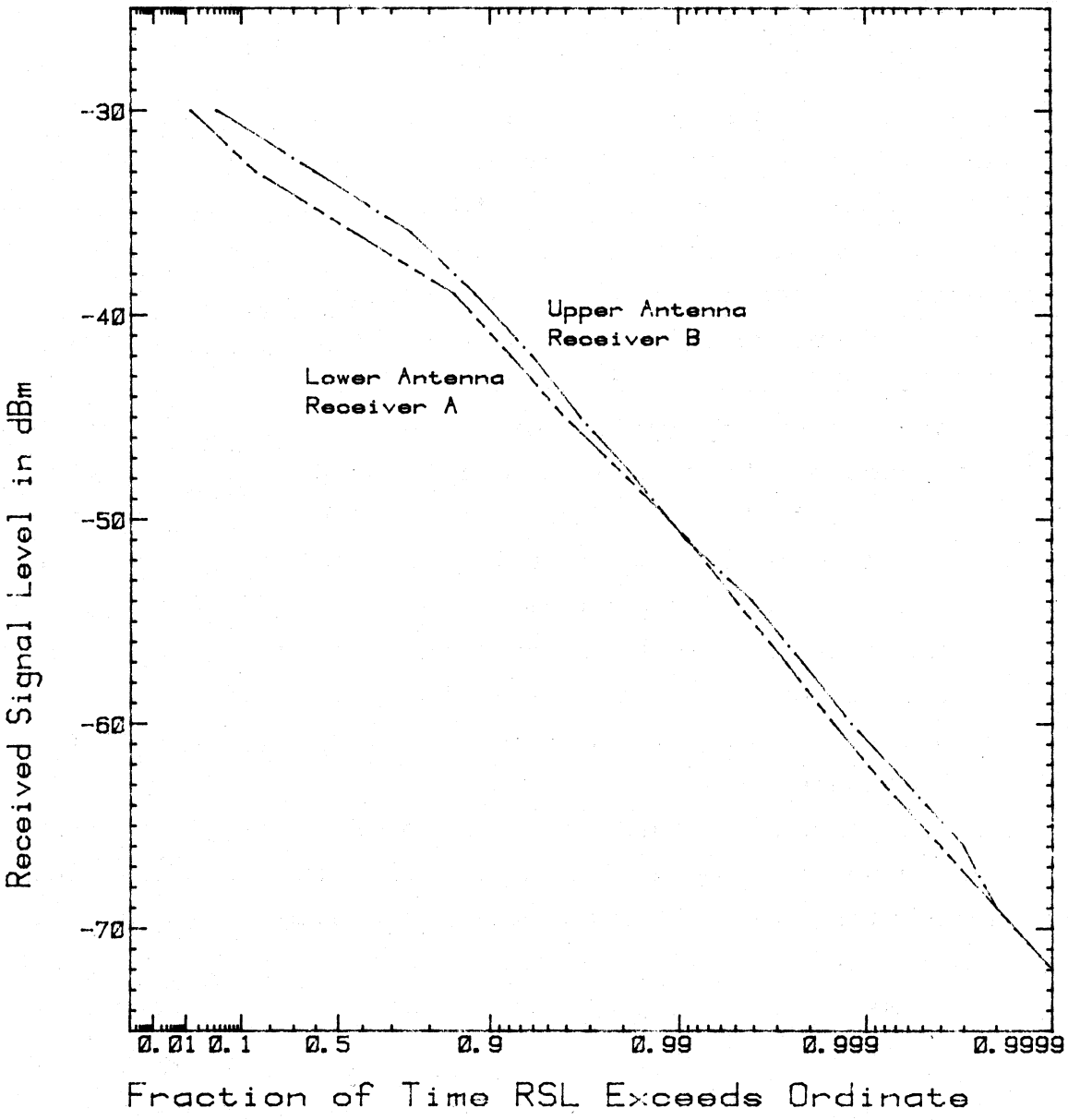

Figure 21. Instantaneous received signal level distributions for all data collected at Hohenstadt.

although a number of long links are currently being investigated. The lack of a well-developed model for predicting the performance of such links has made system designers somewhat reluctant to accept long microwave links as a part of a highly reliable communication system. At one time consideration was given to putting an active relay site in the middle of this link, but the data demonstrate that adequate propagation reliability is provided without such a relay. In fact, the overall reliability of communication between the Hohenstadt and Zugspitze terminals (considering all possible causes for traffic interruption) would be likely to decrease if a relay were to be interposed between these sites. The reason for this is that any small gain in propagation reliability (which could add only about 618 seconds or 10.3 minutes at the very best during the period of observation) would be offset or far exceeded by time lost to station equipment malfunctions. While it is true that such links are possible only in specific physical situations where either one or both terminals is elevated above the intervening terrain or where very tall towers can be built, the practicality and ecomonic utility of such links is more firmly established as additional measurements are reported.

The conclusions reached as a result of studying the fairly extensive amount of propagation data available over this link deserve restating here. One somewhat unexpected conclusion is that even diversity signals which appear to be highly correlated, such as the samples shown in Figures 8 and 9, do not necessarily result in inadequate diversity performance. In the present instance, even though the signals are visually quite similar at high levels, the deep fades which depress the receiver input signal levels below the threshold of adequate performance very seldom occur simultaneously. This permits the diversity protection switch to maintain traffic continuity even during periods of severe fading. In the classical sense, it was possible to achieve good diversity performance in spite of an apparent overall high correlation between the two signals.

The diversity spacing at each end of the path was significantly different as was the relationship between the instantaneous values of received signal level pairs at each end. However, in spite of these differences, effective and nearly equal diversity performance was achieved.

In reviewing the data, several different types of fading were observed. The most frequent type of fading encountered was due to phase interference, either two-ray or multiple component. The distribution of instantaneous signal levels during such periods would presumably be substantially different from a Rayleigh distribution but the overall long-term distribution is very close to Rayleigh. The values of median received signal level (read from Figure 21) are also within one dB of the predicted "free-space" values shown in Table 6-1.

The analysis of the computer-collected fading data included a tabulation of the duration of the fades which dropped 30 dB below the "free space" signal levels and the accumulation of these data into distributions of numbers of fades for given duration windows. As was suggested by the CCIR information, the fade durations are approximately log normally distributed. The median duration of the fades and the standard deviations of the fade duration distributions (in dB) of the Hohenstadt computer-collected data compare favorably with the information from CCIR documents.

All of the above conclusions support the idea that it is definitely possible to achieve reliable propagation at 8 GHz on a link as long as 160 km and with less than normal diversity spacing. This is not to imply that all such systems will perform the same way but with careful engineering it is possible to achieve comparable performance.

8. ACKNOWLEDGEMENTS

The authors wish to express their appreciation to the United States Air Force, Electronic Systems Division for their support of the measurement project. We would also like to thank the site personnel at Hohenstadt (members of the U.S. Army 252nd Signal Company) and at the Zugspitze (members of the U.S. Air Force 1945th Communication Group) for their continuing assistance in collecting the data. Without their generous help the project could not have been accomplished. Particular thanks are offered to SGT Peter Moran of the 252nd Signal Company who nursed the computer system at Hohenstadt through several periods of failing health.

9. REFERENCES

Barnett, W.T. (1972), Multipath Propagation at 4, 6, and 11 GHz, Bell System Tech. J., 51, No. 2.

CCIR (1978), Recommendations and Reports of the CCIR, 1978 XIVth Plenary Assembly, Kyoto, 1978, Volume V, Report 338-3.

Dougherty, H.T. (1968), A Survey of Microwave Fading Mechanisms: Remedies and Applications, ESSA Technical Report ERL69-WPL4. (NTIS Access. No. COM-71-50288, National Technical Information Service, Springfield, VA 22161.)

Hause, L.G., and D.R. Wortendyke (1979), Automated Digital System Engineering Model, NTIA-Report-79-18.

Mc Gavin, R.E., H.T. Dougherty, and C.B. Emmanuel (1970), Microwave Space and Frequency Diversity Performance Under Adverse Conditions, IEEE Trans. COM-18, No. 3, June, 261 - 263.

Samson, C.A., B.A. Hart, and R.E. Skerjanec (1970), Weather Effects on Approach and Landing Systems, FAA Report No. FAA-RD-70-47.

Thompson, M.C. Harris B. Janes, Lockett E. Wood, and Dean Smith (1975), Phase and Amplitude Scintillations at 9.6 GHz on an Elevated Path, IEEE, Vol. AP-23, No. 6, November 1975.

Vigants, A. (1975), Space Diversity Engineering, Bell System Tech. J., 54, No. 1.

White, R.F. (1970), Engineering Considerations for Microwave Communication Systems, Lenkurt Electric Company. (GTE-Lenkurt, Dept. C134, San Carlos, CA 94070).

APPENDIX

This appendix contains plots of hourly median and inter-decile range values for each of the receivers at Hohenstadt. The upper trace corresponds to the lower antenna and the lower trace to the upper antenna in each figure. The ordinate scales are received signal level in negative dBm corresponding to the upper edges of the 3 dB wide histogram bins. Apparent discontinuities in the early data are artifacts of the data collection procedure which have proven impossible to remove.

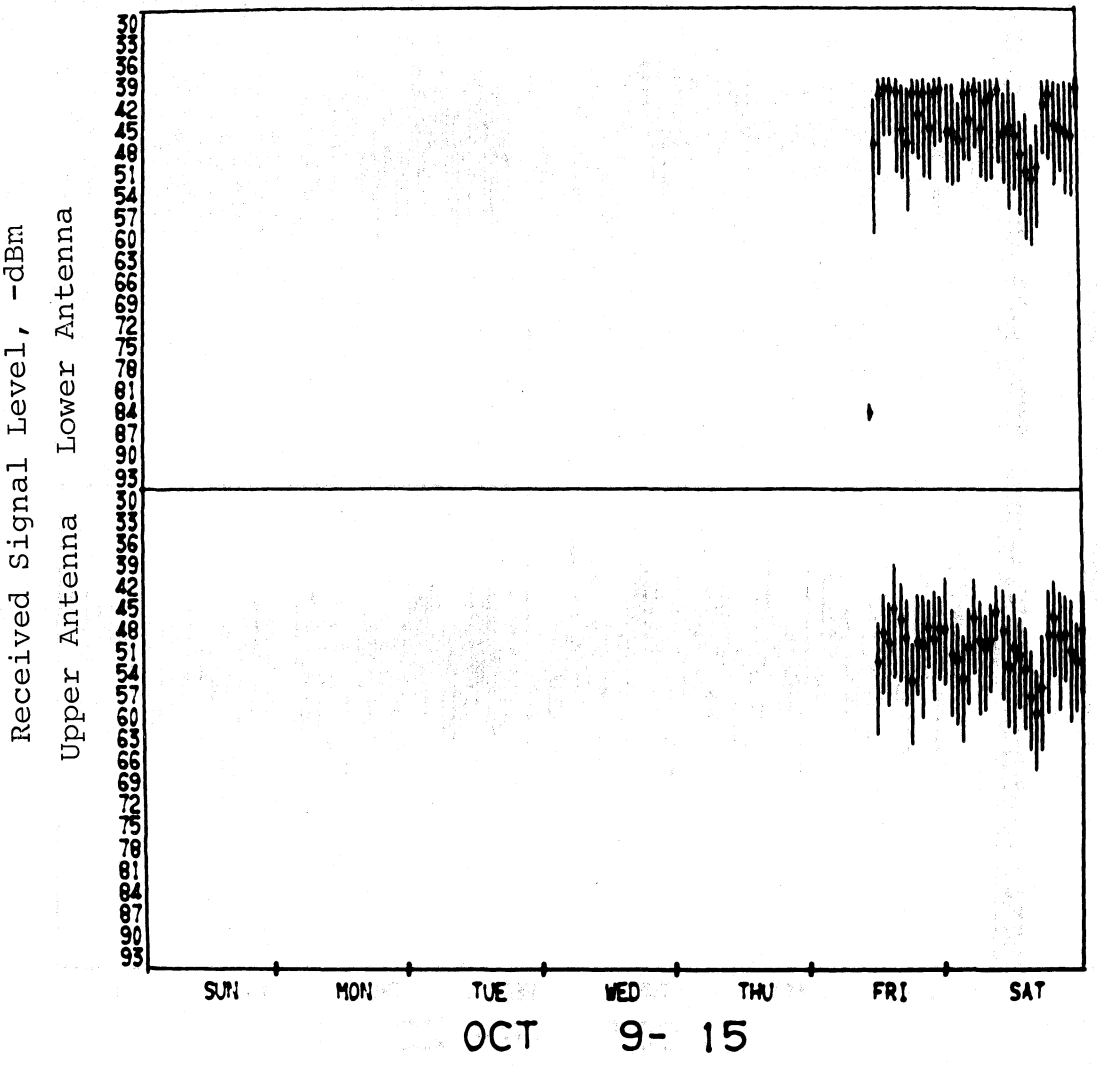

Figure A-1. Hourly histogram data, 1977.

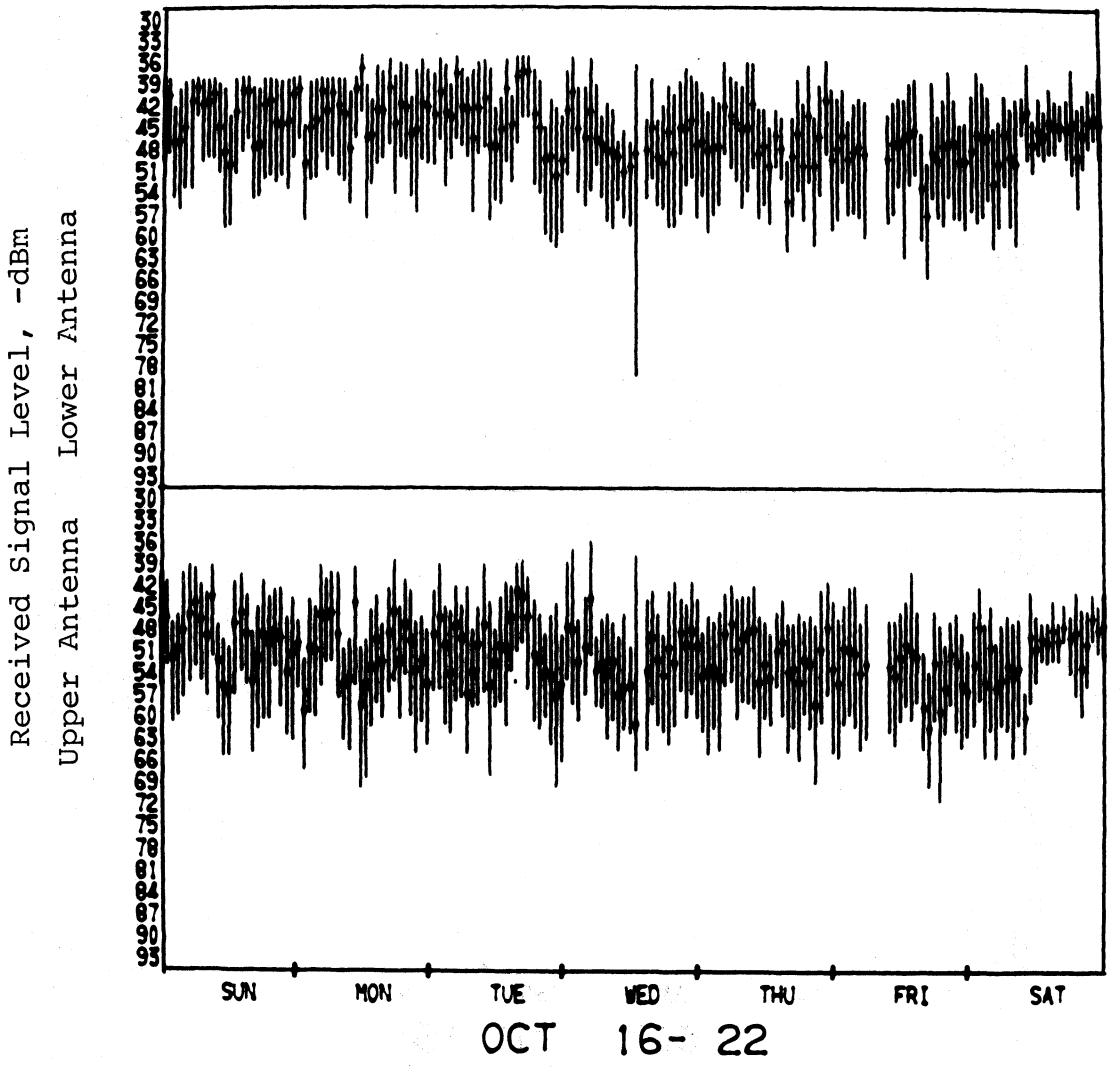

Figure A-2. Hourly histogram data, 1977.

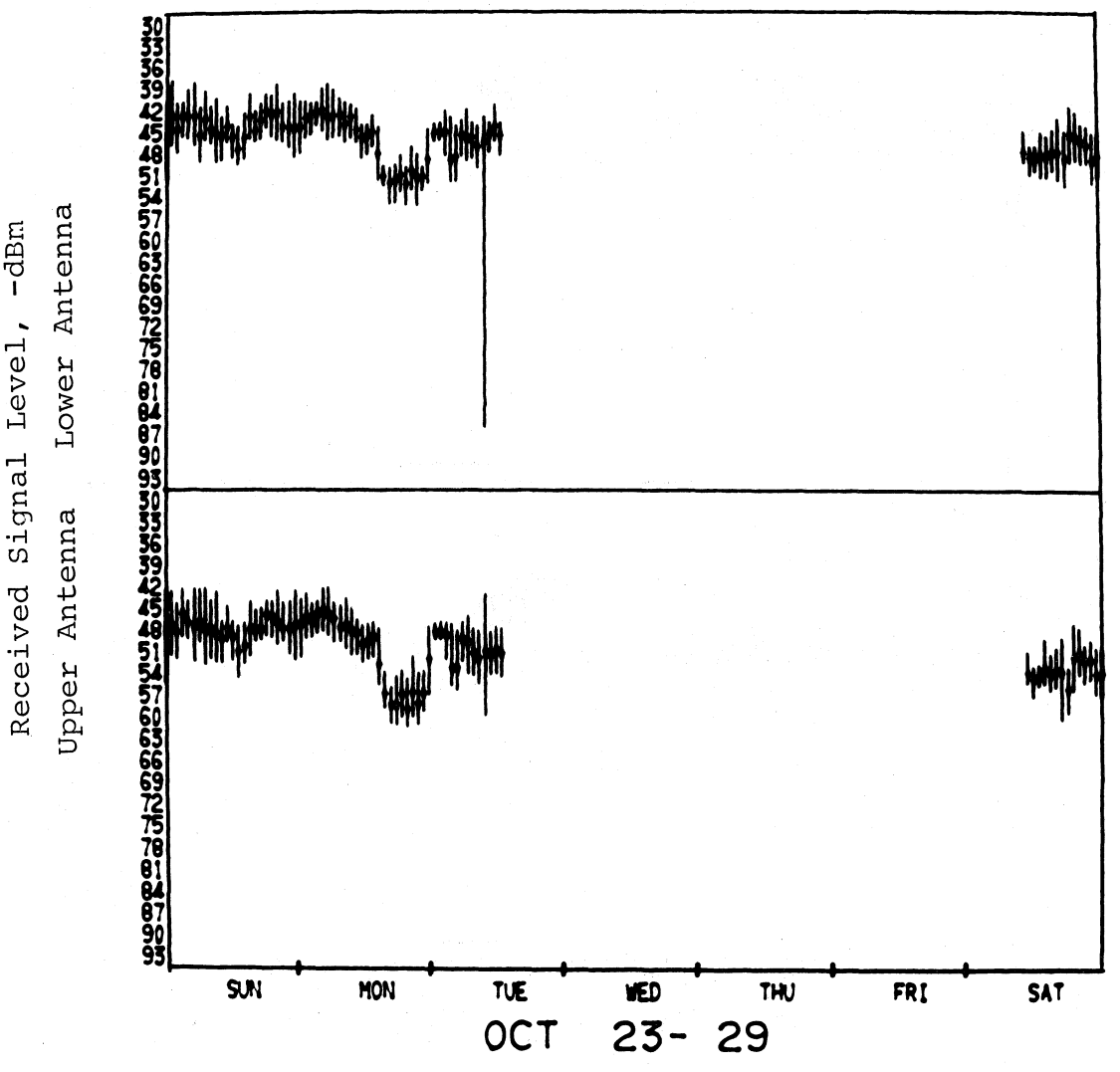

Figure A-3. Hourly histogram data, 1977.

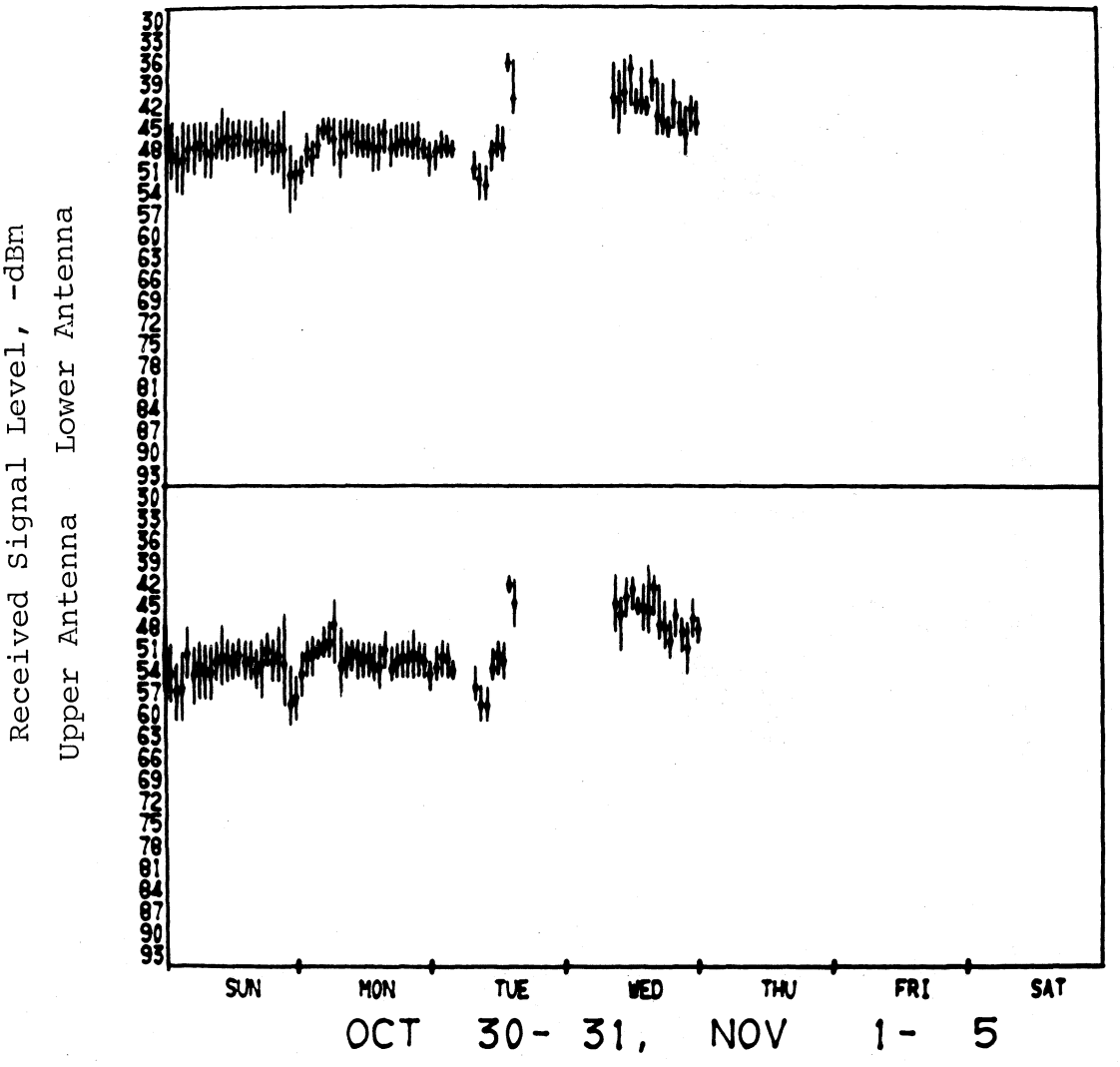

Figure A-4. Hourly histogram data, 1977.

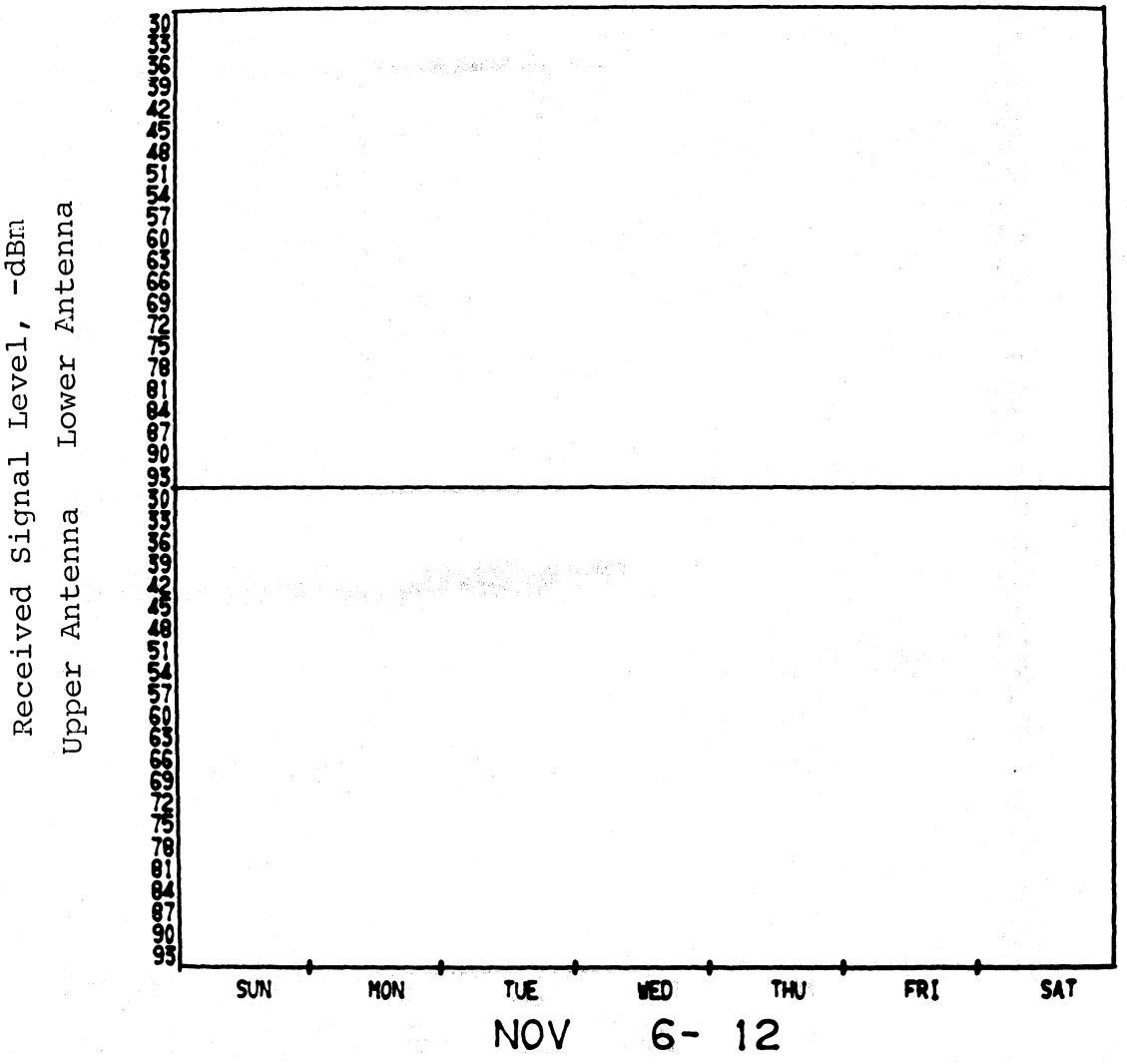

Figure A-5. Hourly histogram data, 1977.

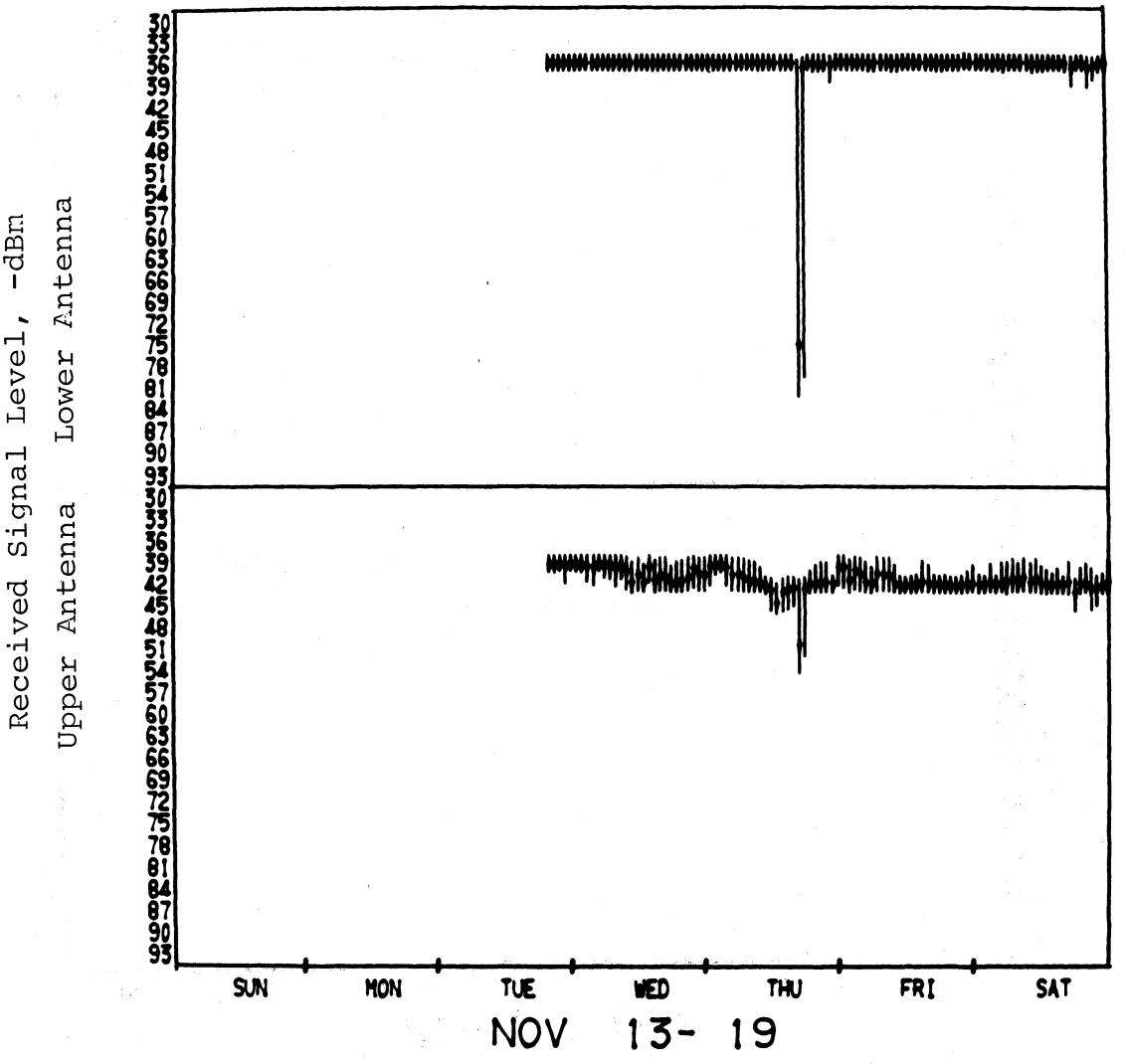

Figure A-6. Hourly histogram data, 1977.

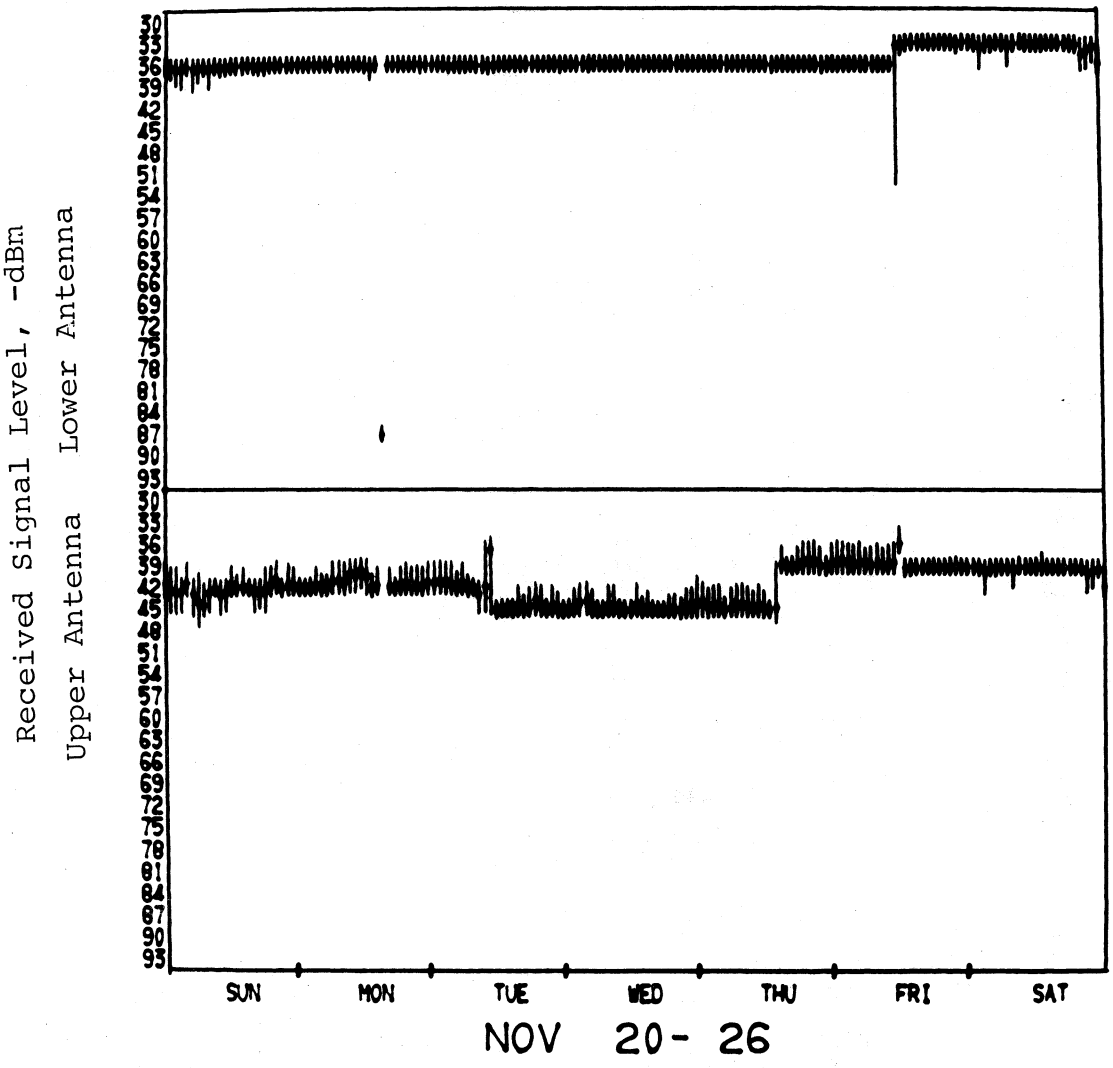

Figure A-7. Hourly histogram data, 1977.

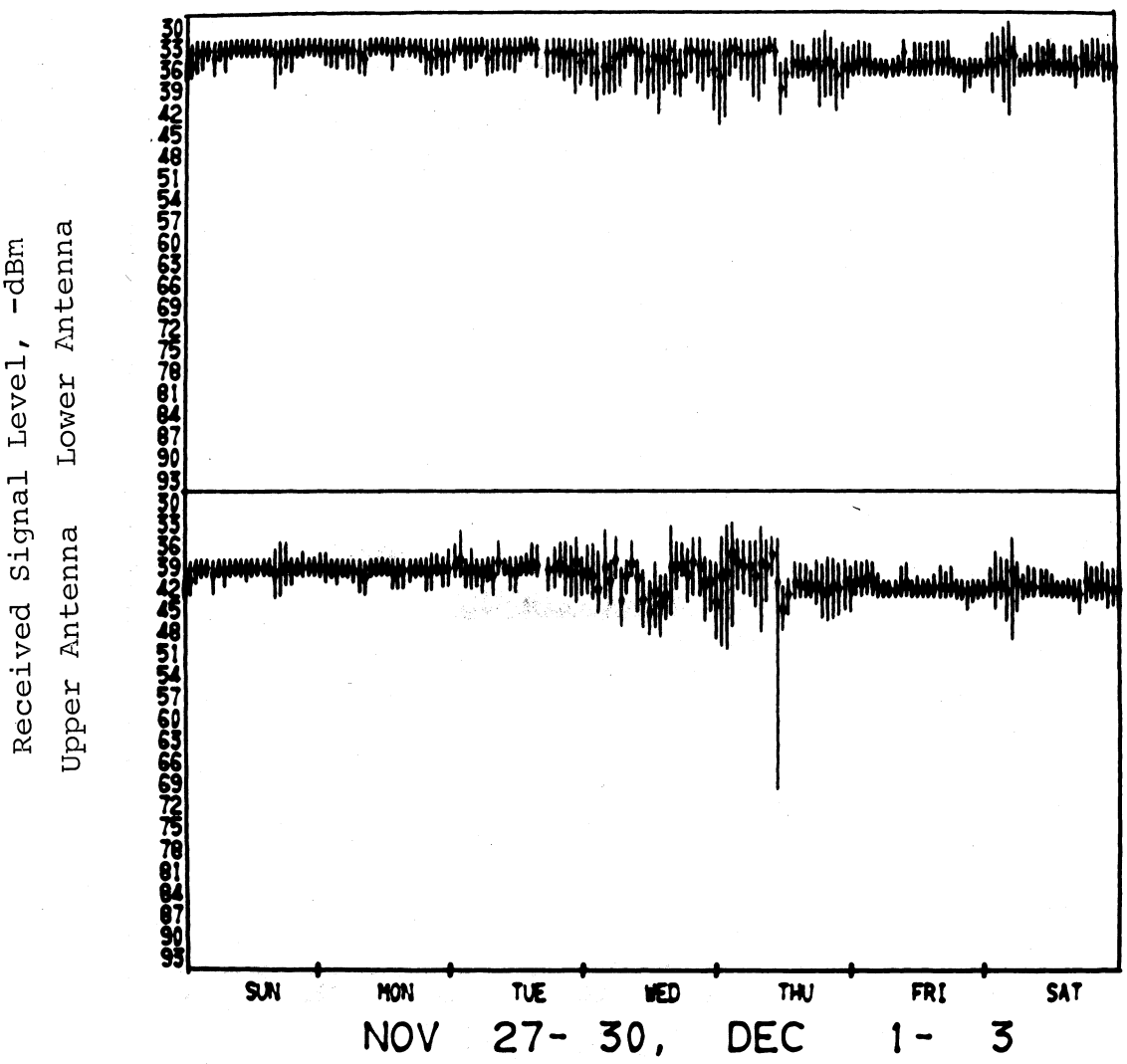

Figure A-8. Hourly histogram data, 1977.

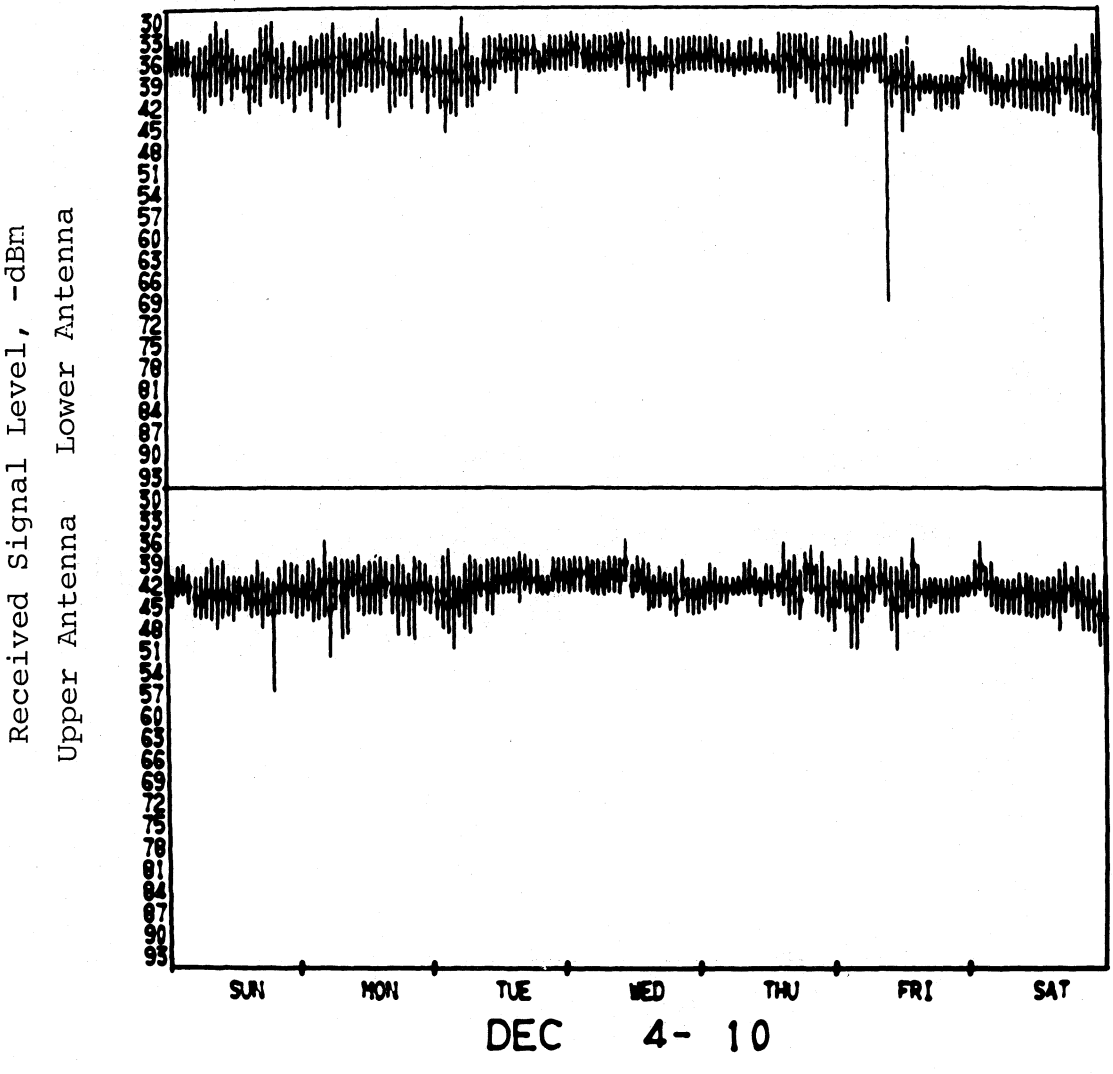

Figure A-9. Hourly histogram data, 1977.

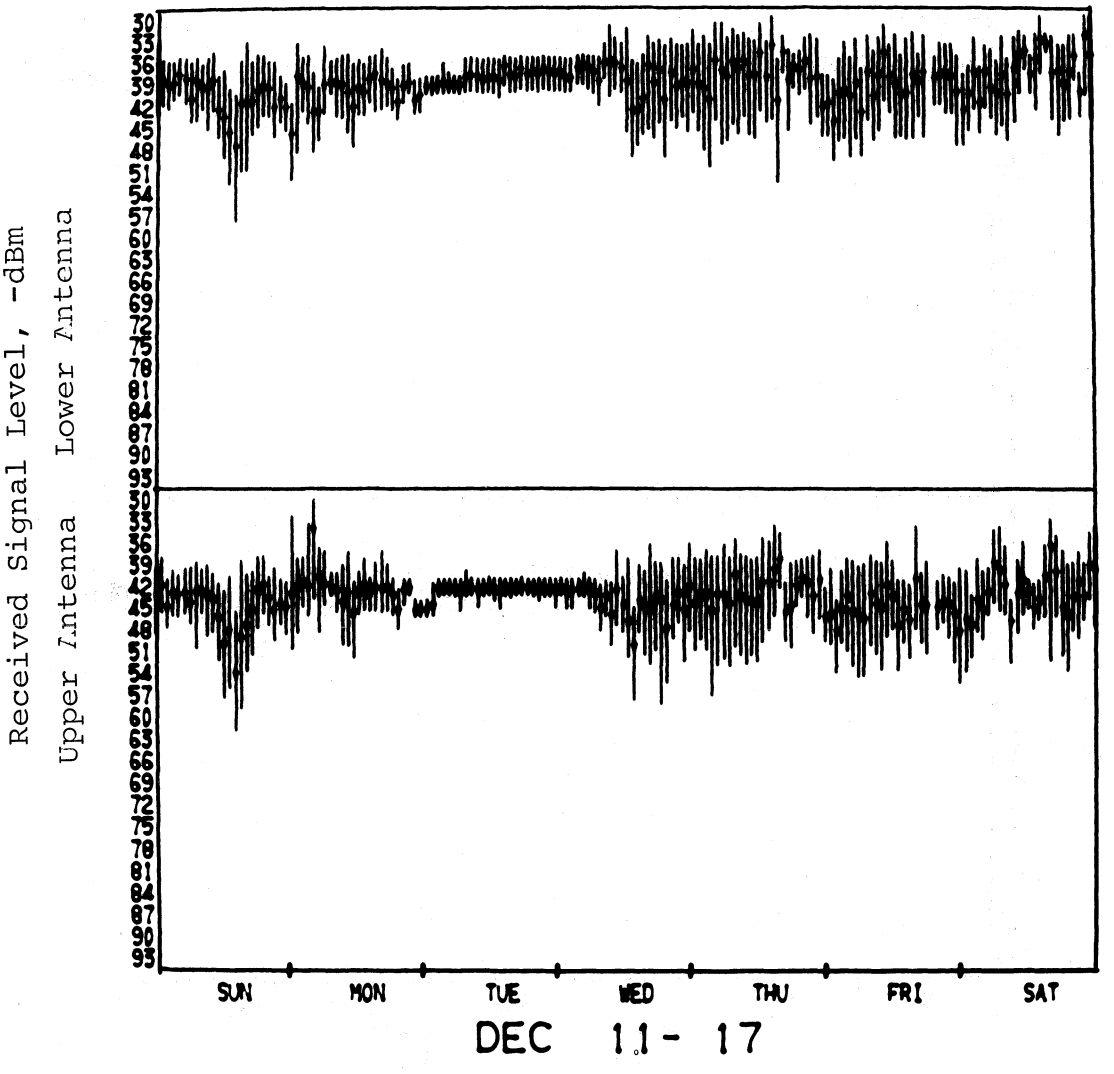

Figure A-10. Hourly histogram data, 1977.

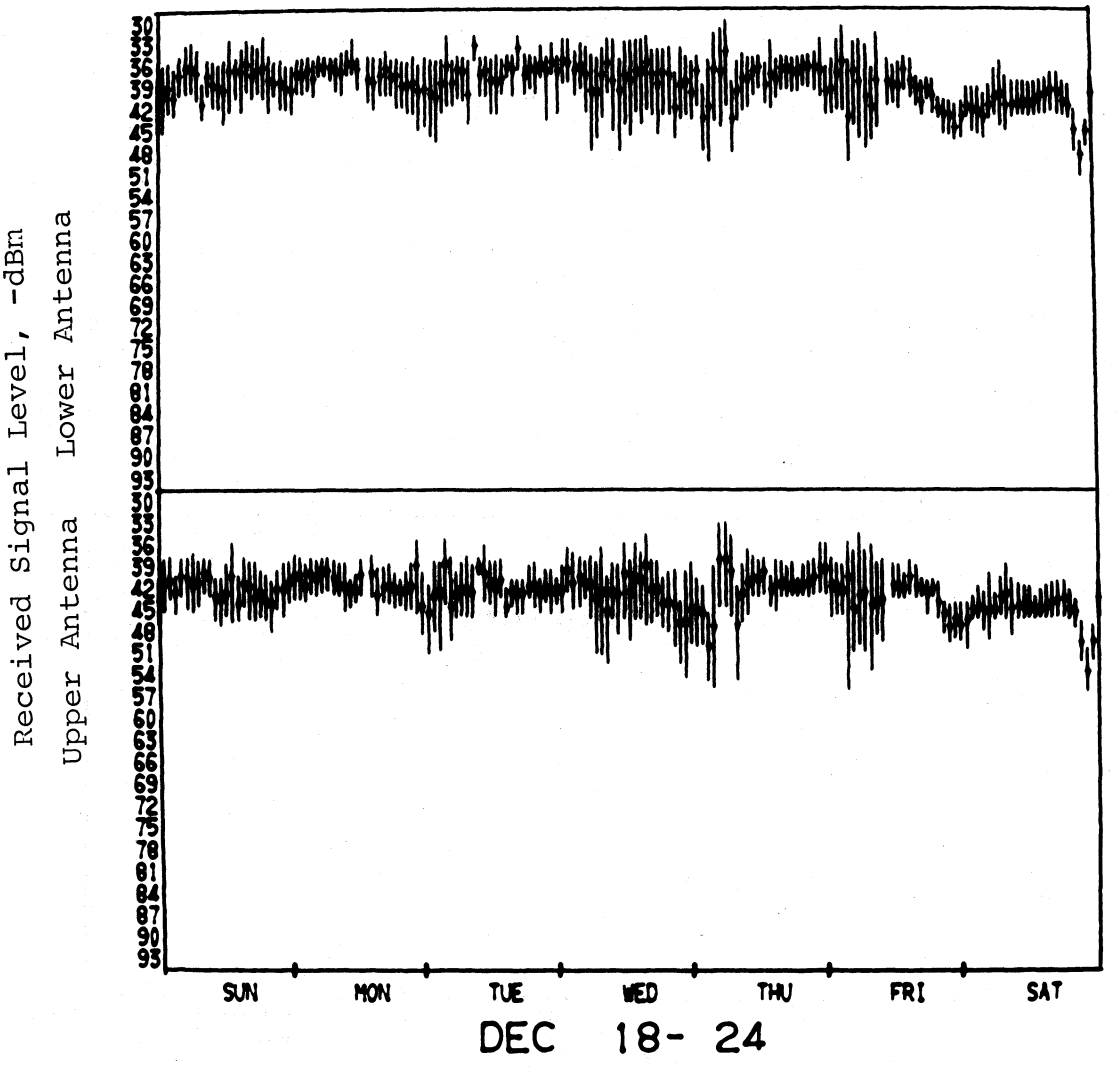

Figure A-11. Hourly histogram data, 1977.

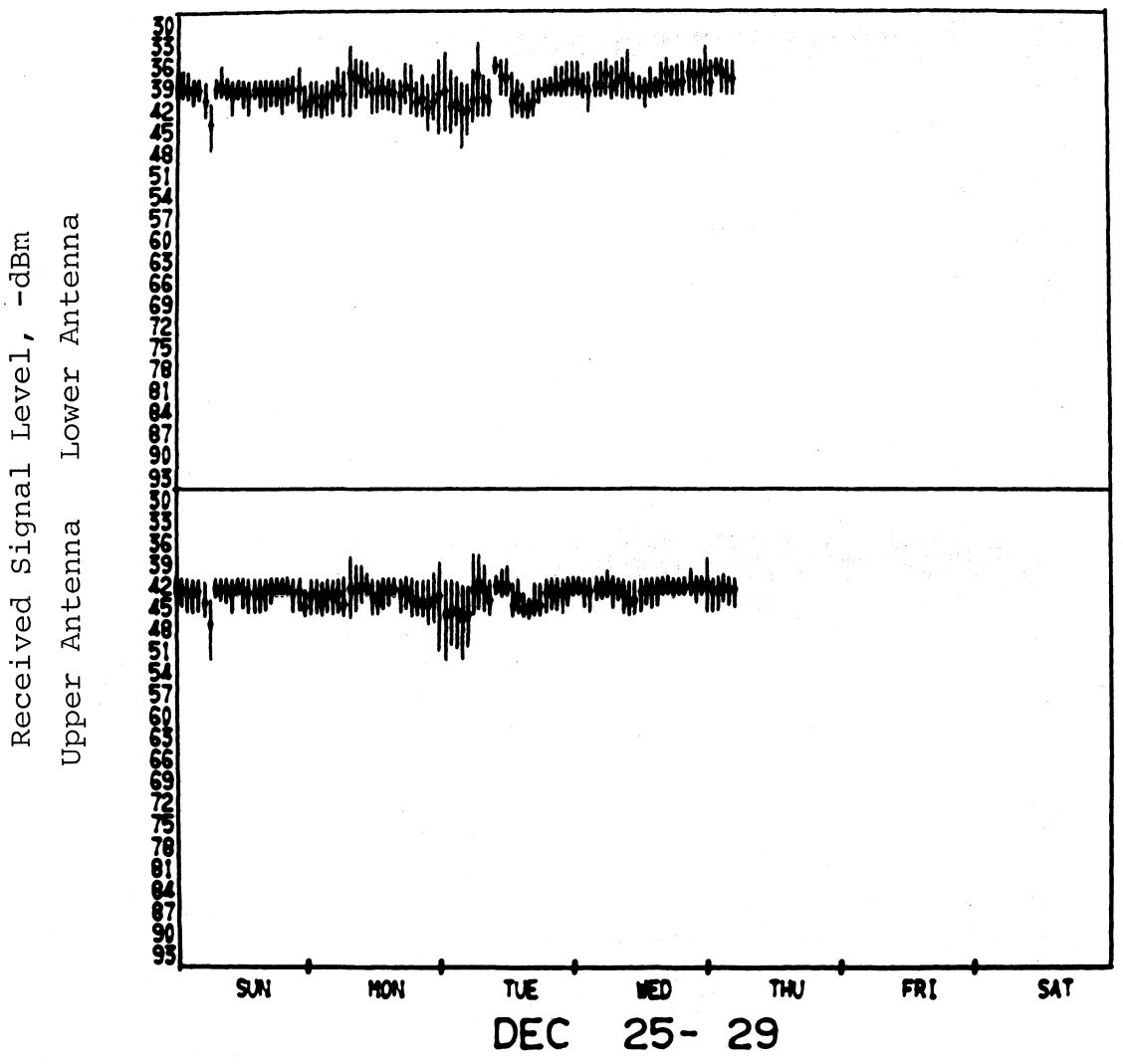

Figure A-12. Hourly histogram data, 1977.

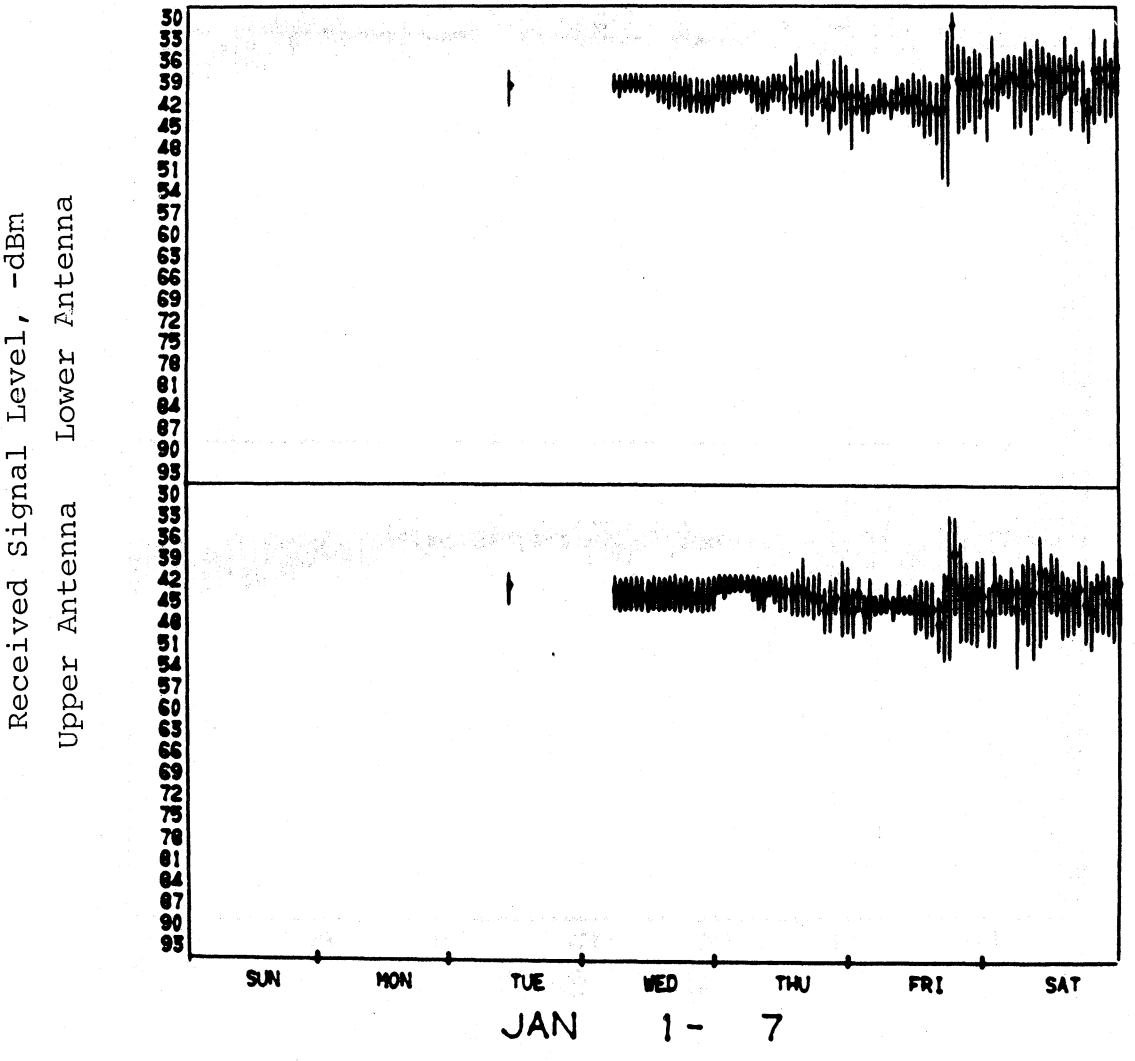

Figure A-13. Hourly histogram data, 1978.

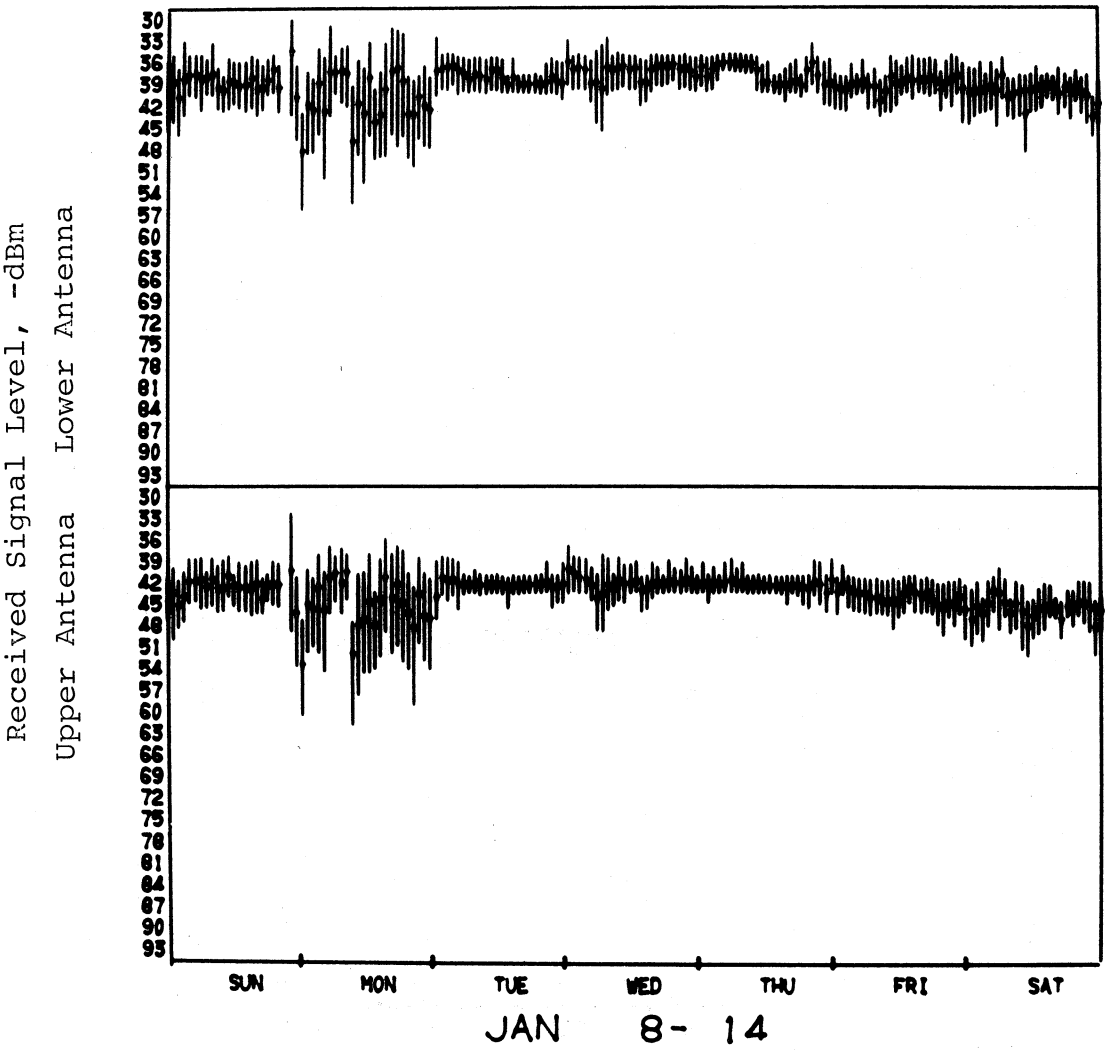

Figure A-14. Hourly histogram data, 1978.

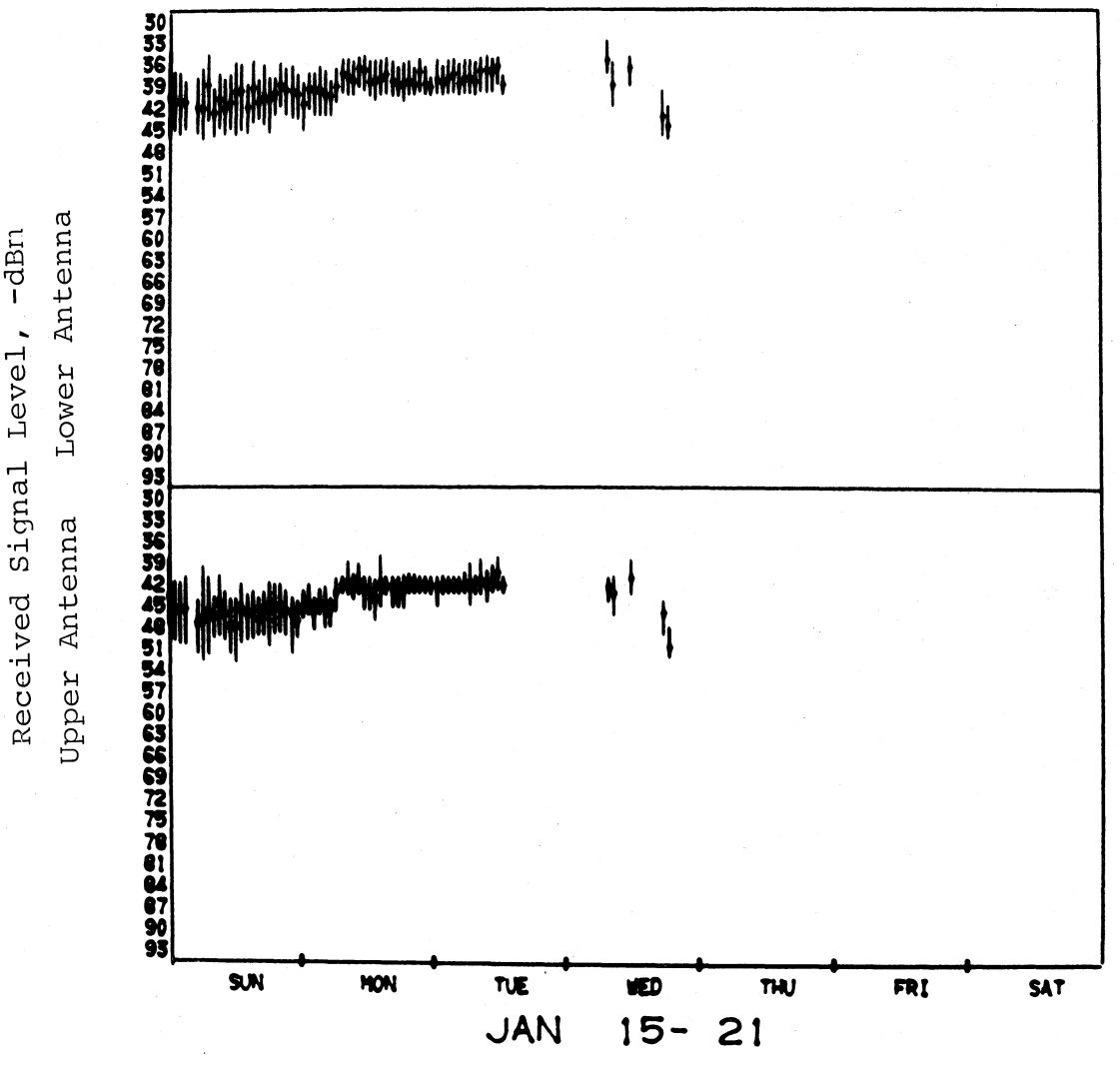

Figure A-15. Hourly histogram data, 1978.

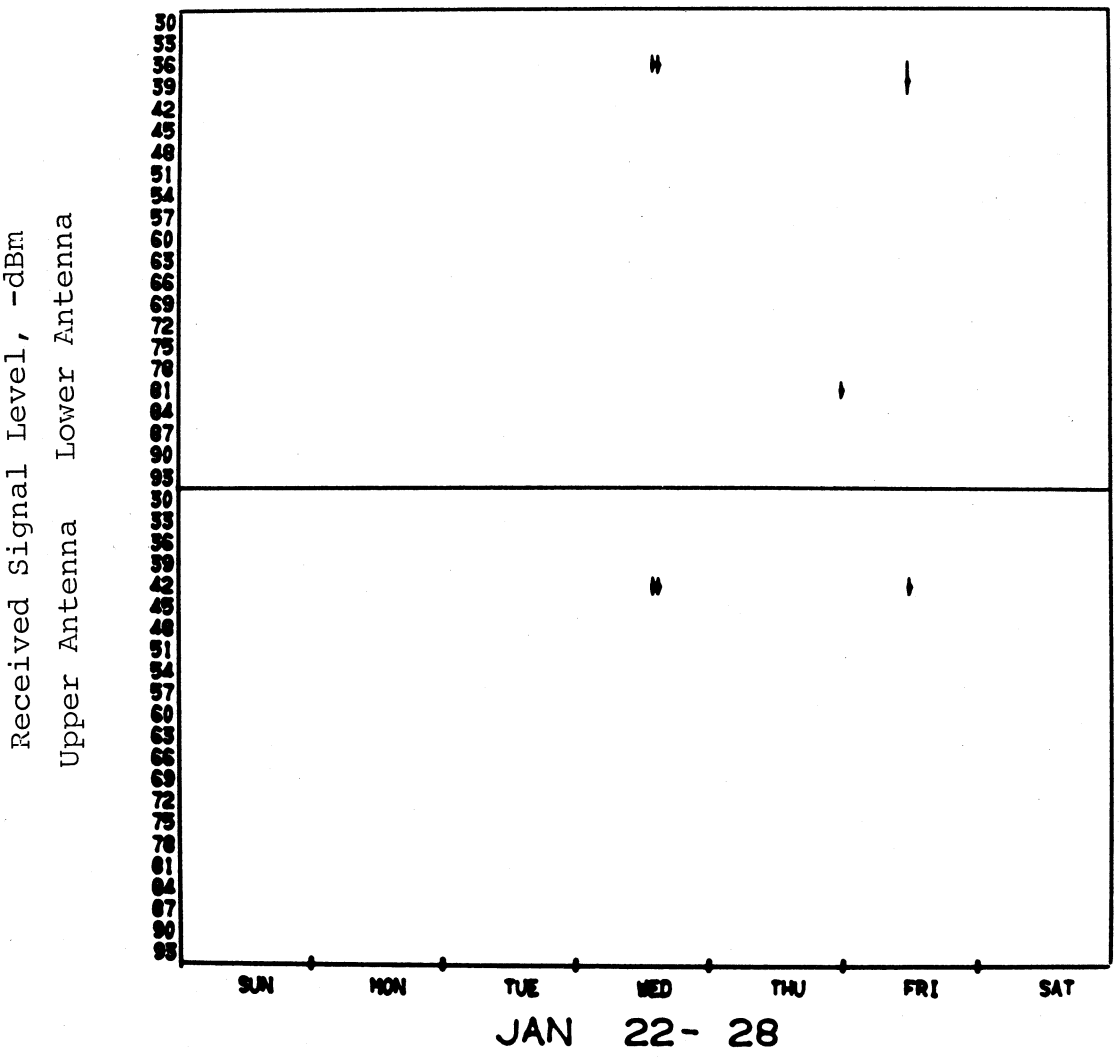

Figure A-16. Hourly histogram data, 1978.

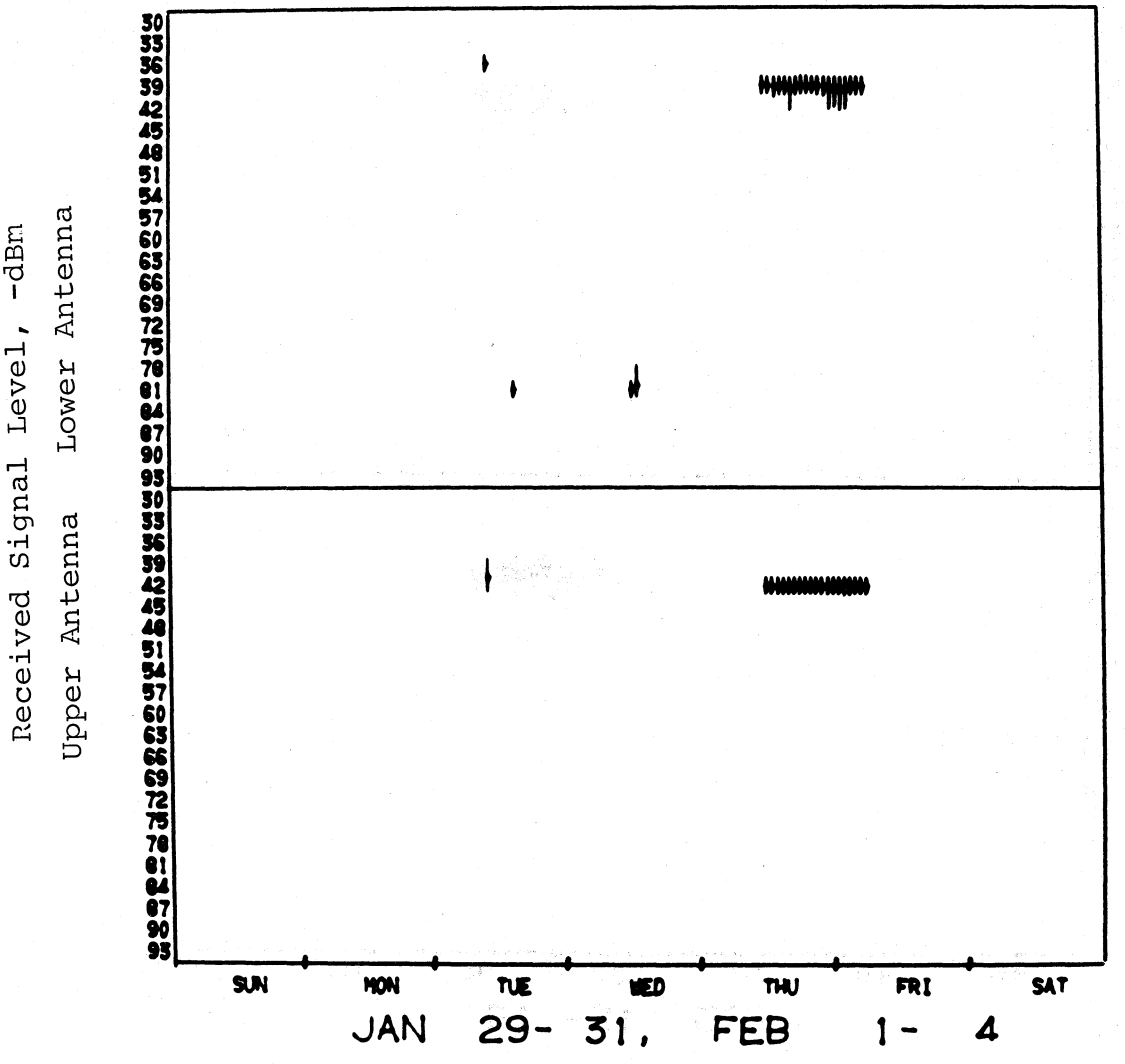

Figure A-17. Hourly histogram data, 1978.

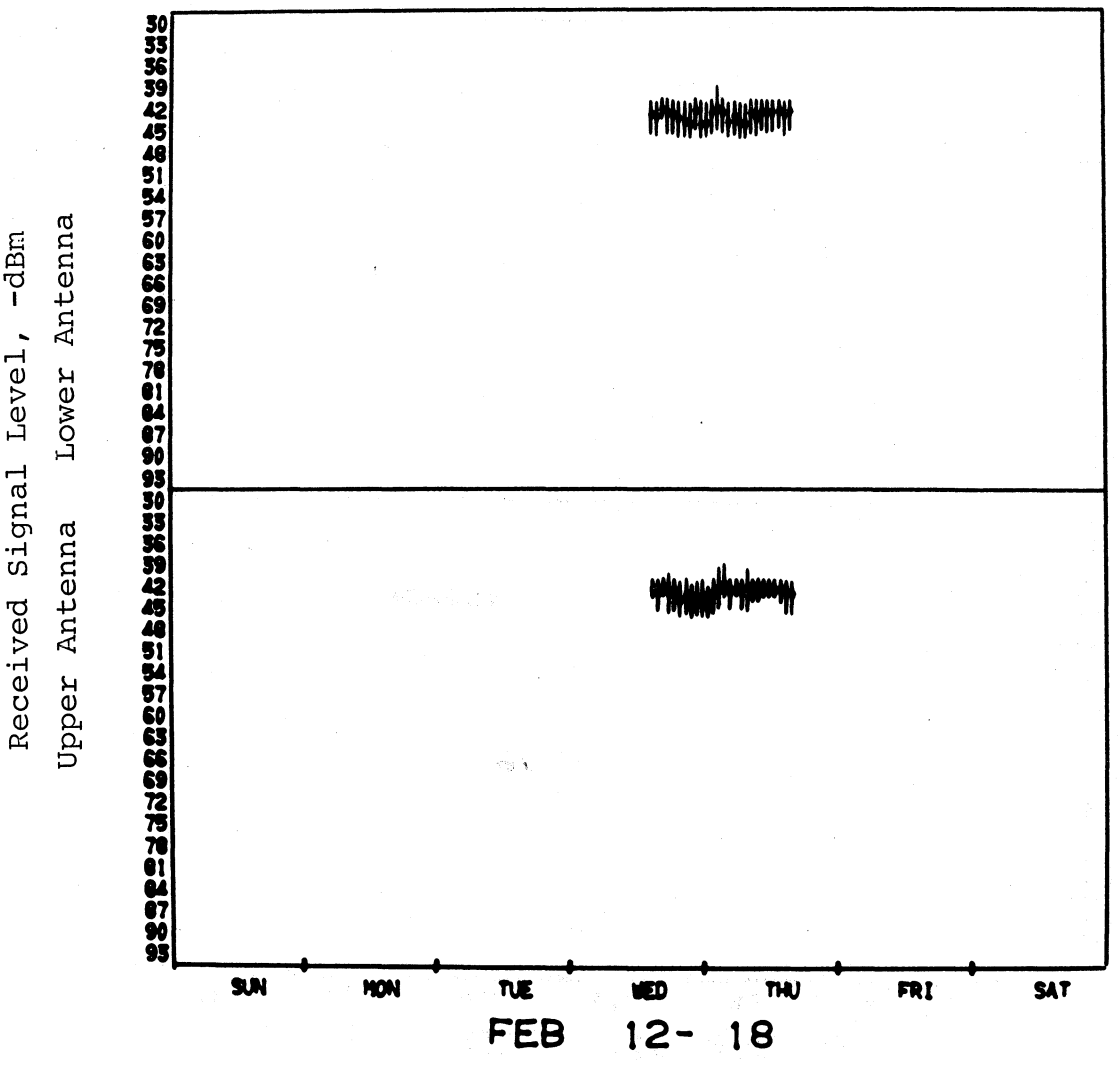

Figure A-18. Hourly histogram data, 1978.

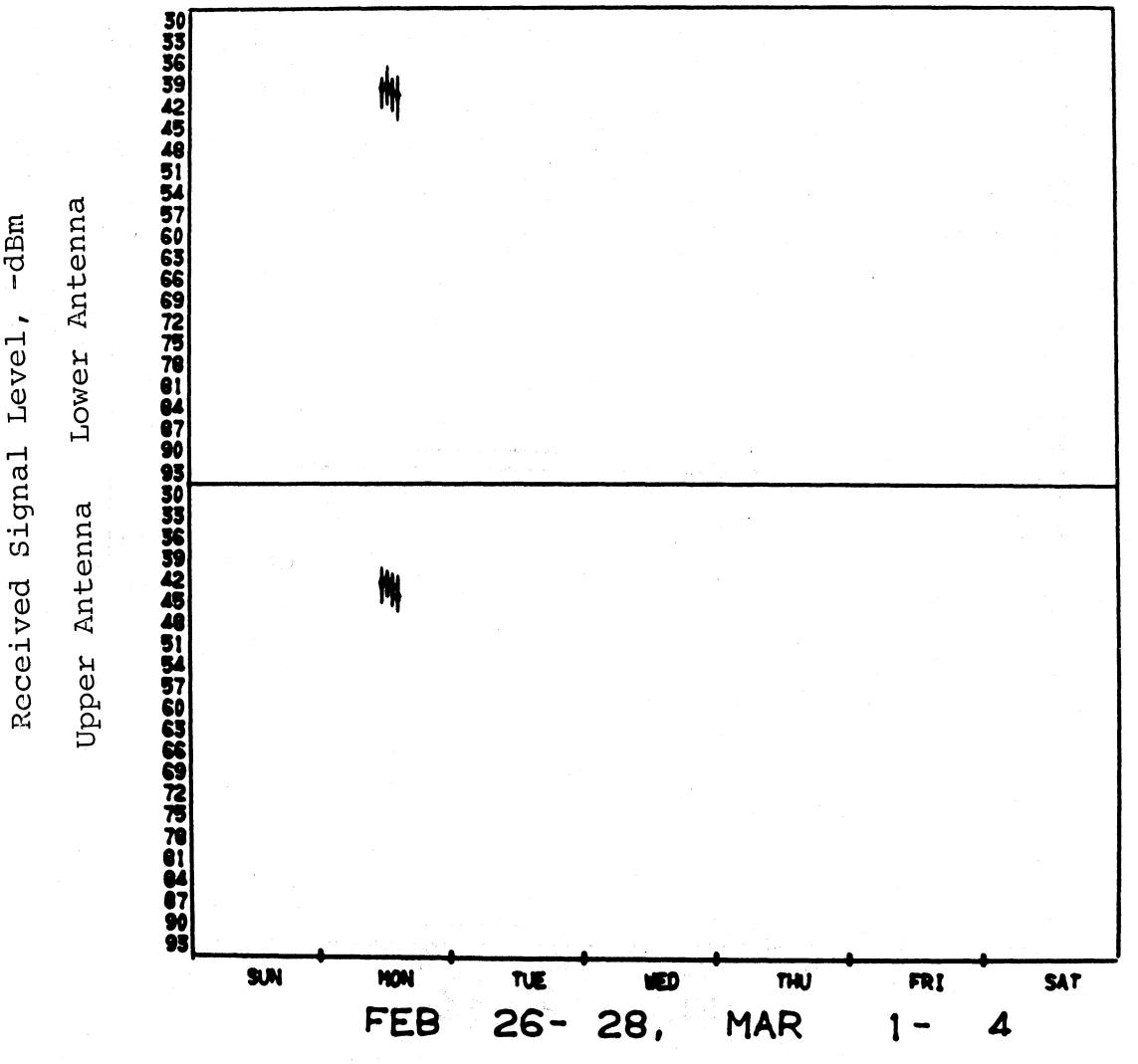

Figure A-19. Hourly histogram data, 1978.

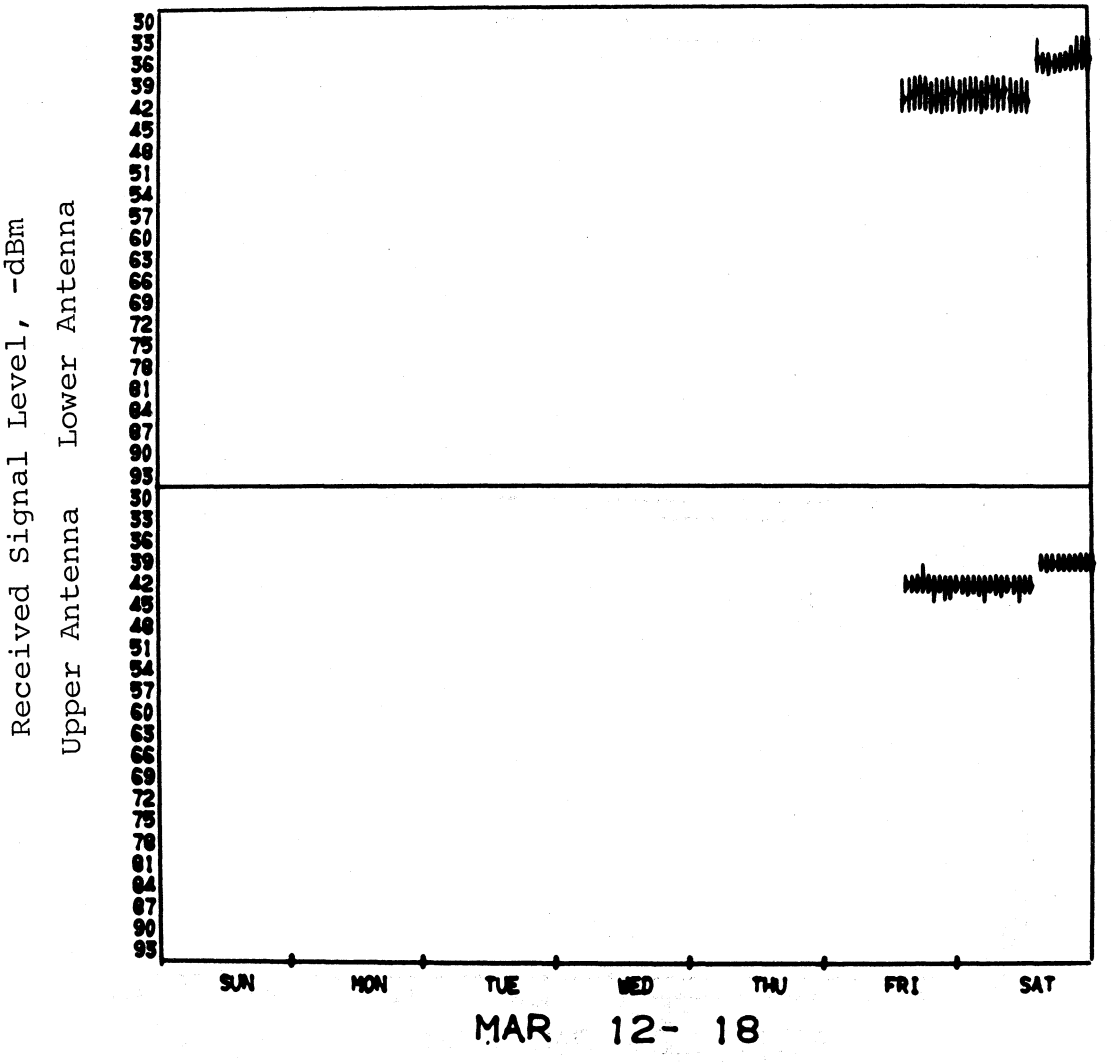

Figure A-20. Hourly histogram data, 1978.

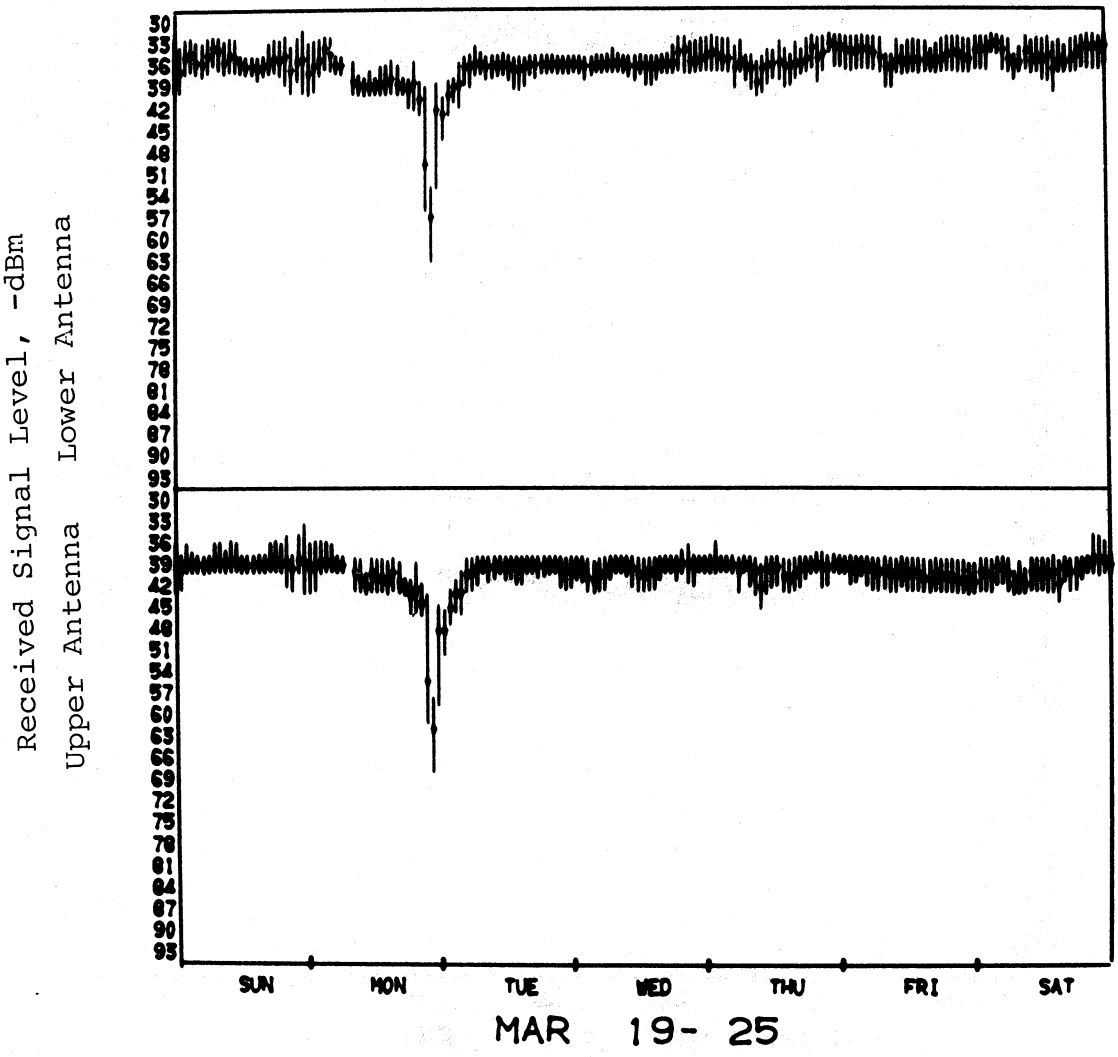

Figure A-21. Hourly histogram data, 1978.

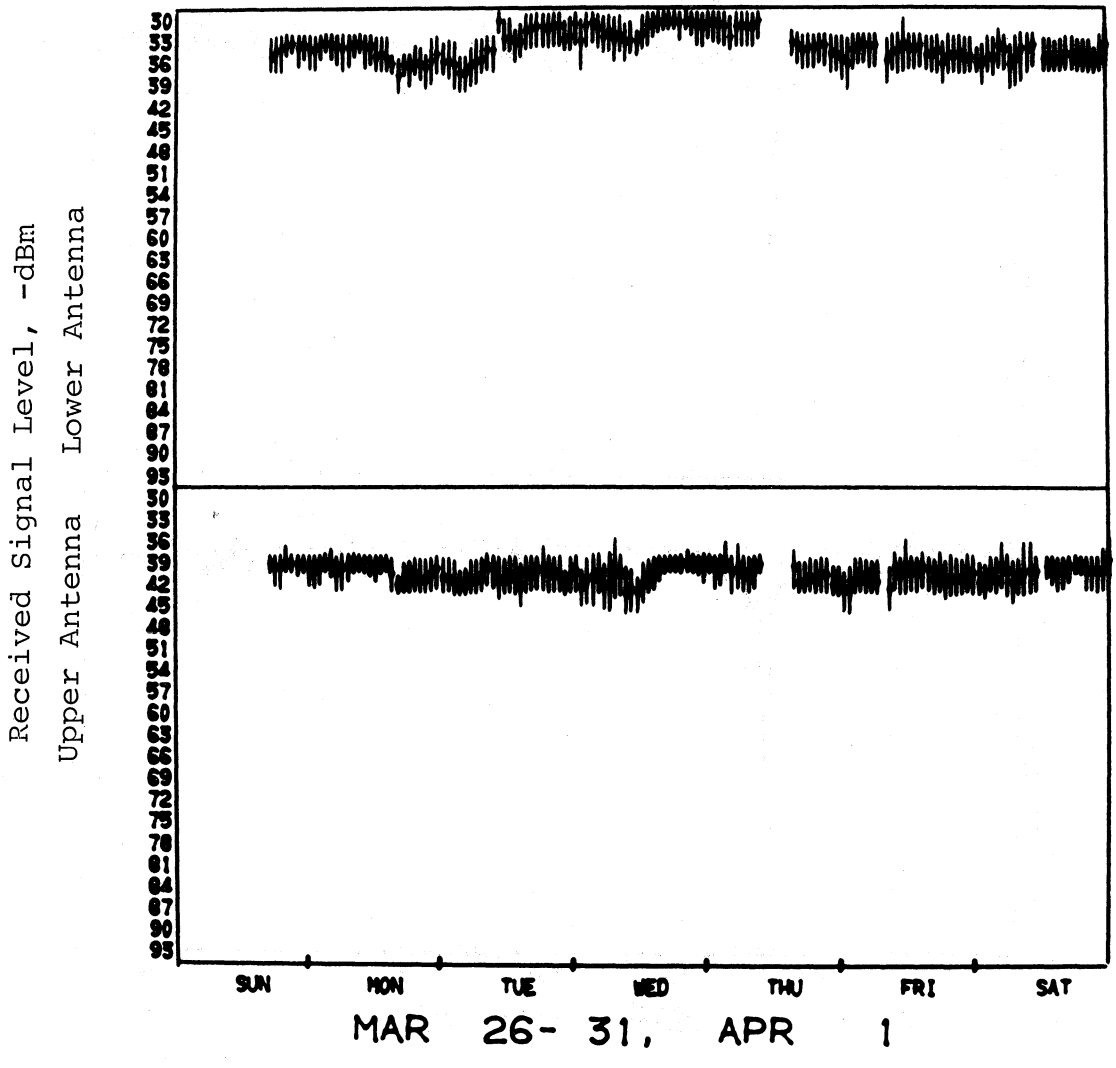

Figure A-22. Hourly histogram data, 1978.

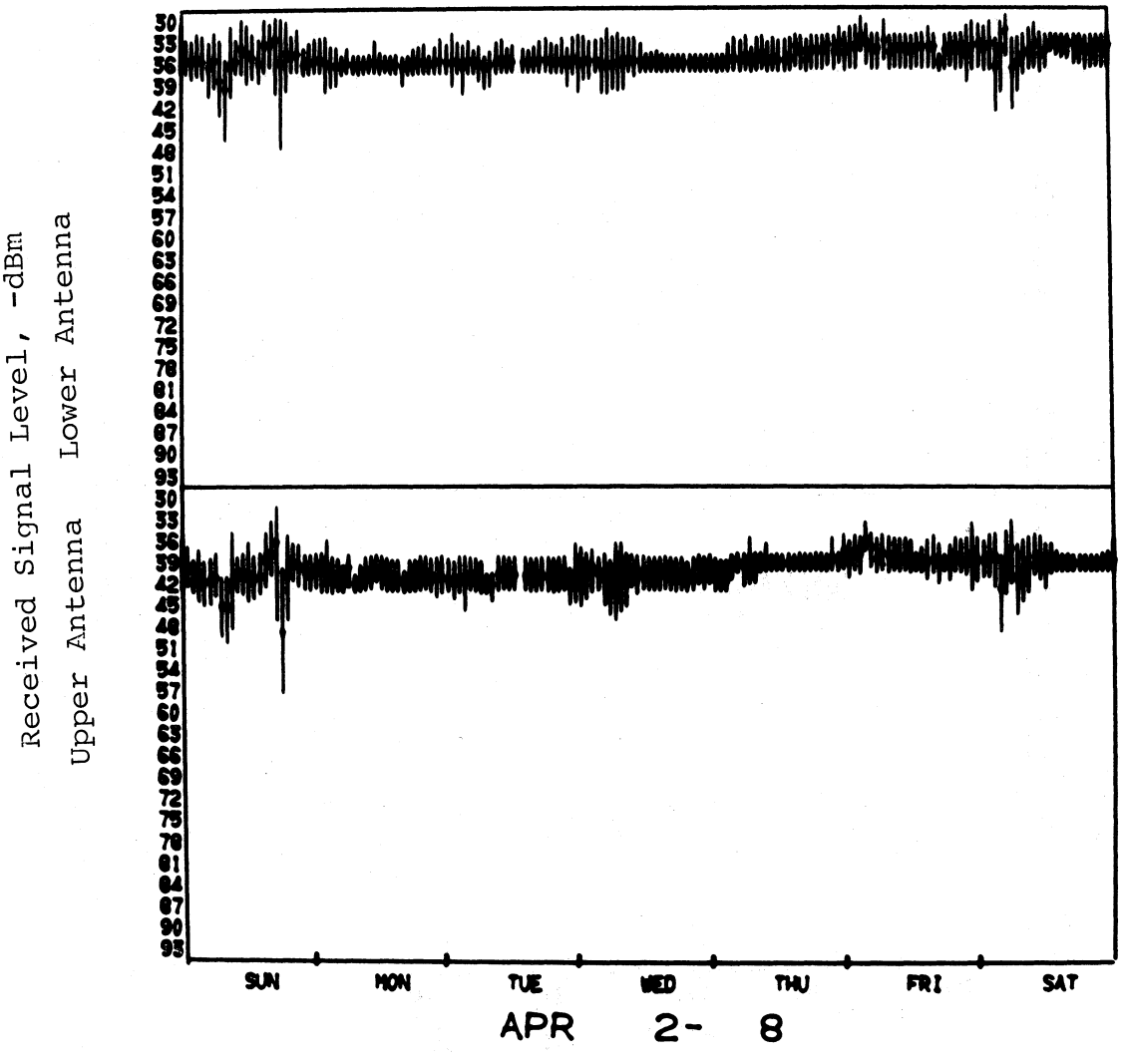

Figure A-23. Hourly histogram data, 1978.

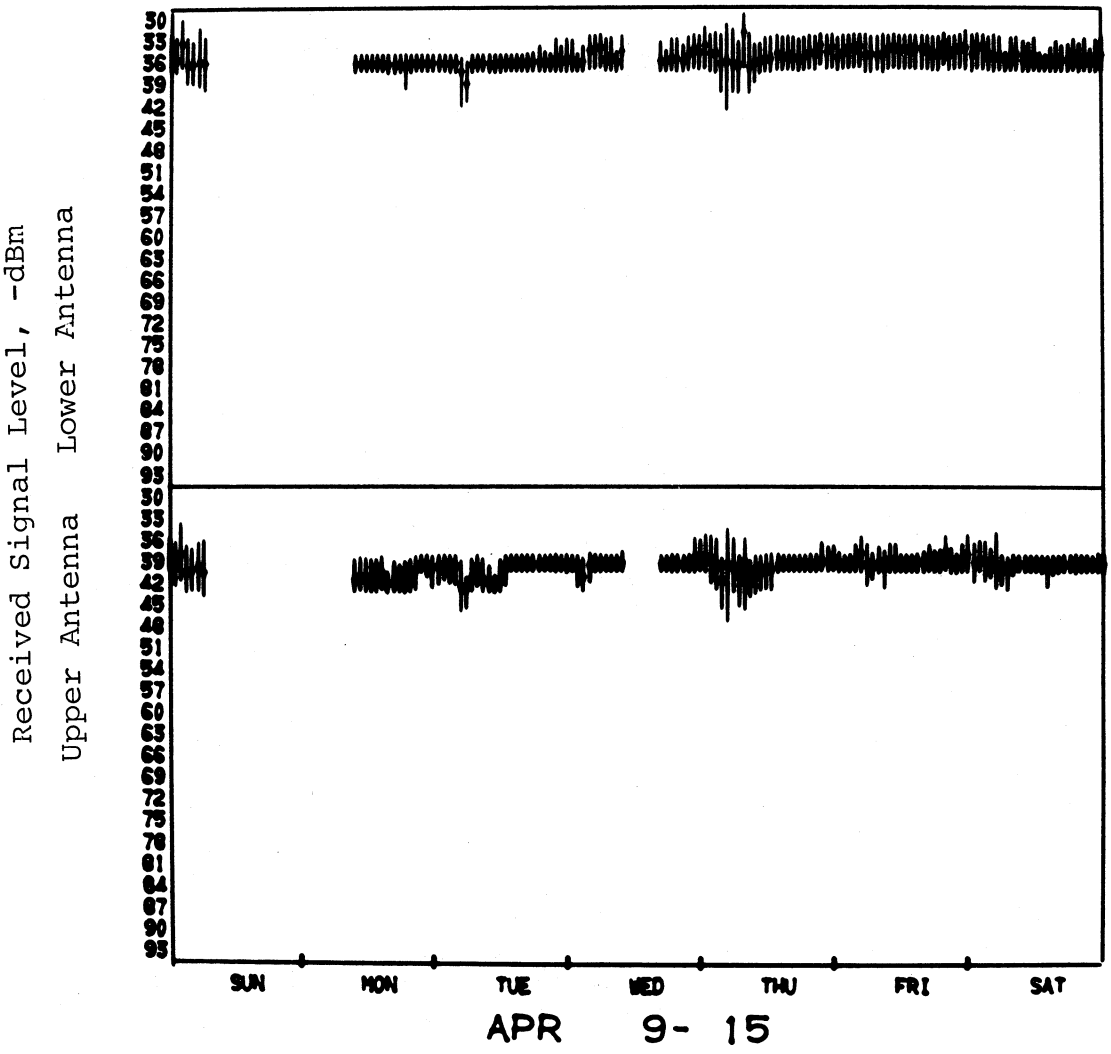

Figure A-24. Hourly histogram data, 1978.

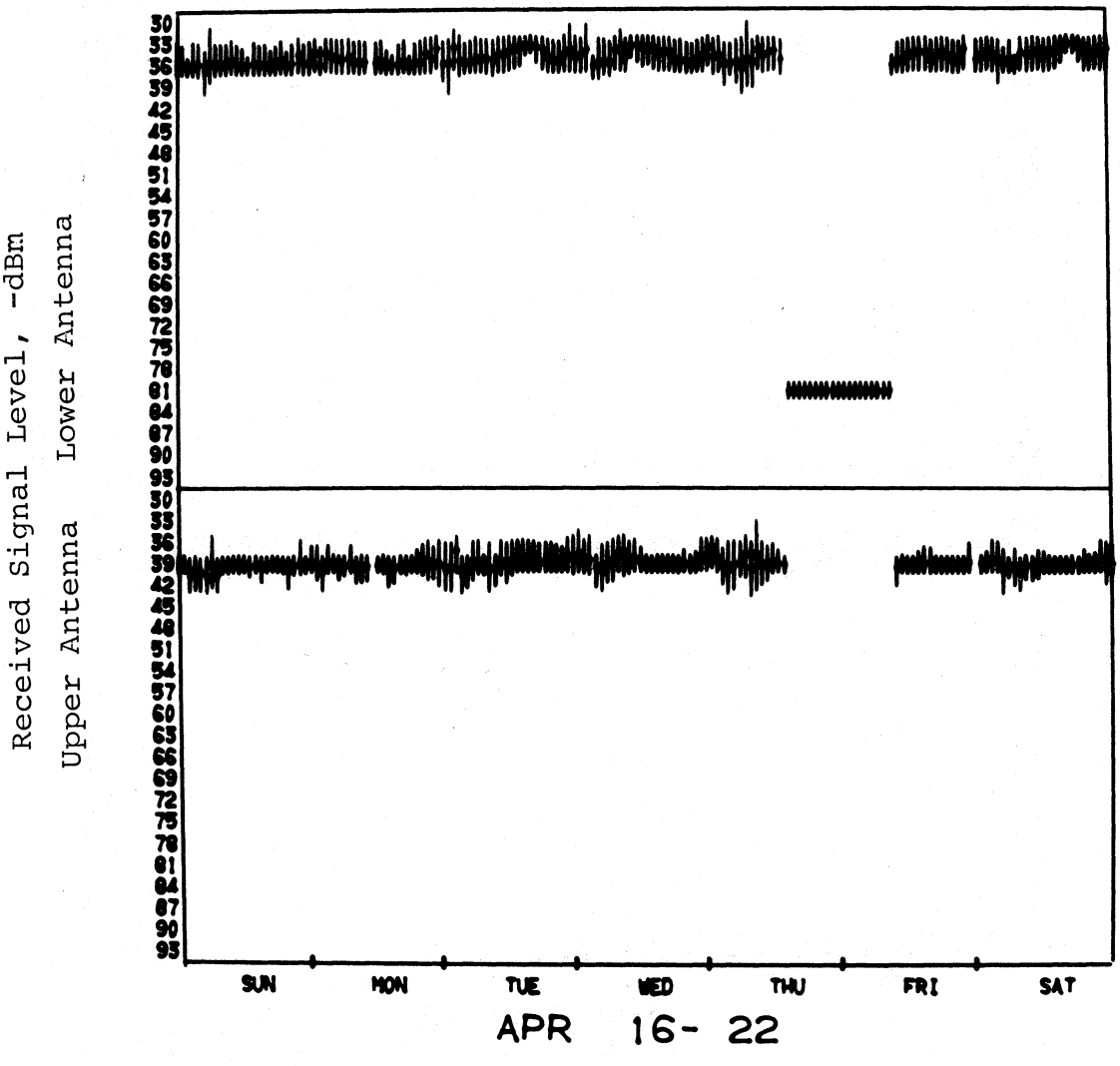

Figure A-25. Hourly histogram data, 1978.

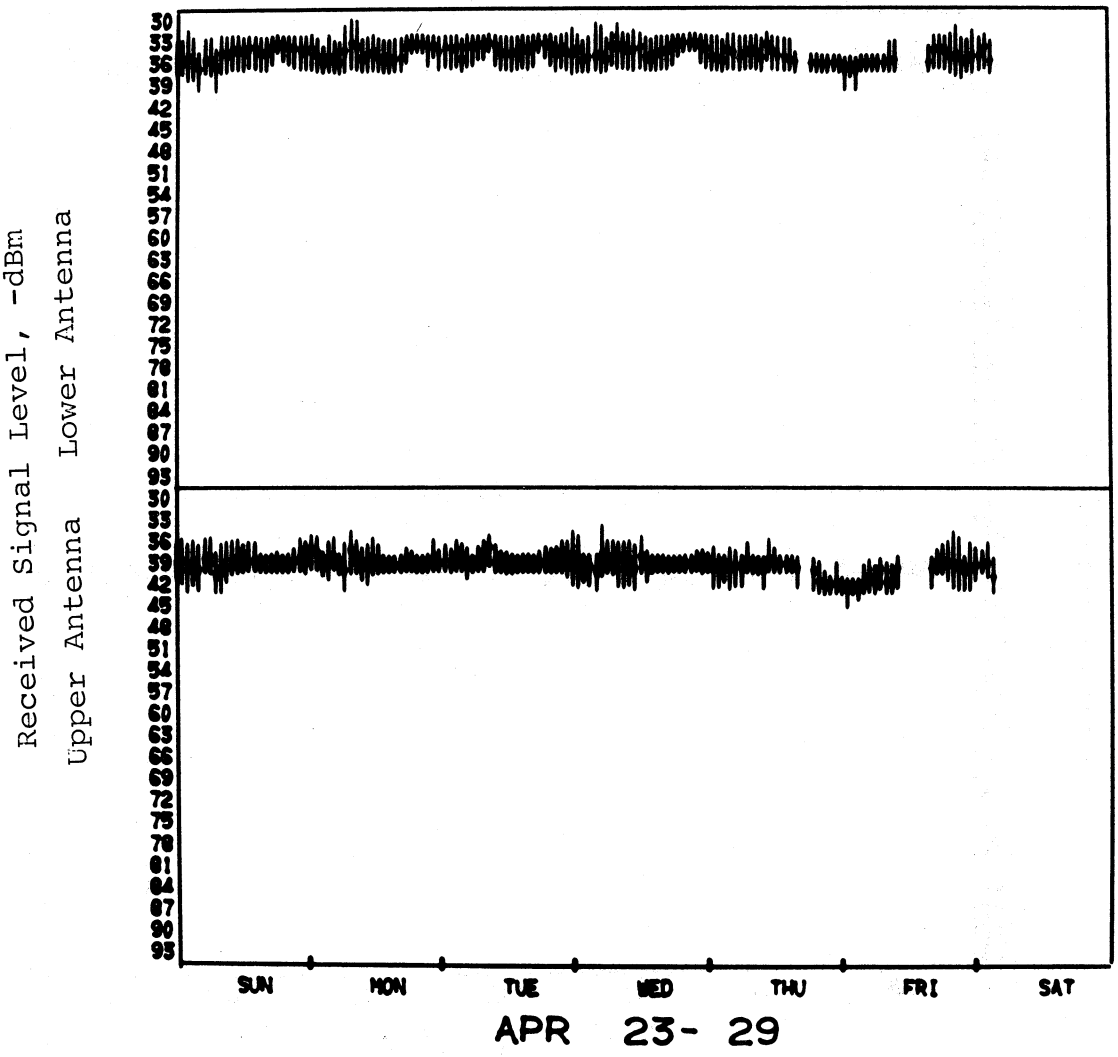

Figure A-26. Hourly histogram data, 1978.

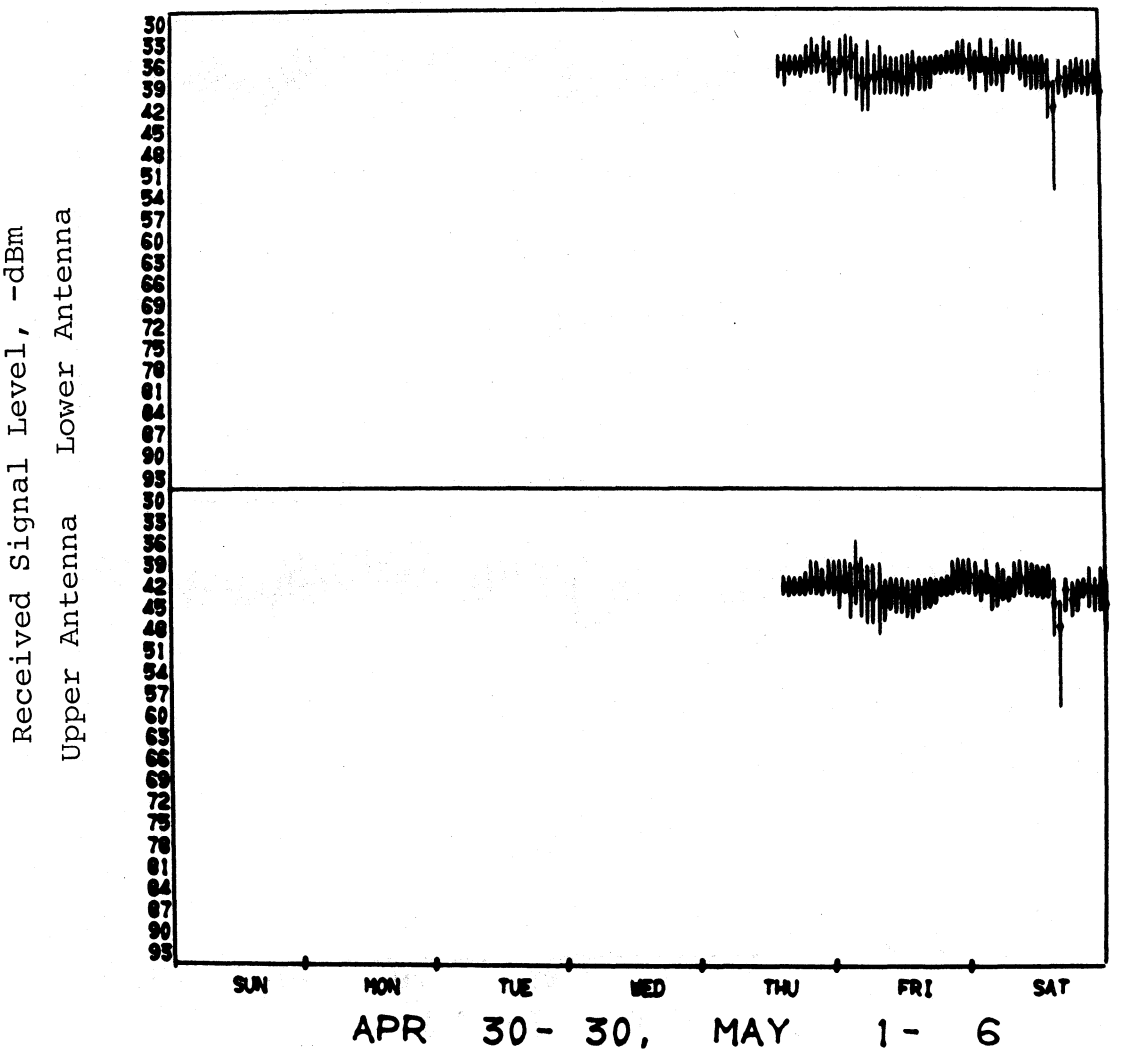

Figure A-27. Hourly histogram data, 1978.

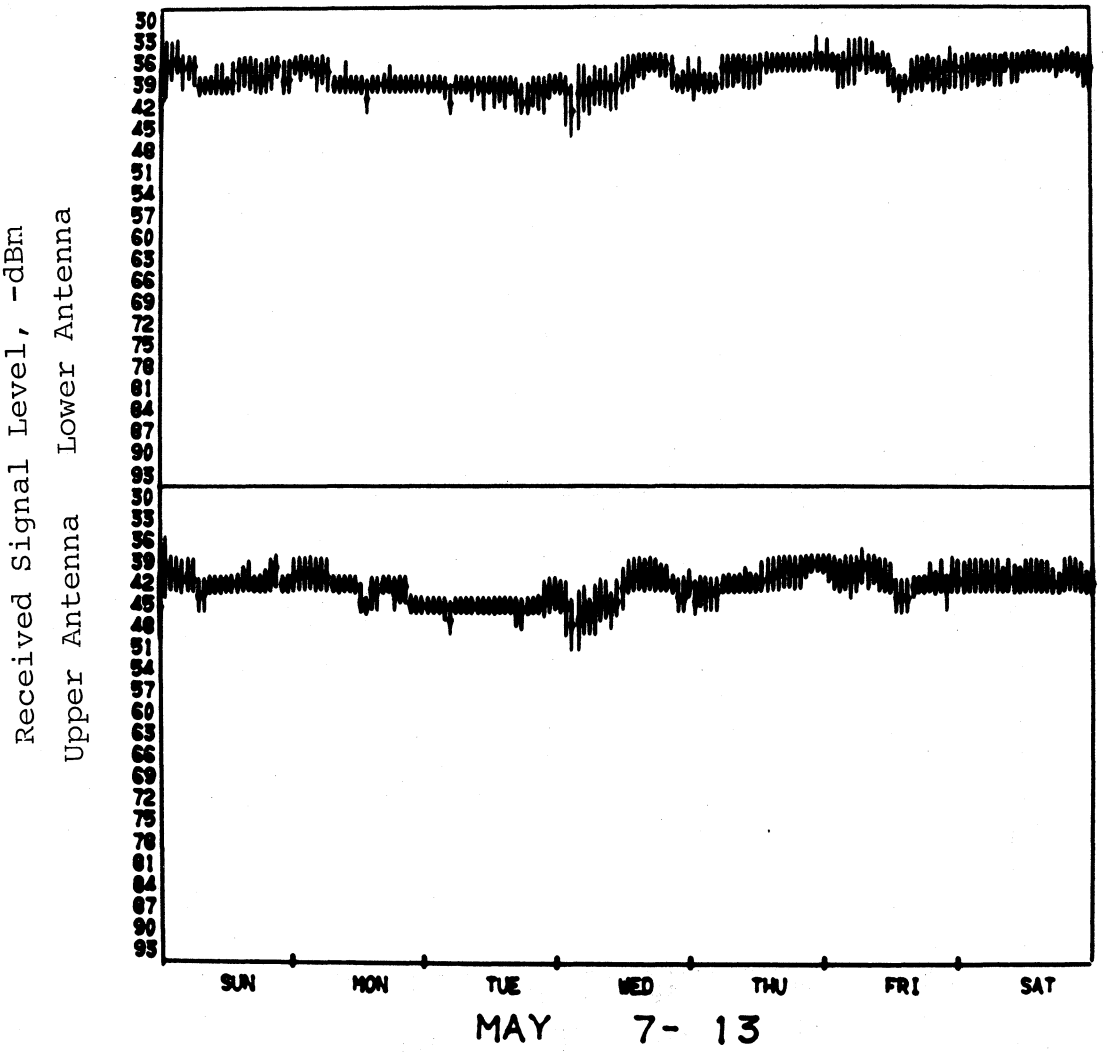

Figure A-28. Hourly histogram data, 1978.

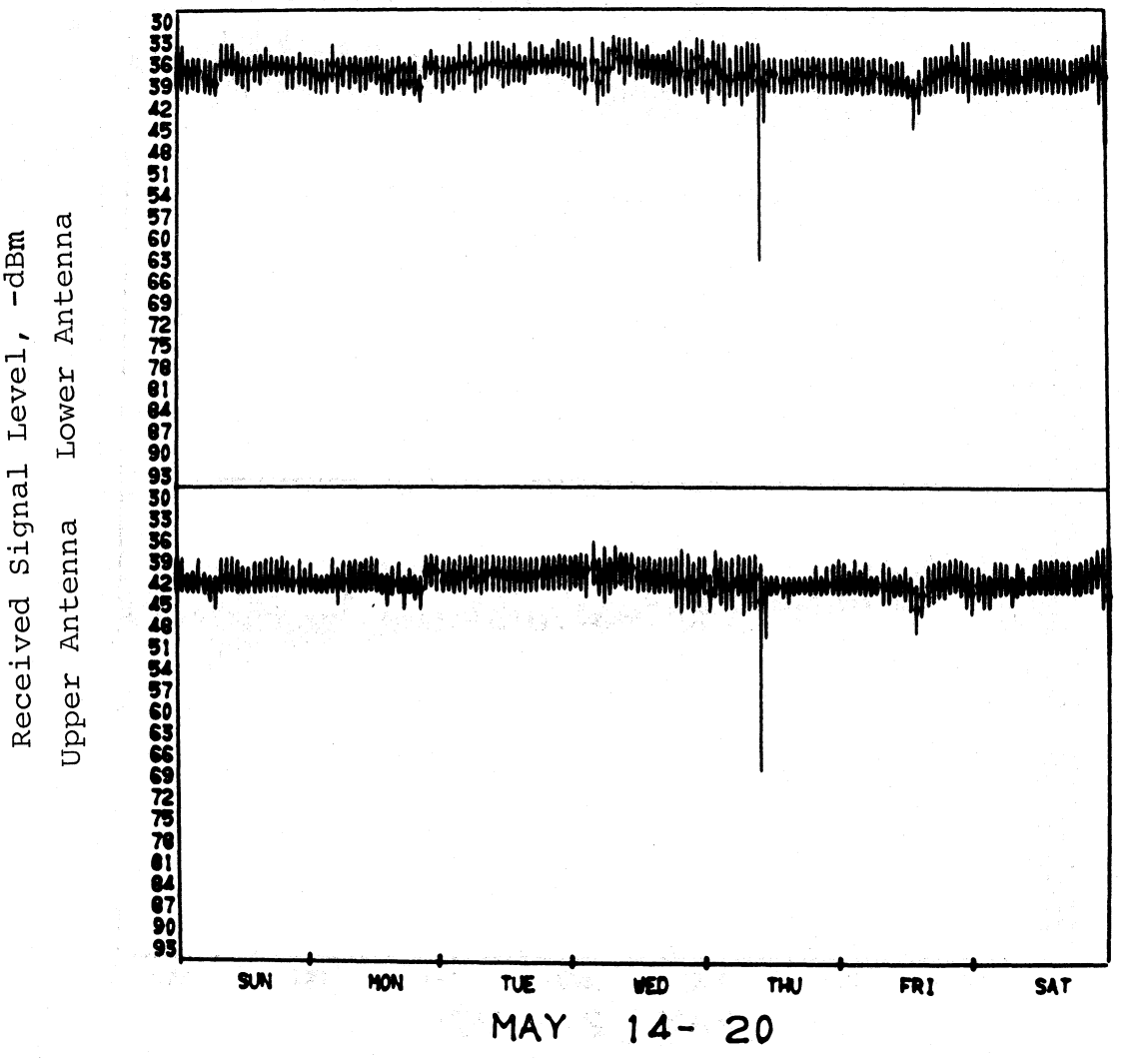

Figure A-29. Hourly histogram data, 1978.

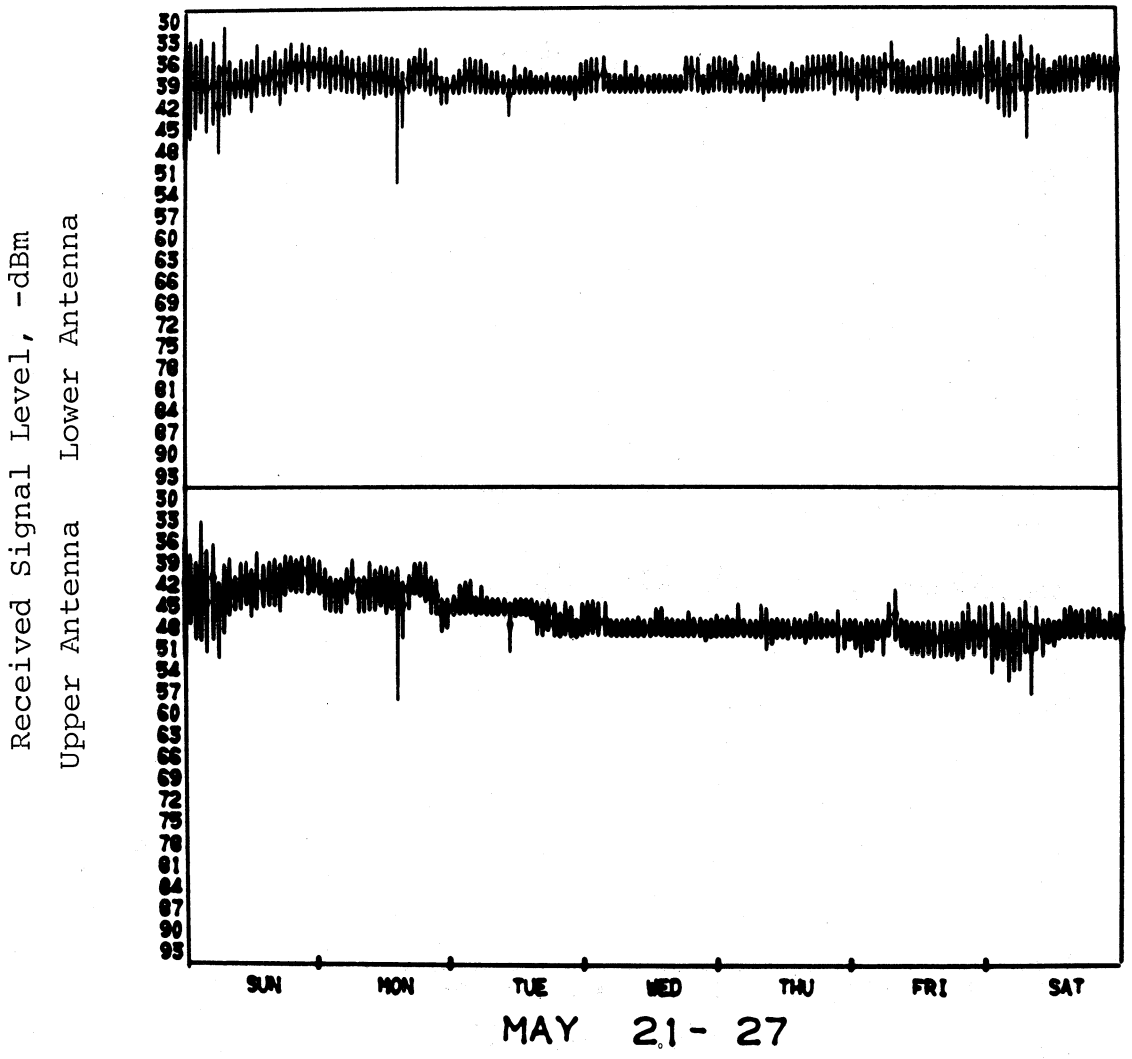

Figure A-30. Hourly histogram data, 1978.

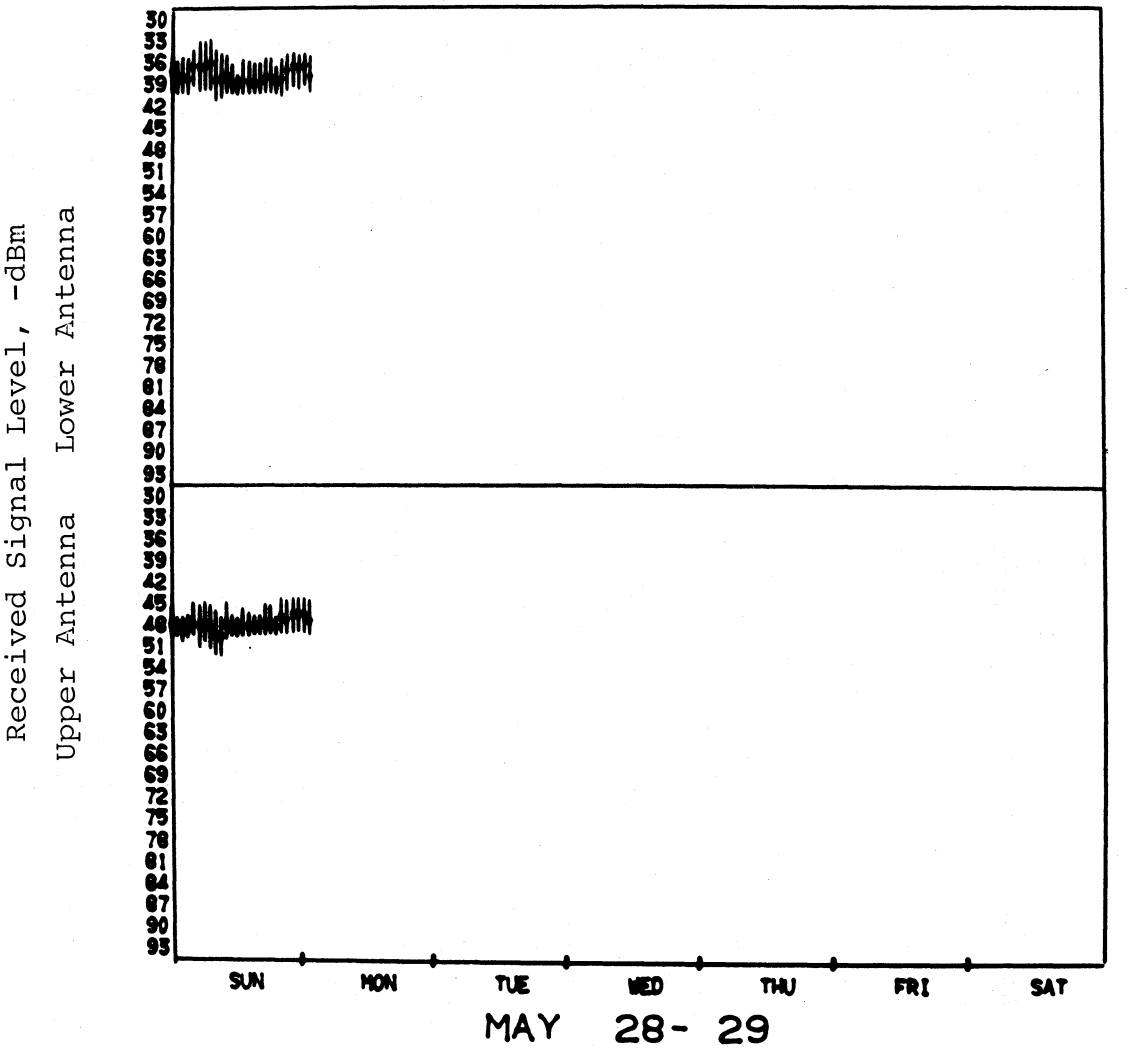

Figure A-31. Hourly histogram data, 1978.

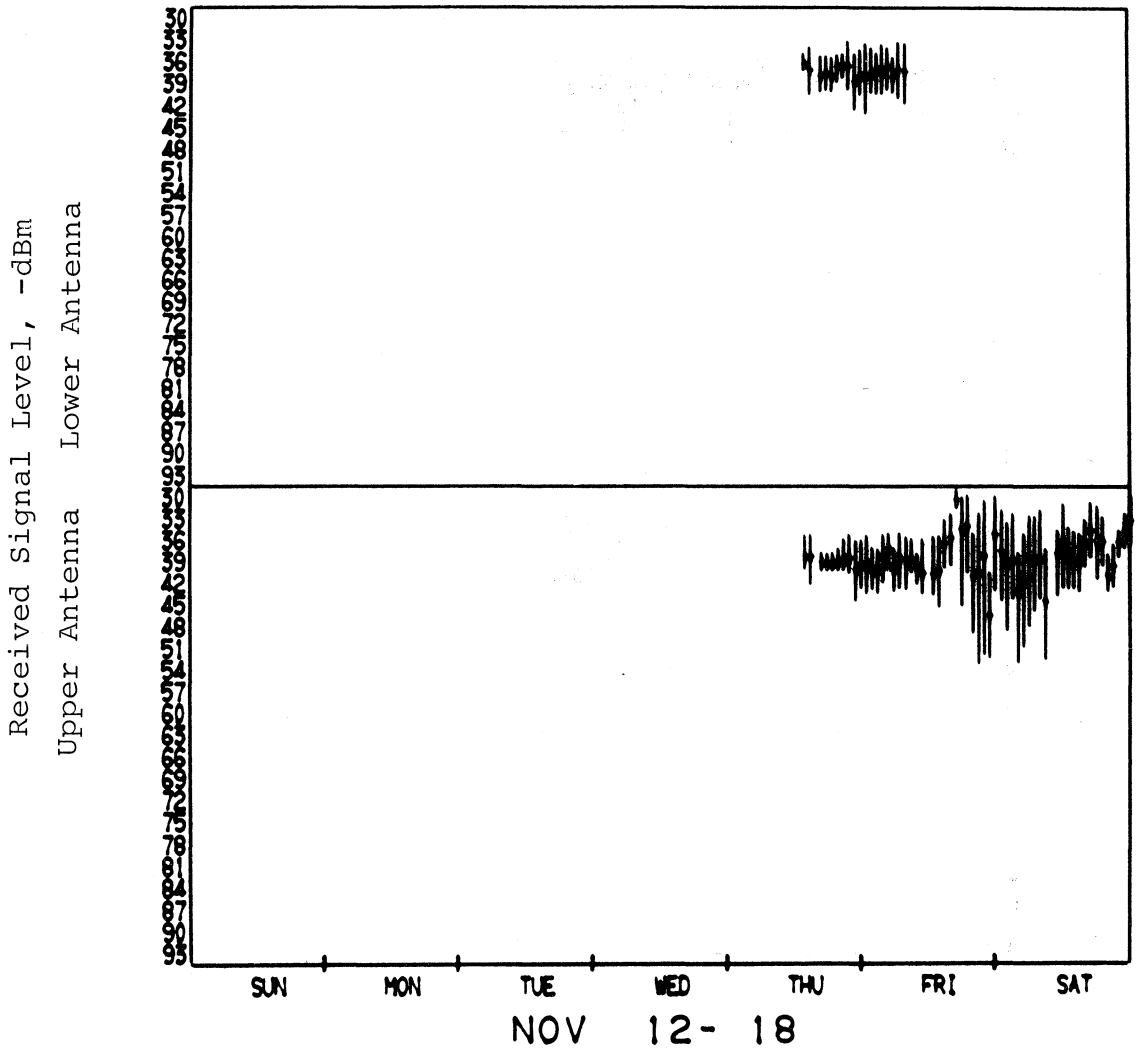

Figure A-32. Hourly histogram data, 1978.

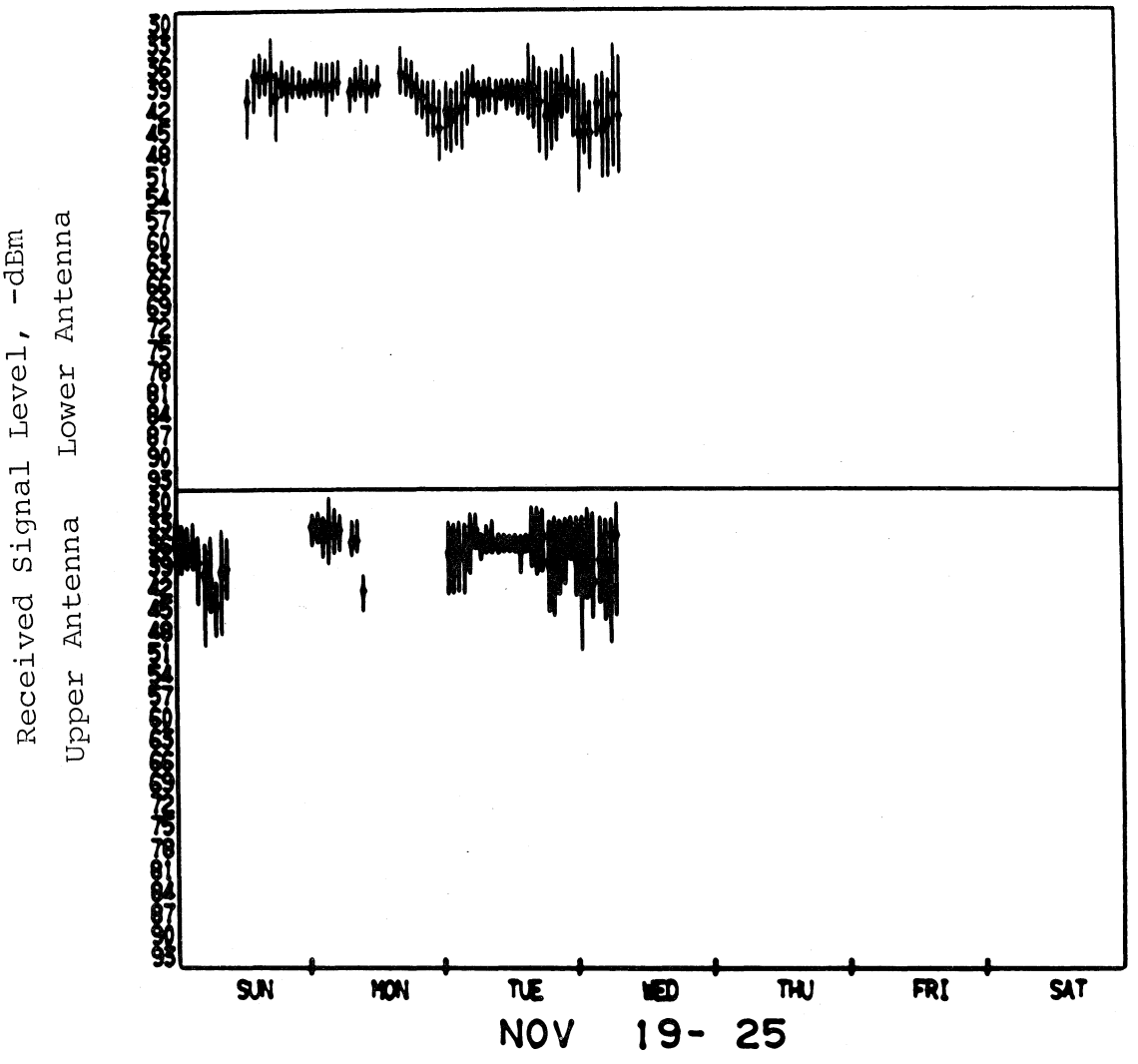

Figure A-33. Hourly histogram data, 1978.

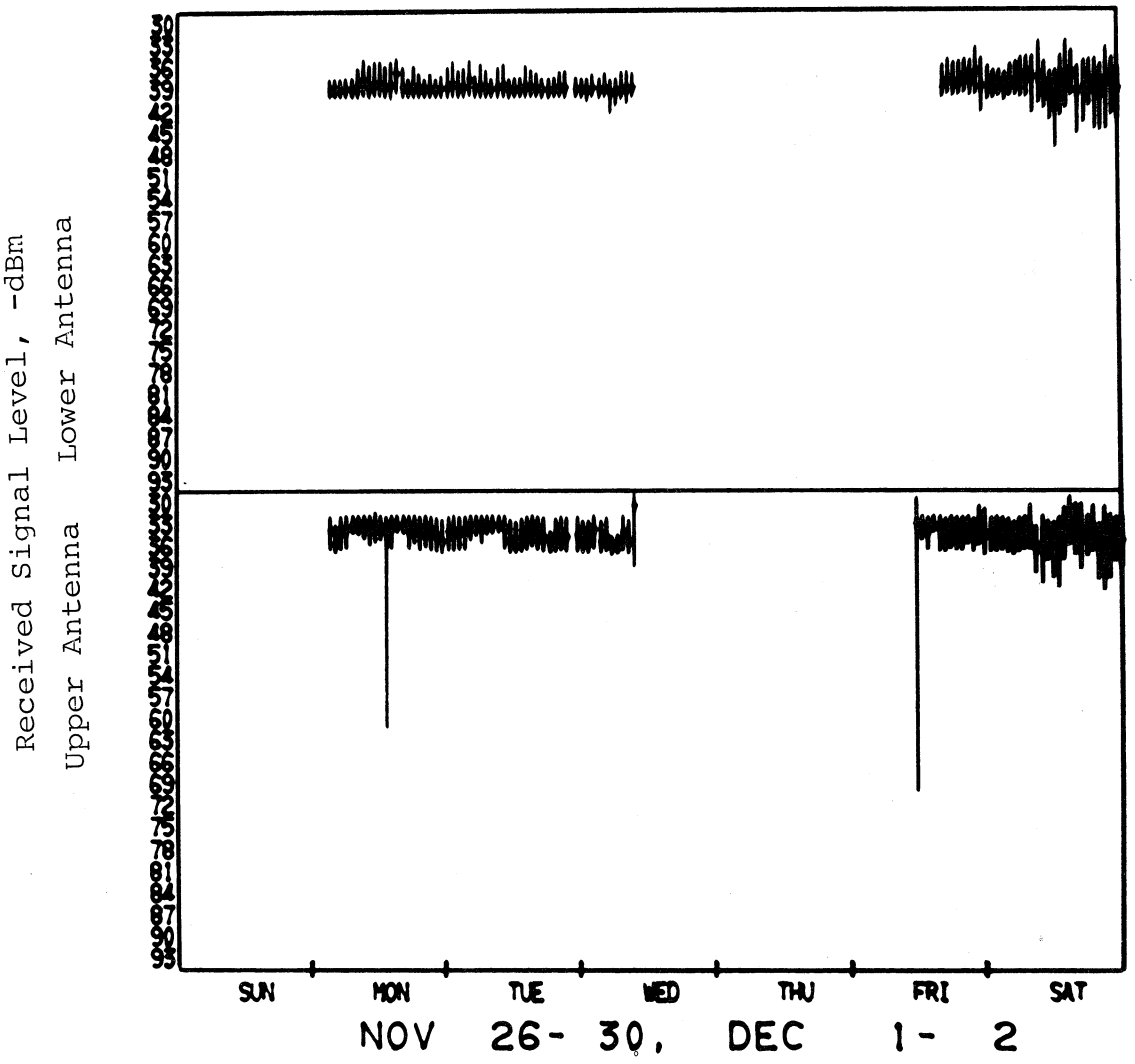

Figure A-34. Hourly histogram data, 1978.

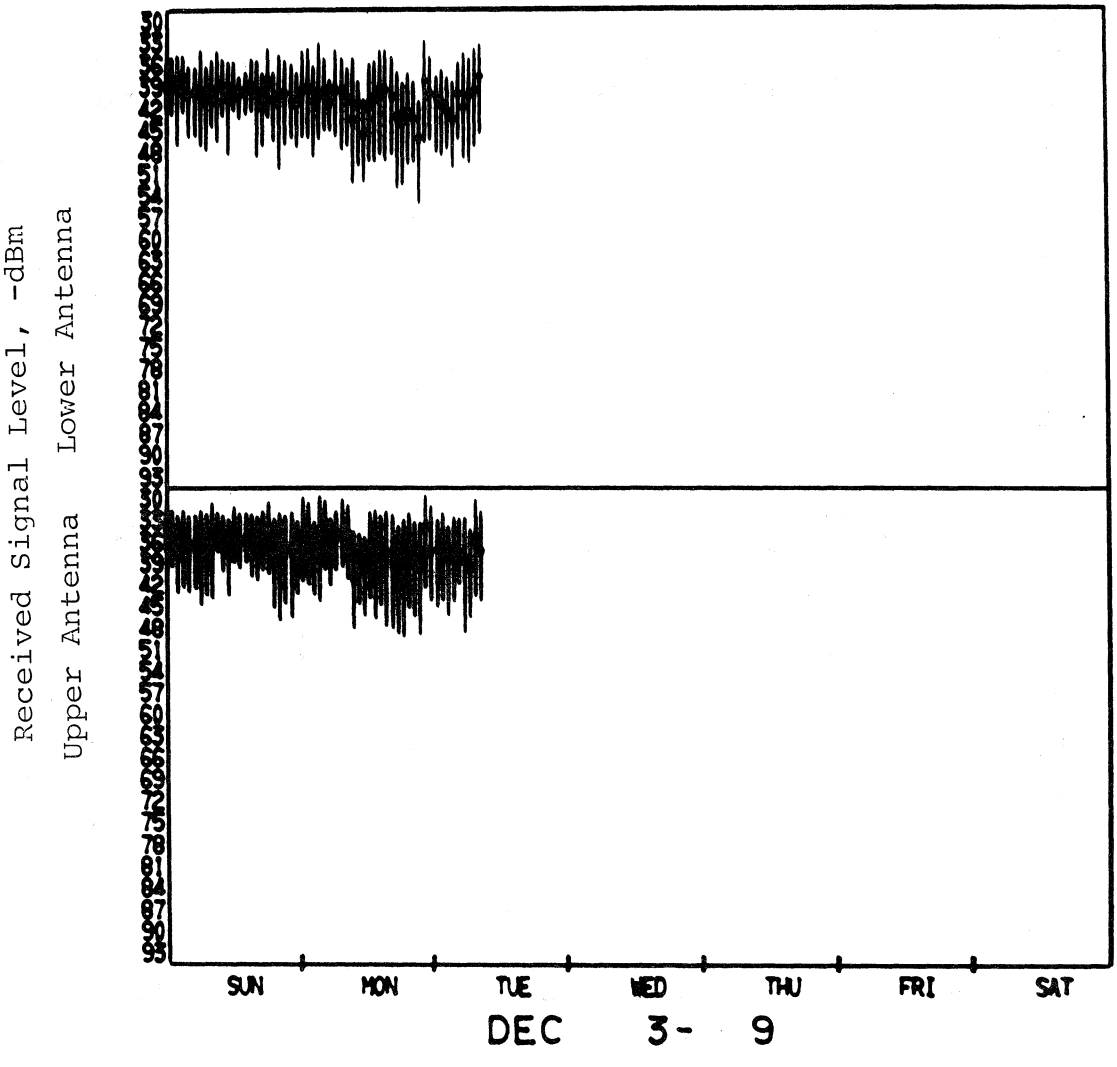

Figure A-35. Hourly histogram data, 1978.

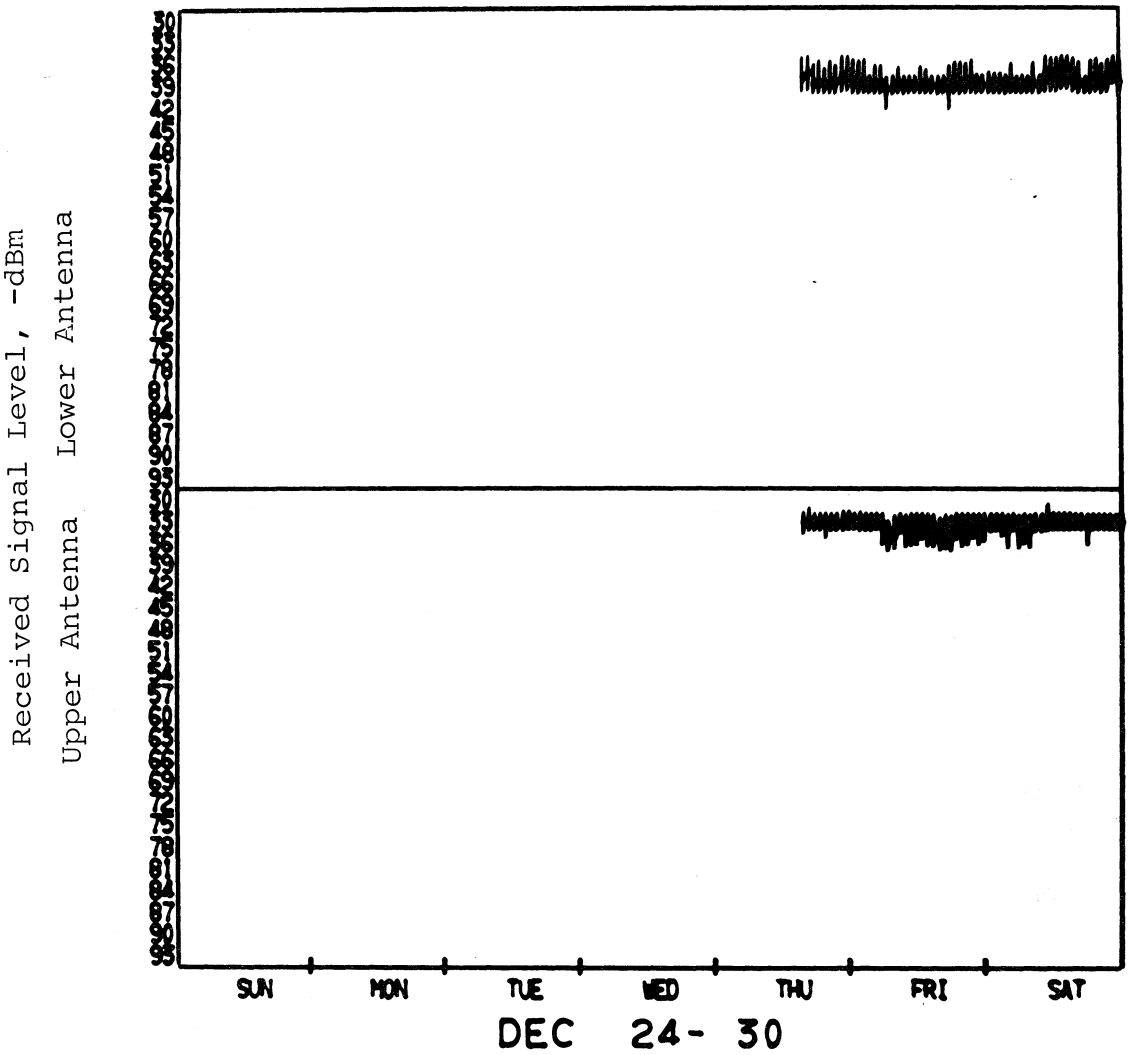

Figure A-36. Hourly histogram data, 1978.

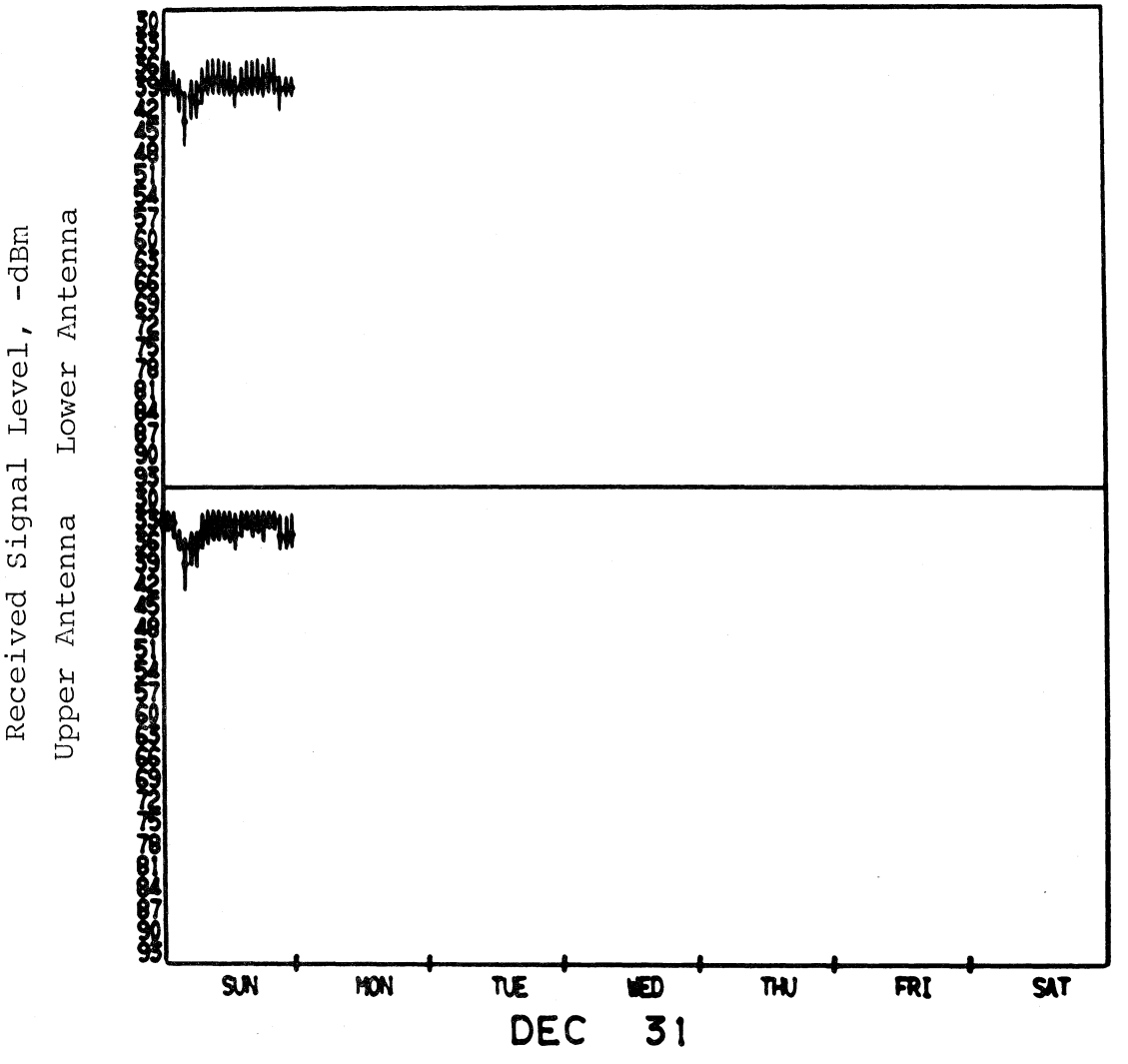

Figure A-37. Hourly histogram data, 1978.

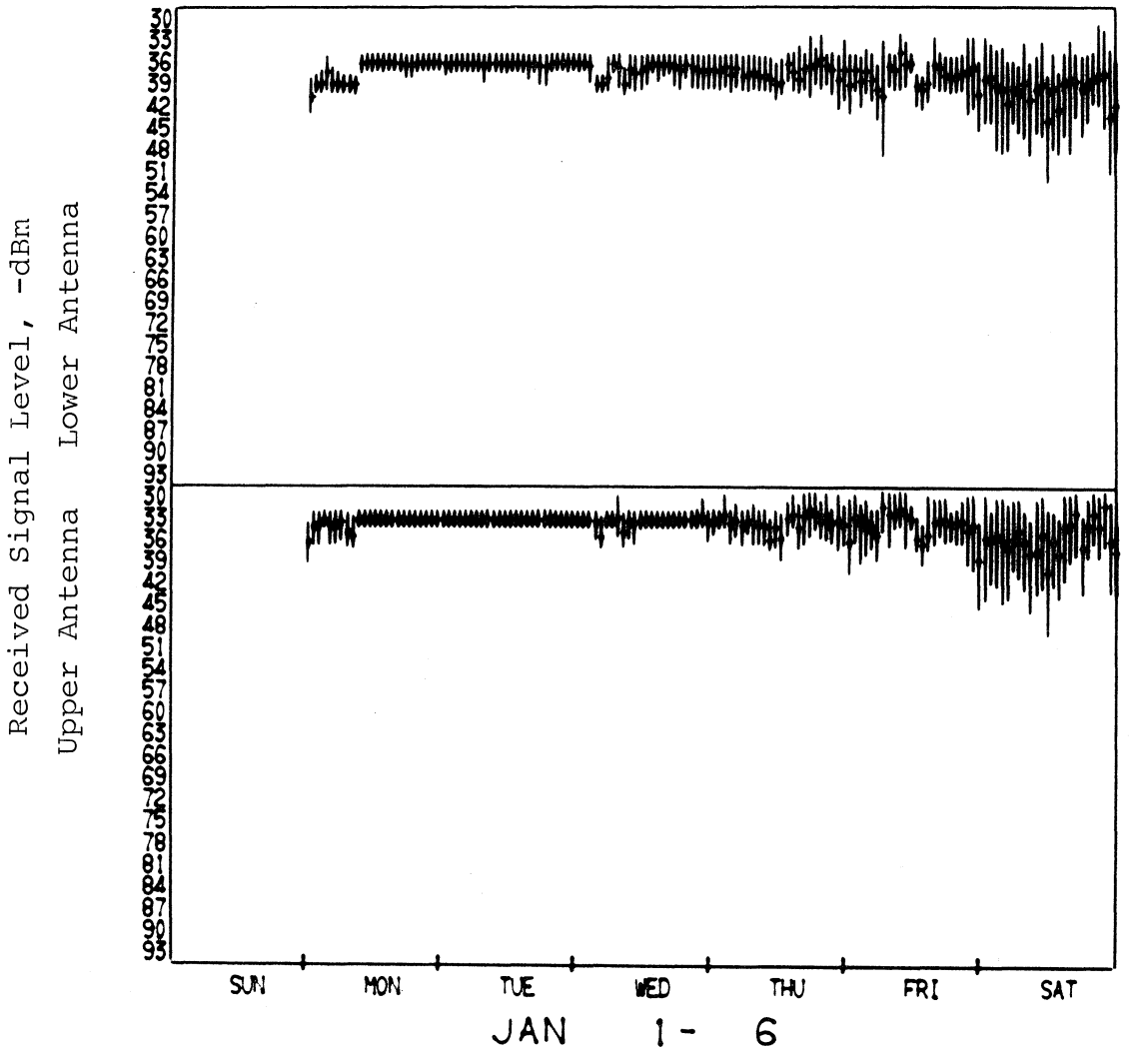

Figure A-38. Hourly histogram data, 1979.

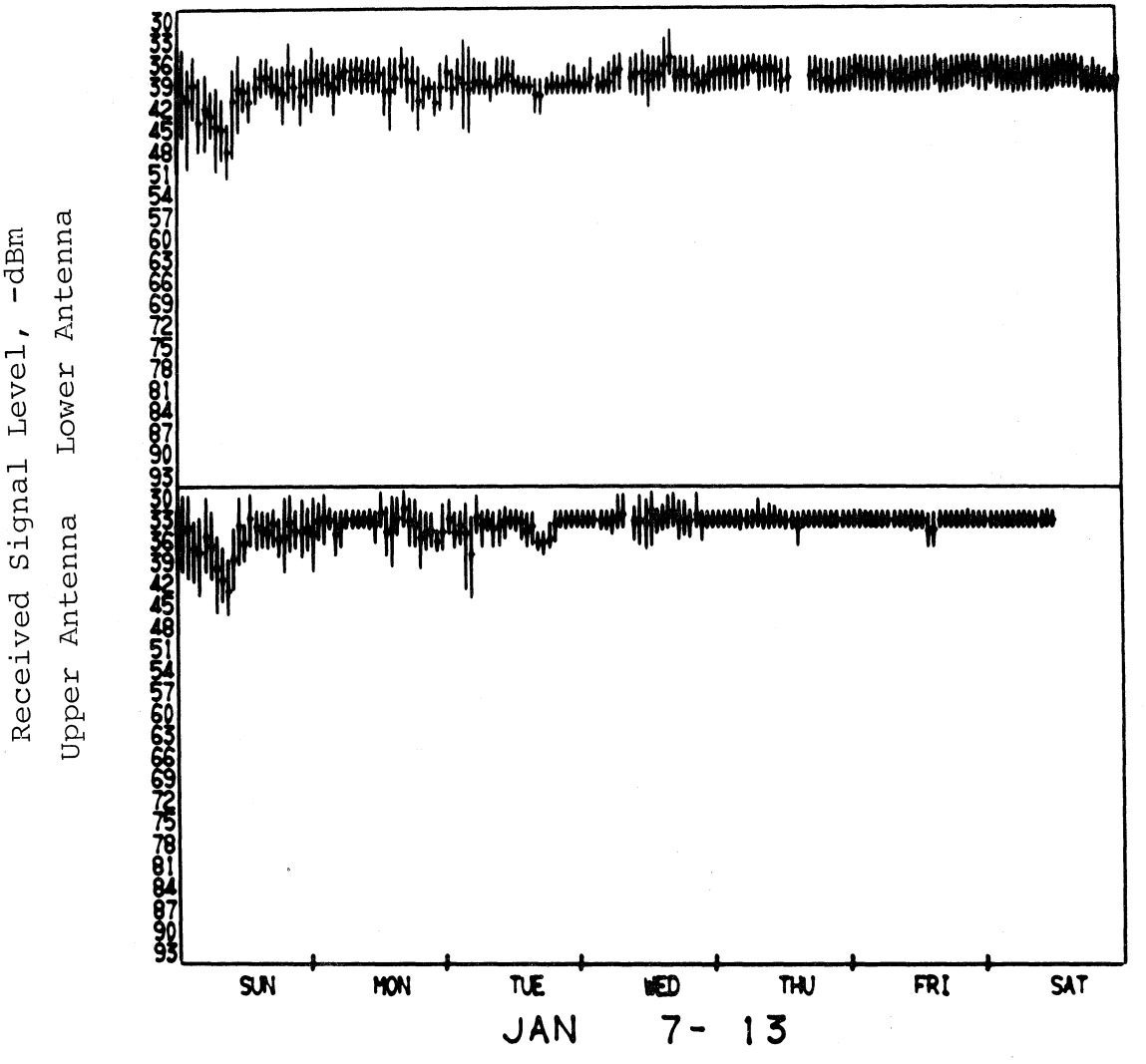

Figure A-39. Hourly histogram data, 1979.

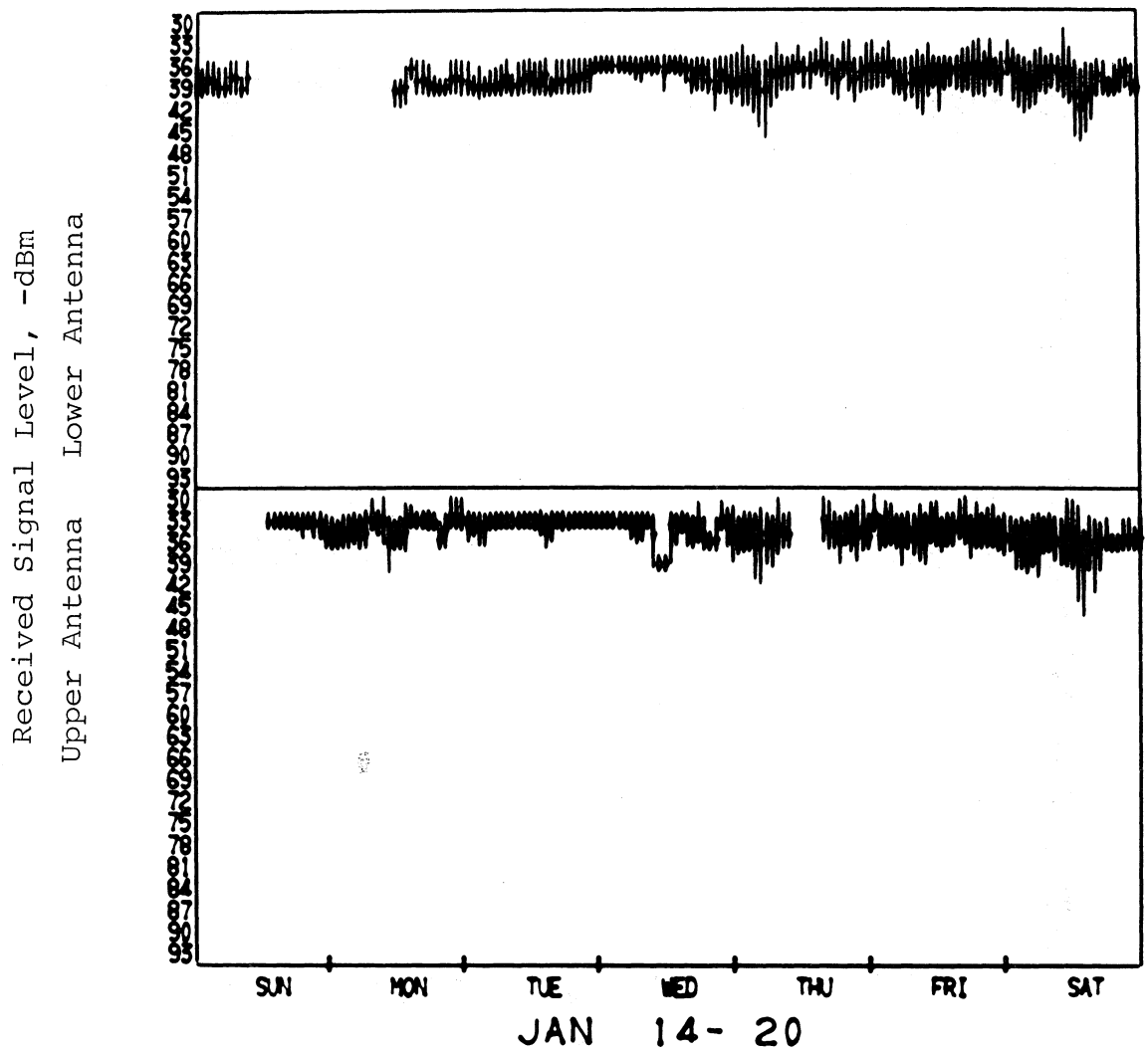

Figure A-40. Hourly histogram data, 1979.

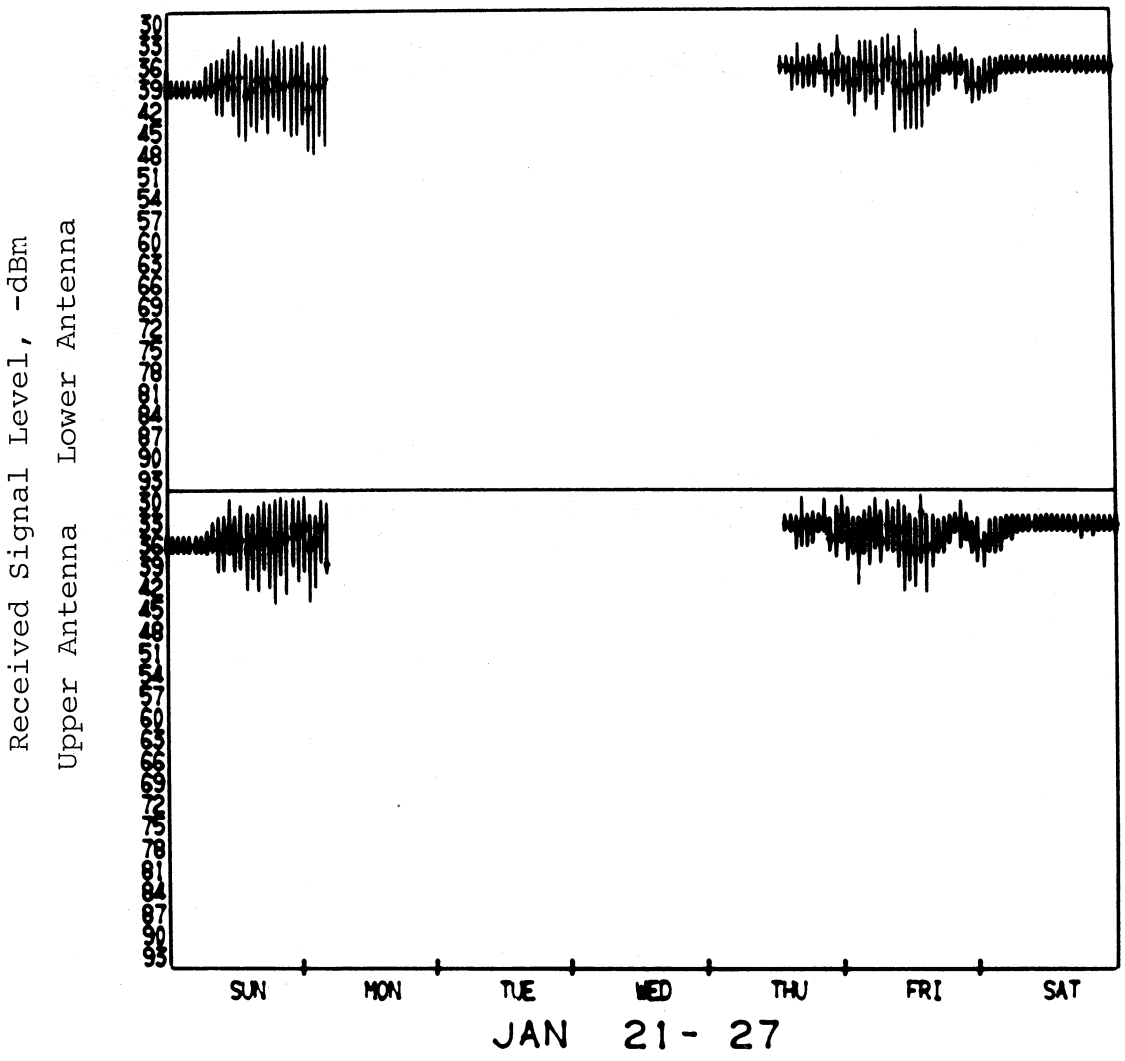

Figure A-41. Hourly histogram data, 1979.

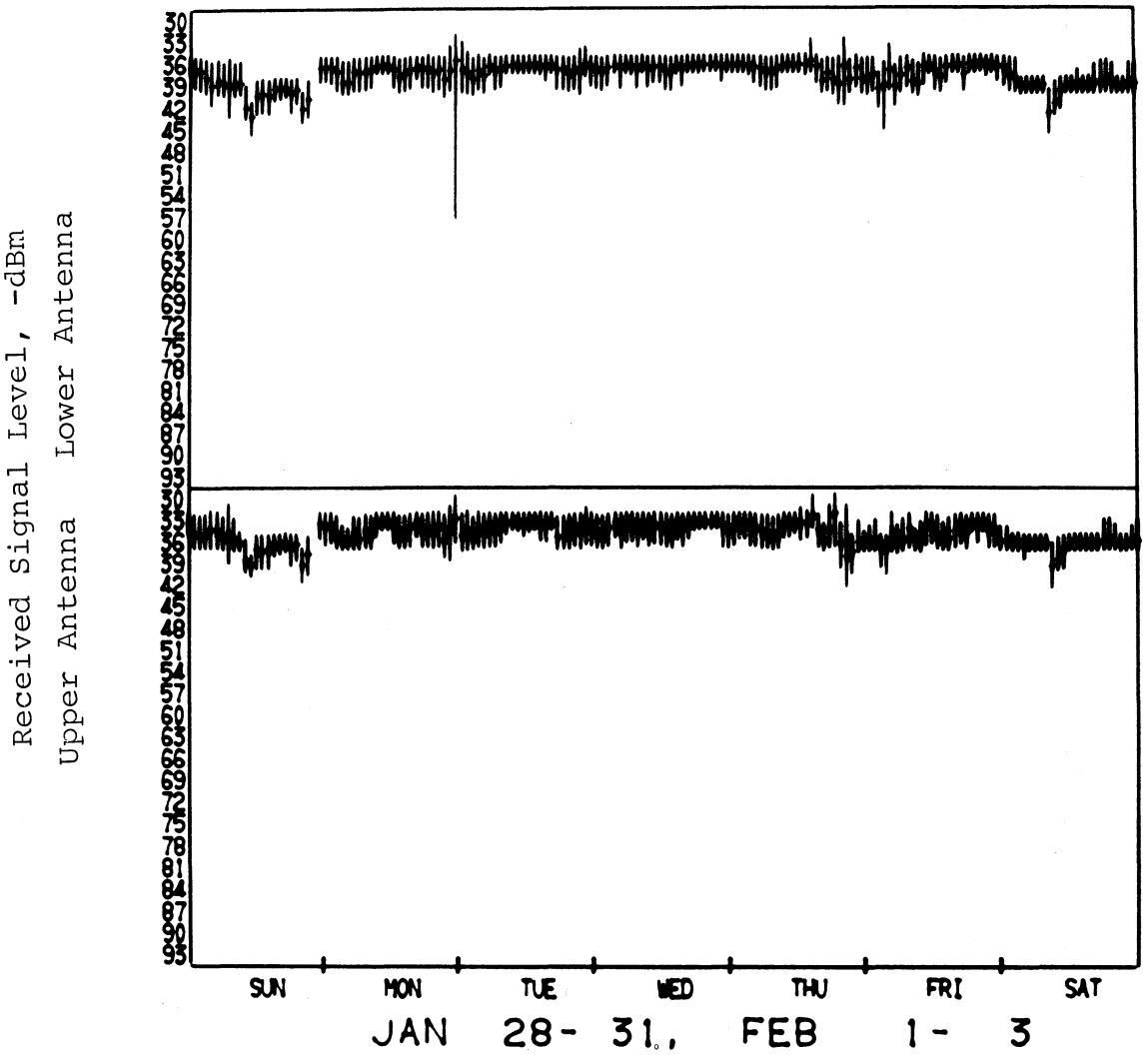

Figure A-42. Hourly histogram data, 1979.

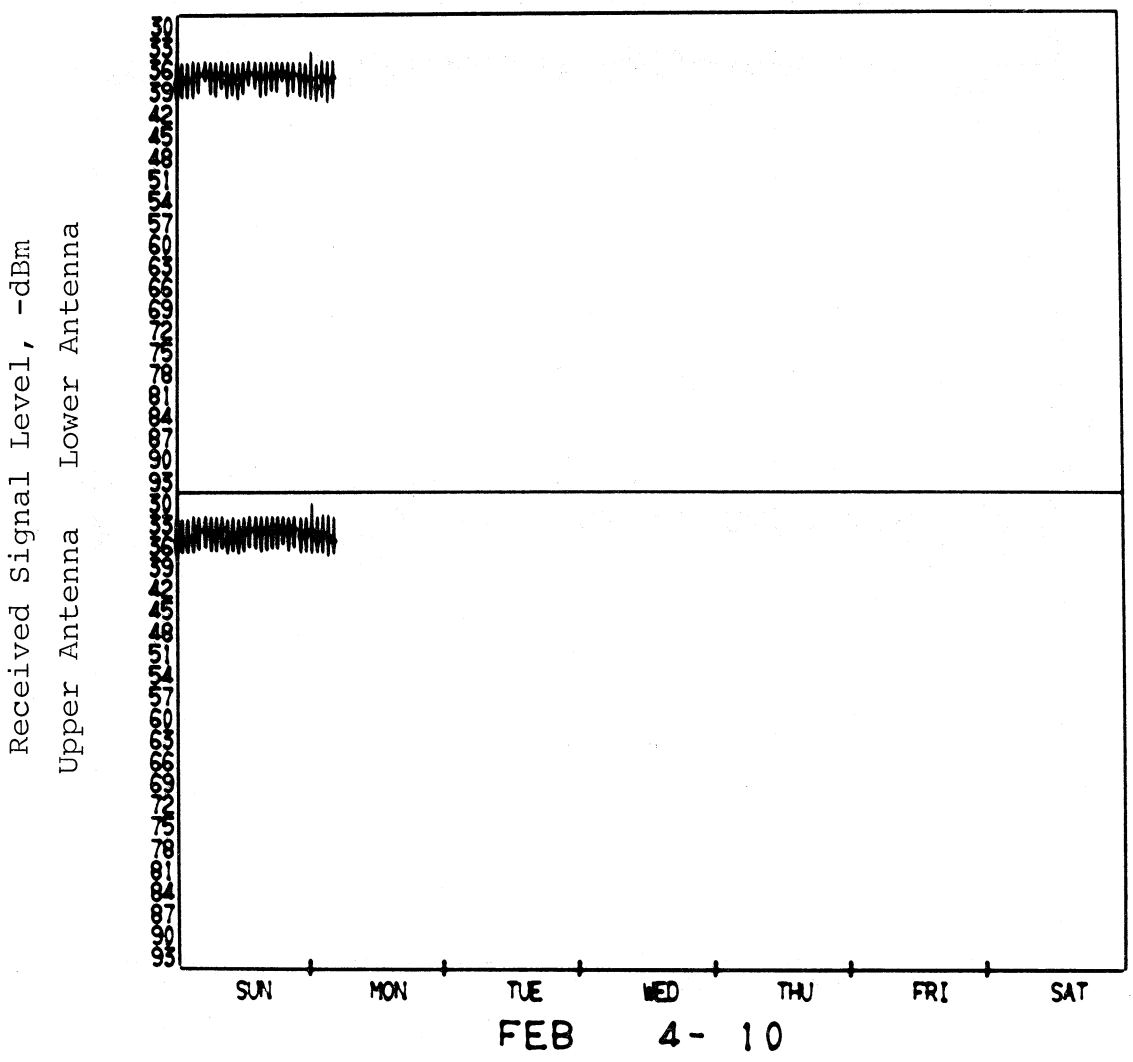

Figure A-43. Hourly histogram data, 1979.

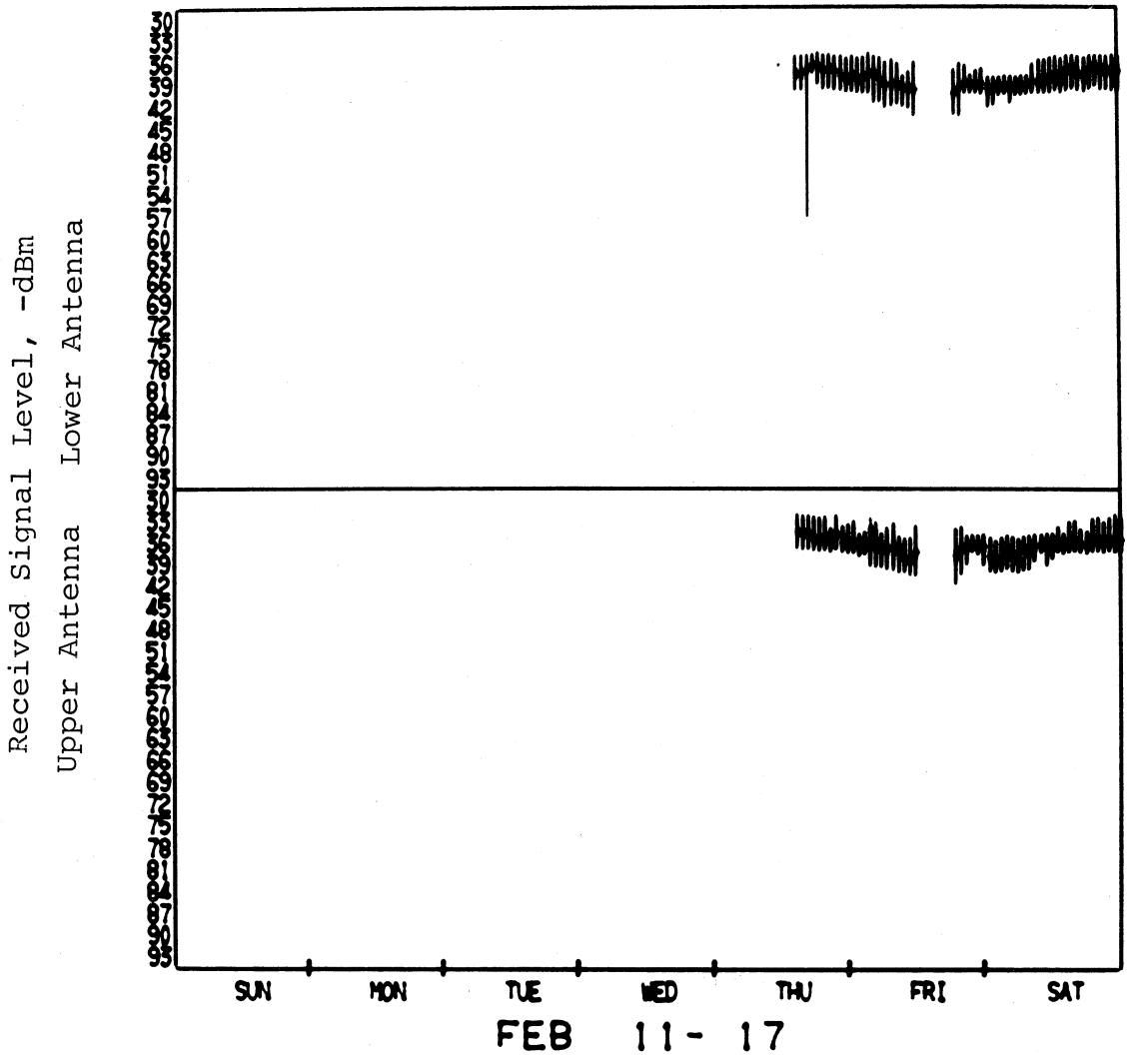

Figure A-44. Hourly histogram data, 1979.

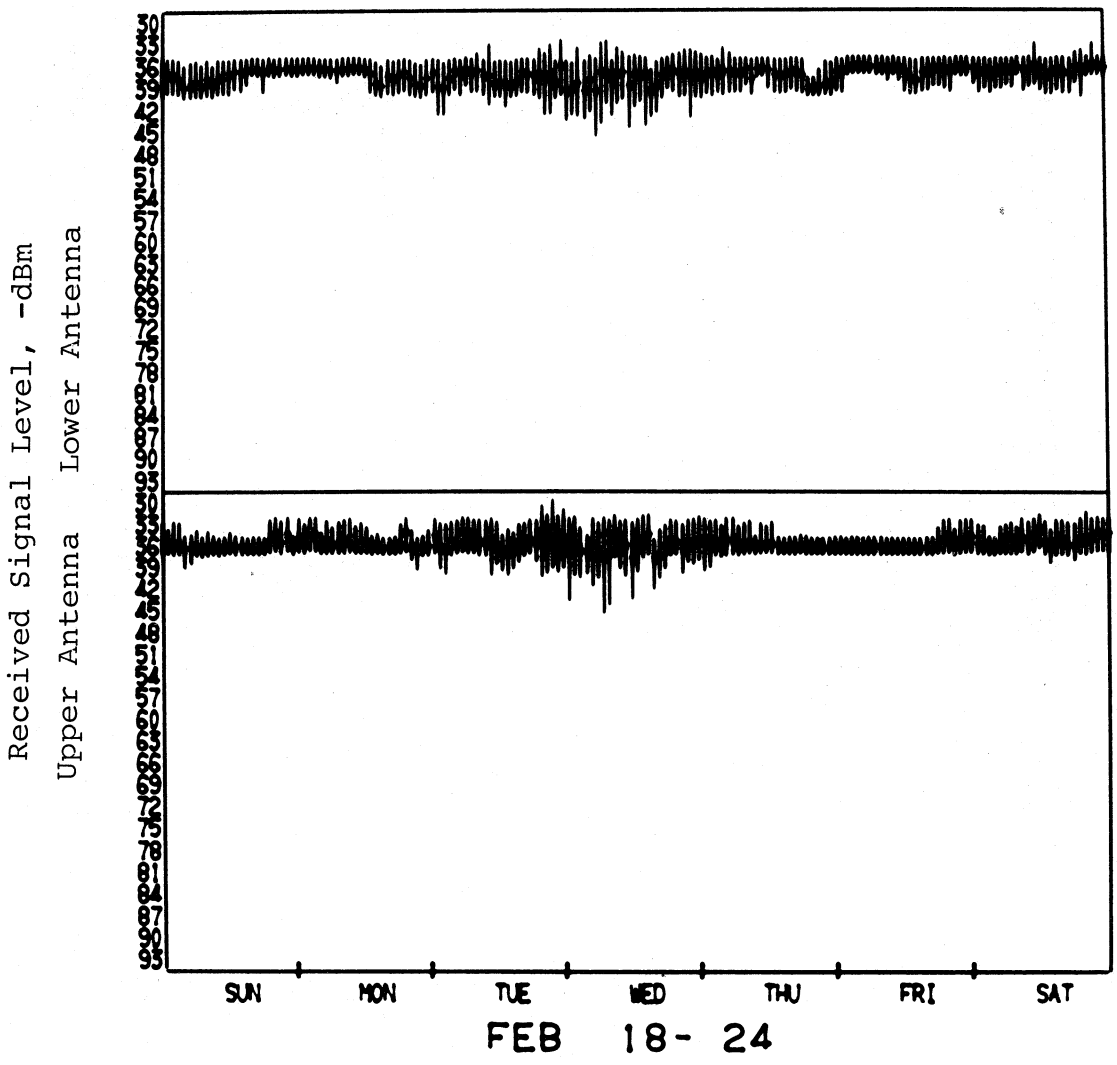

Figure A-45. Hourly histogram data, 1979.

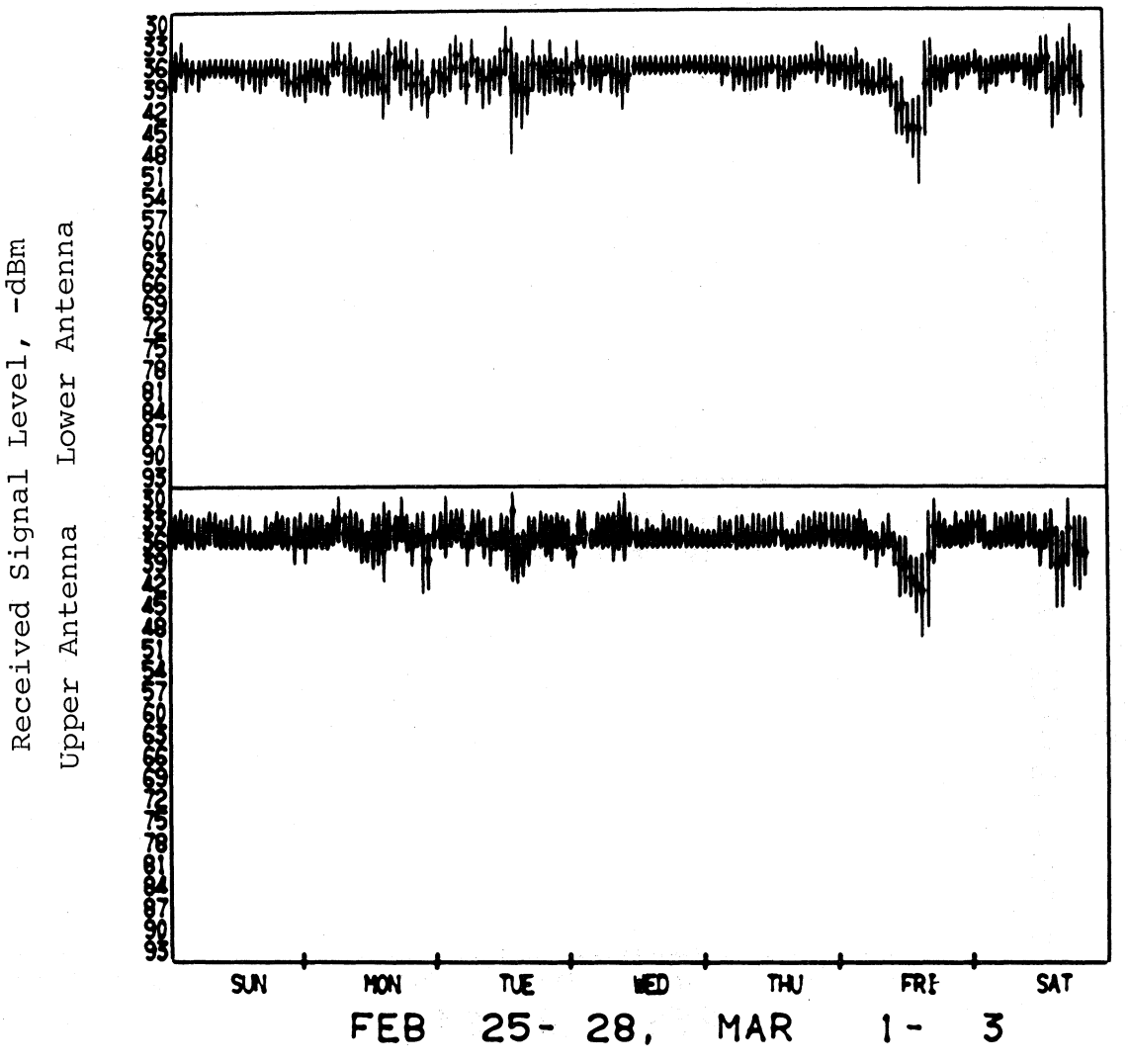

Figure A-46. Hourly histogram data, 1979.

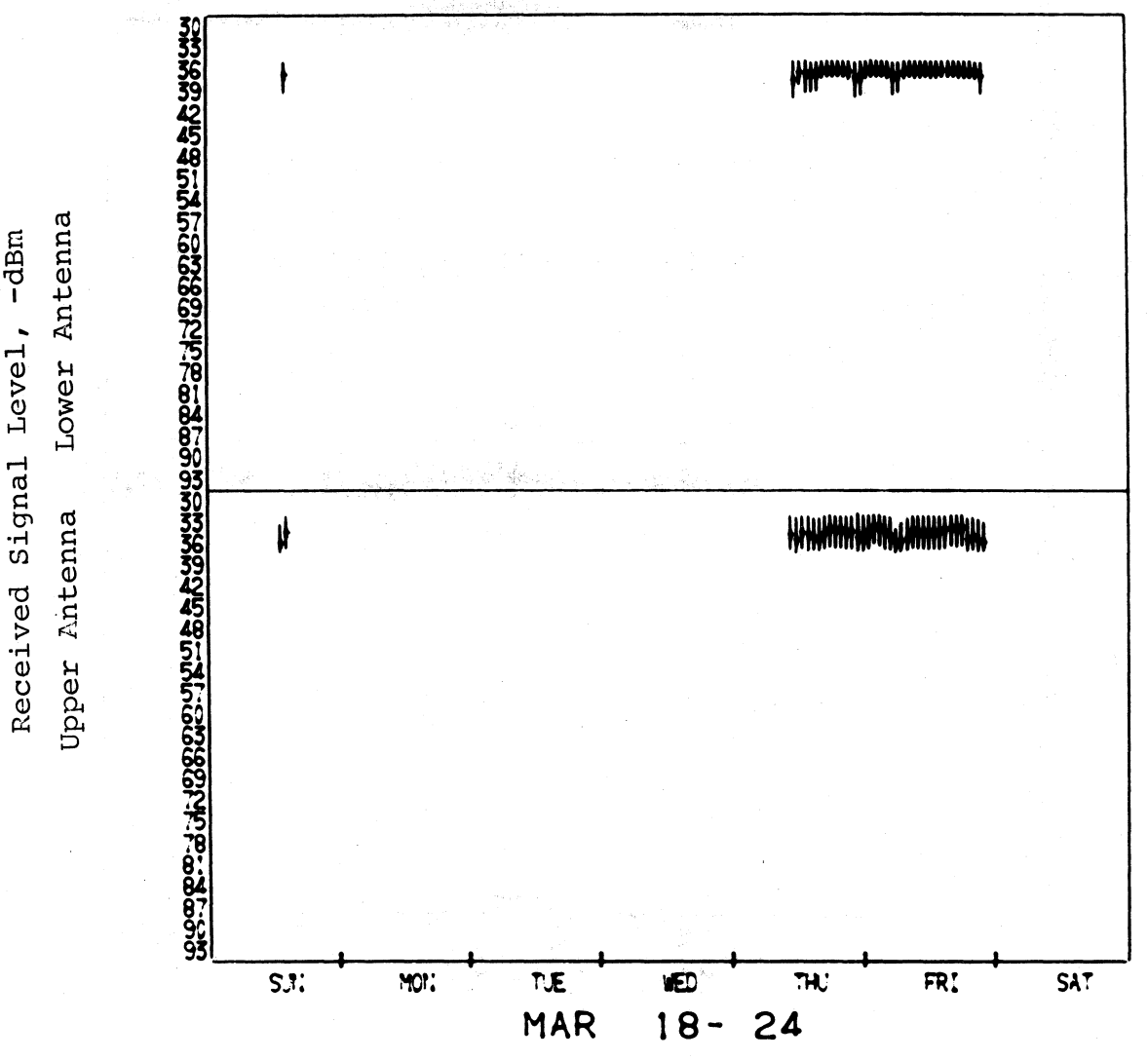

Figure A-47. Hourly histogram data, 1979.

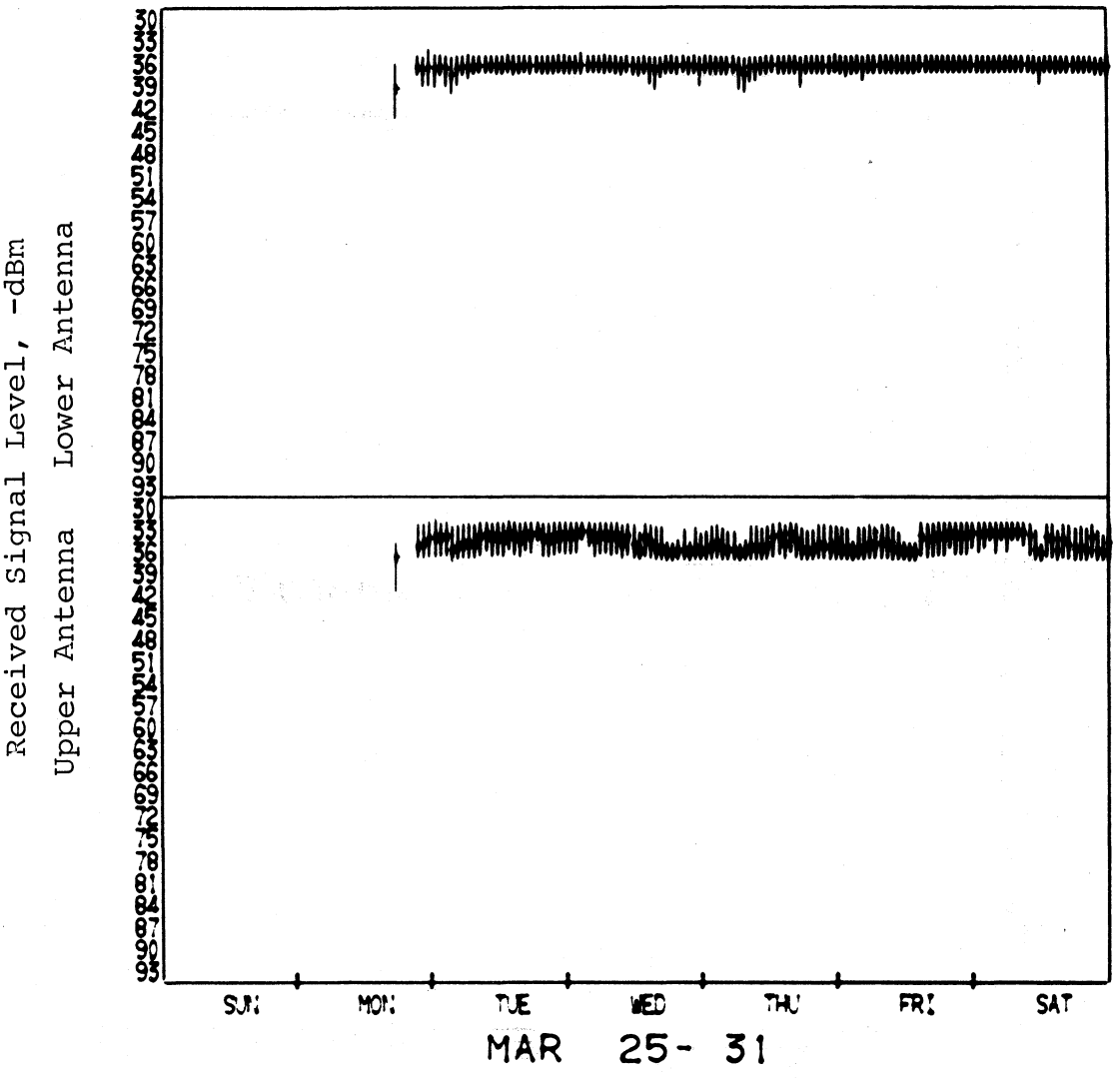

Figure A-48. Hourly histogram data, 1979.

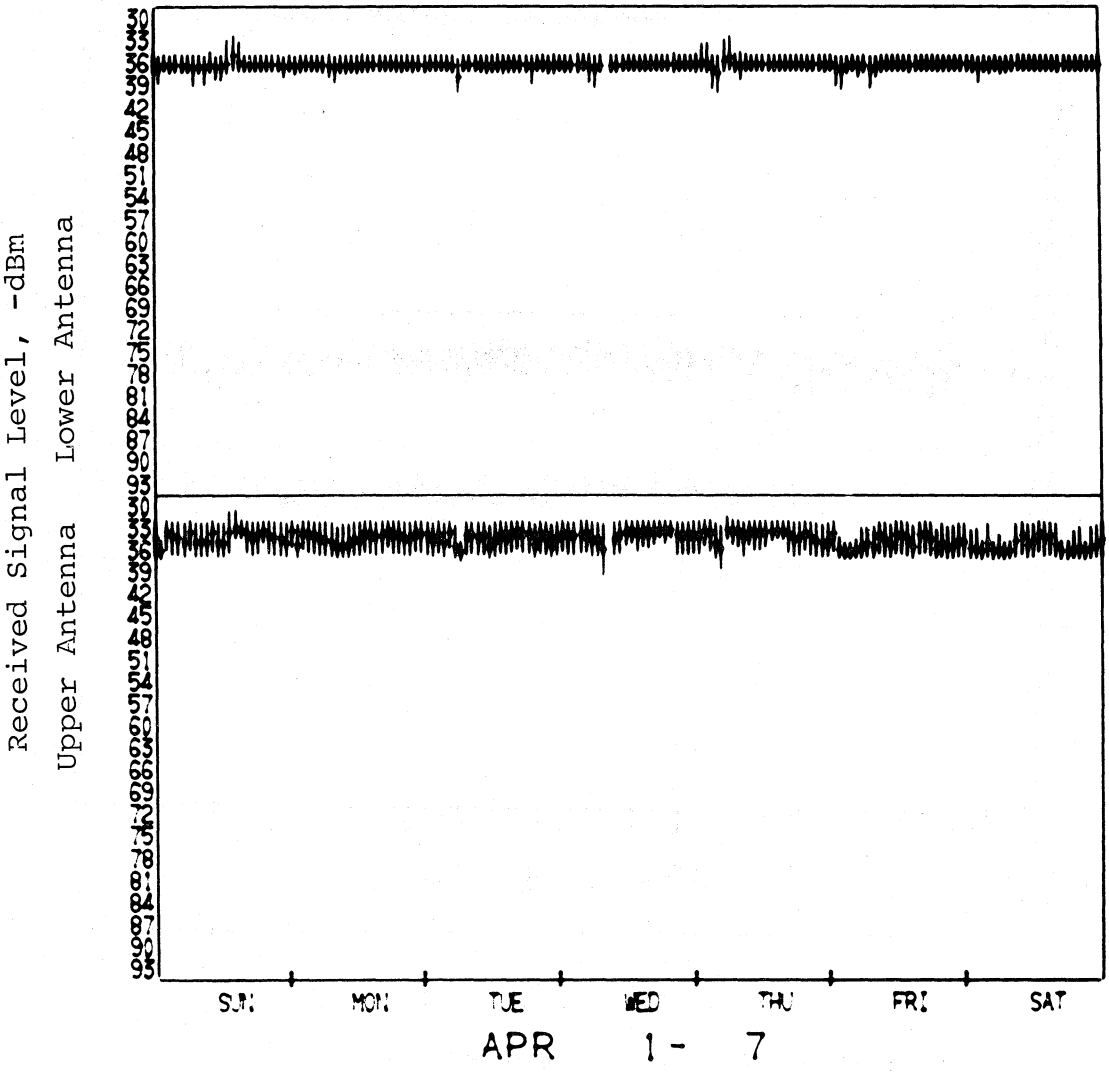

Figure A-49. Hourly histogram data, 1979.

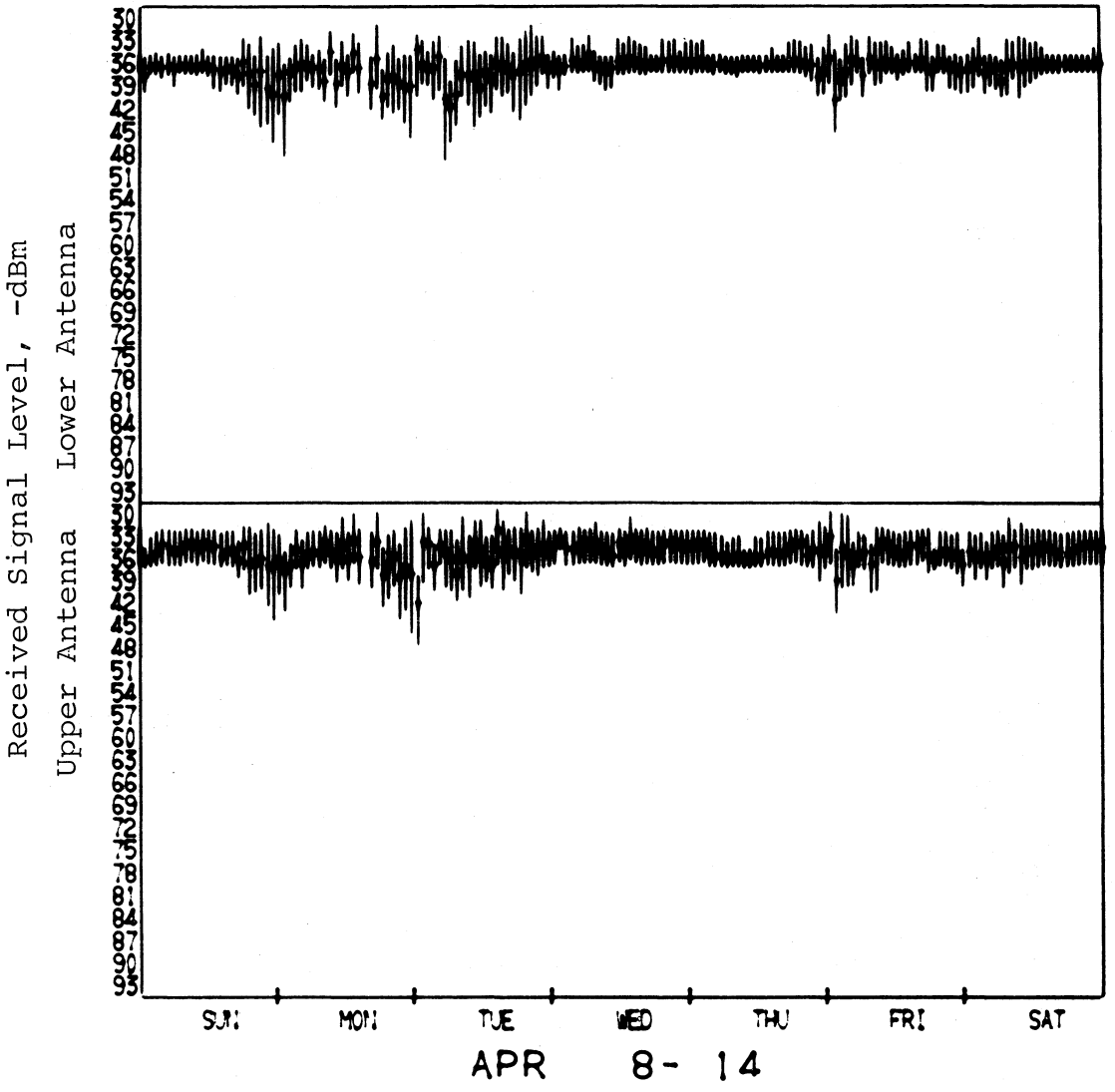

Figure A-50. Hourly histogram data, 1979.

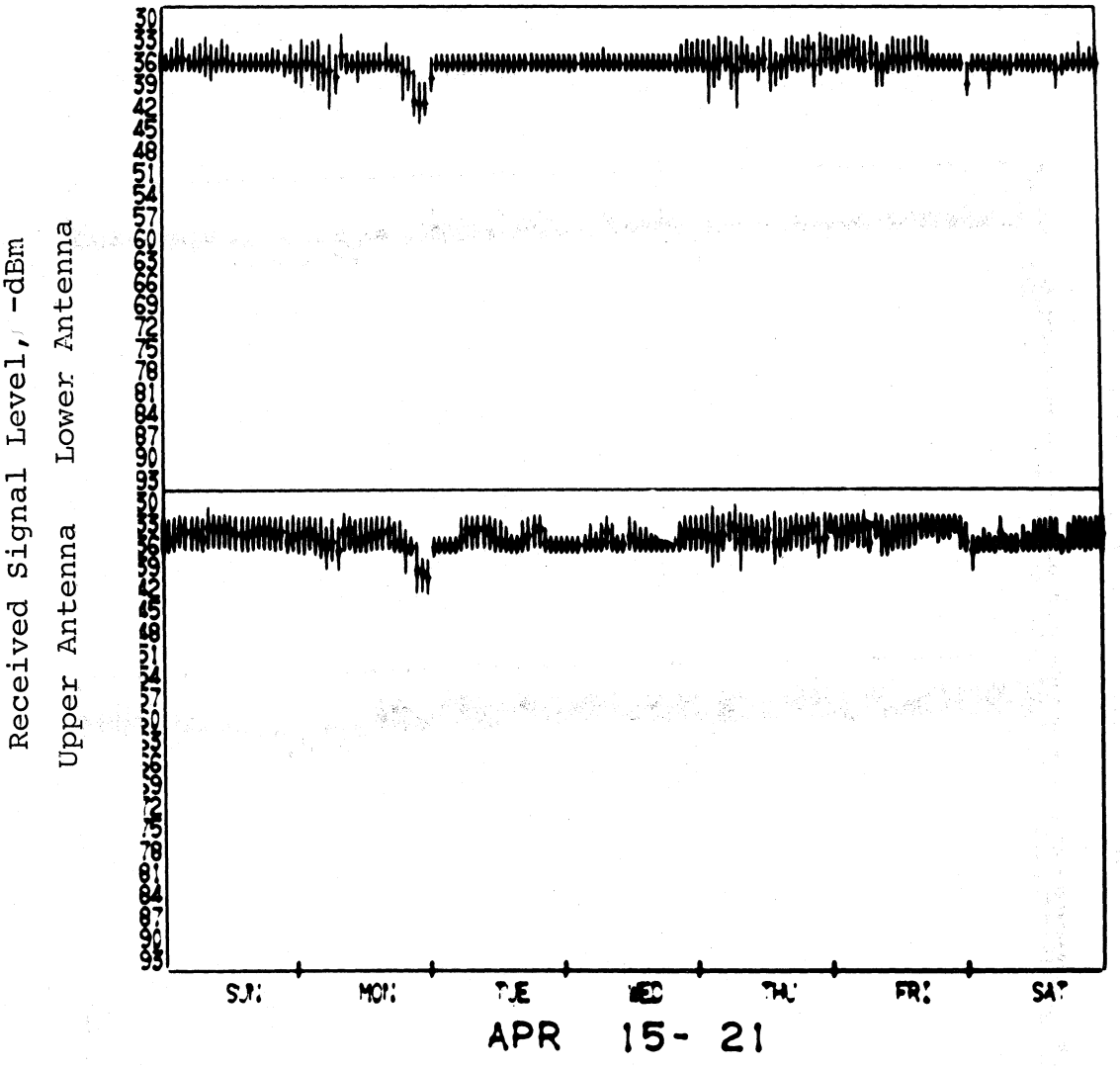

Figure A-51. Hourly histogram data, 1979.

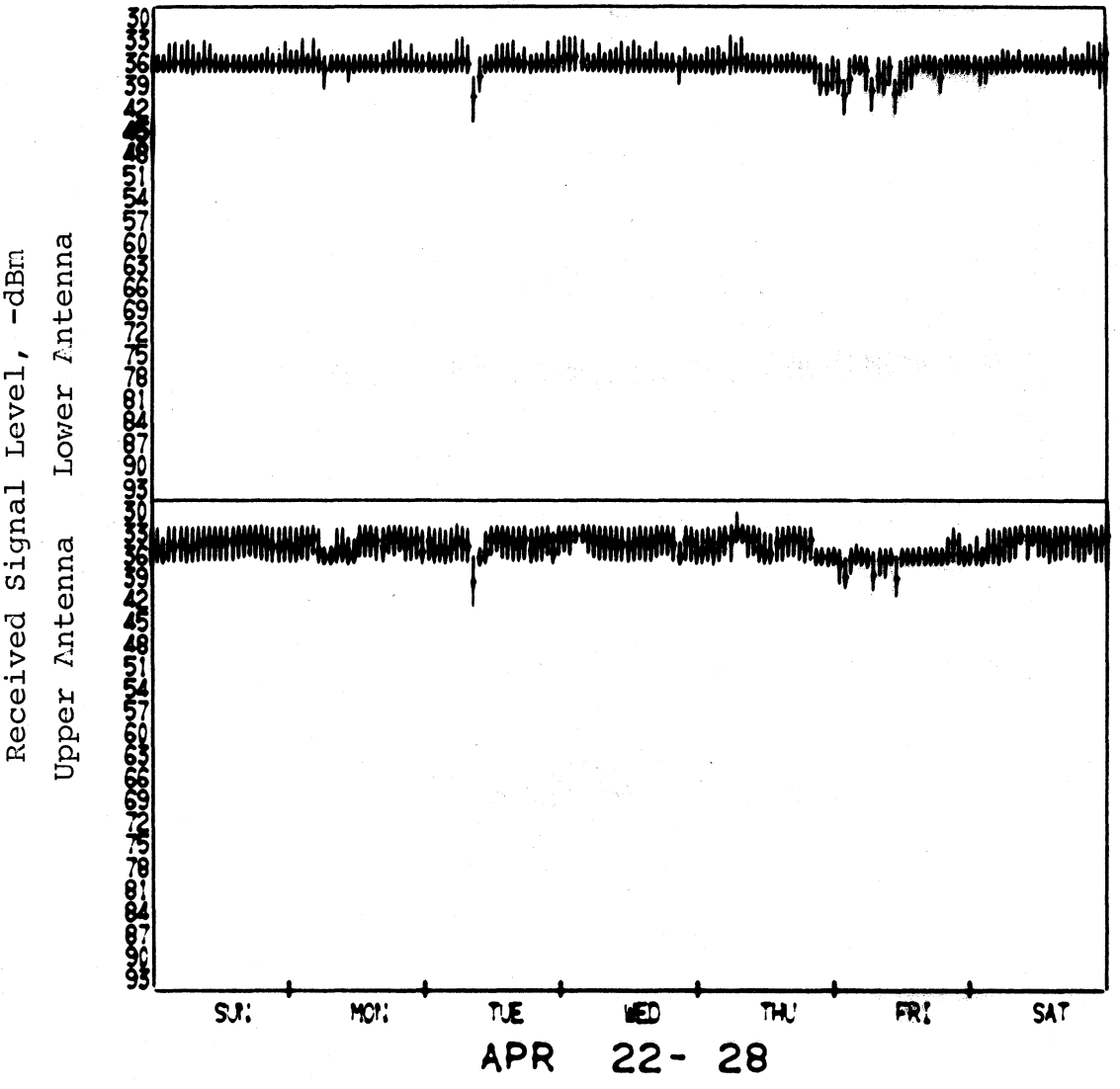

Figure A-52. Hourly histogram data, 1979.

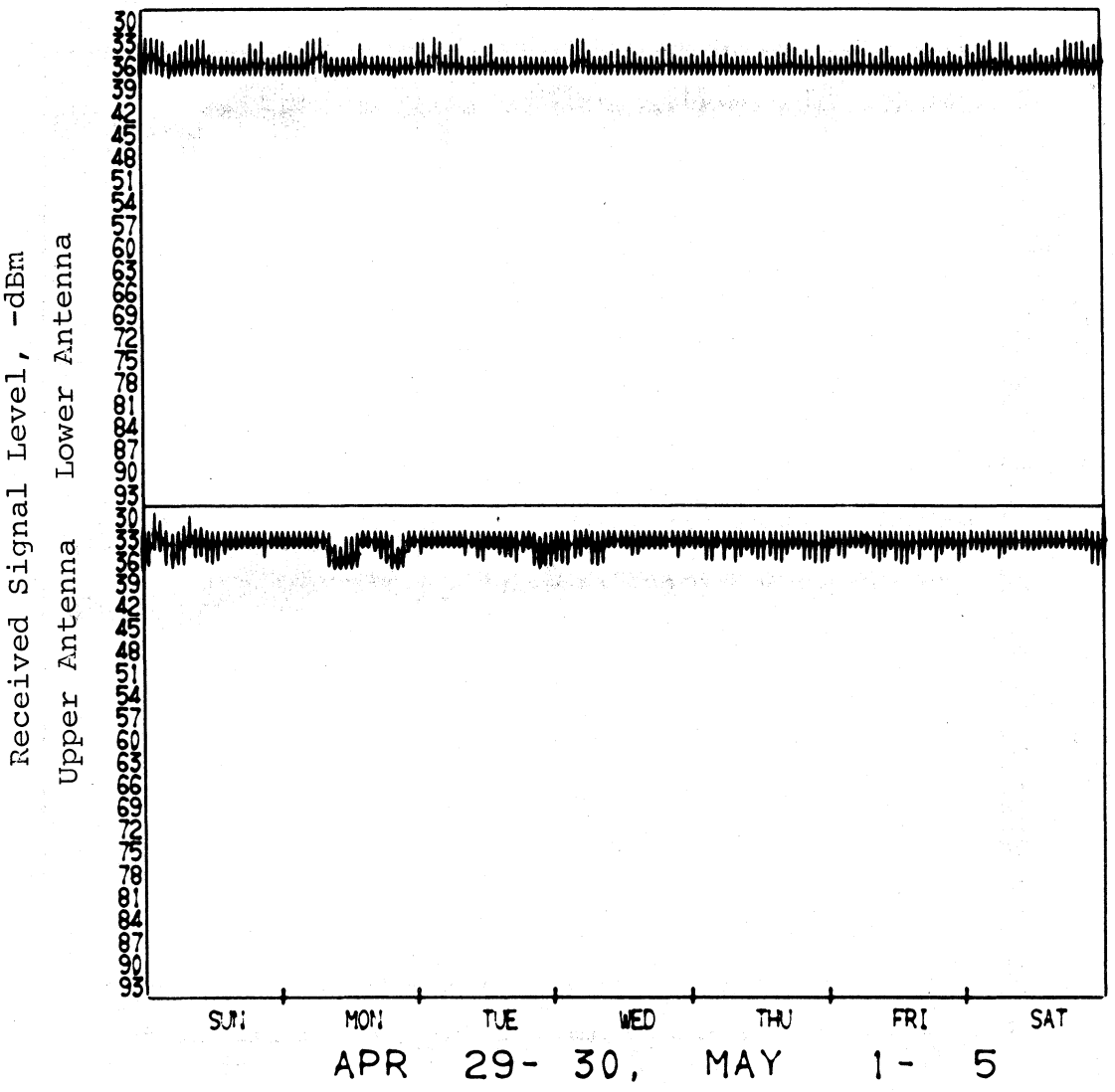

Figure A-53. Hourly histogram data, 1979.

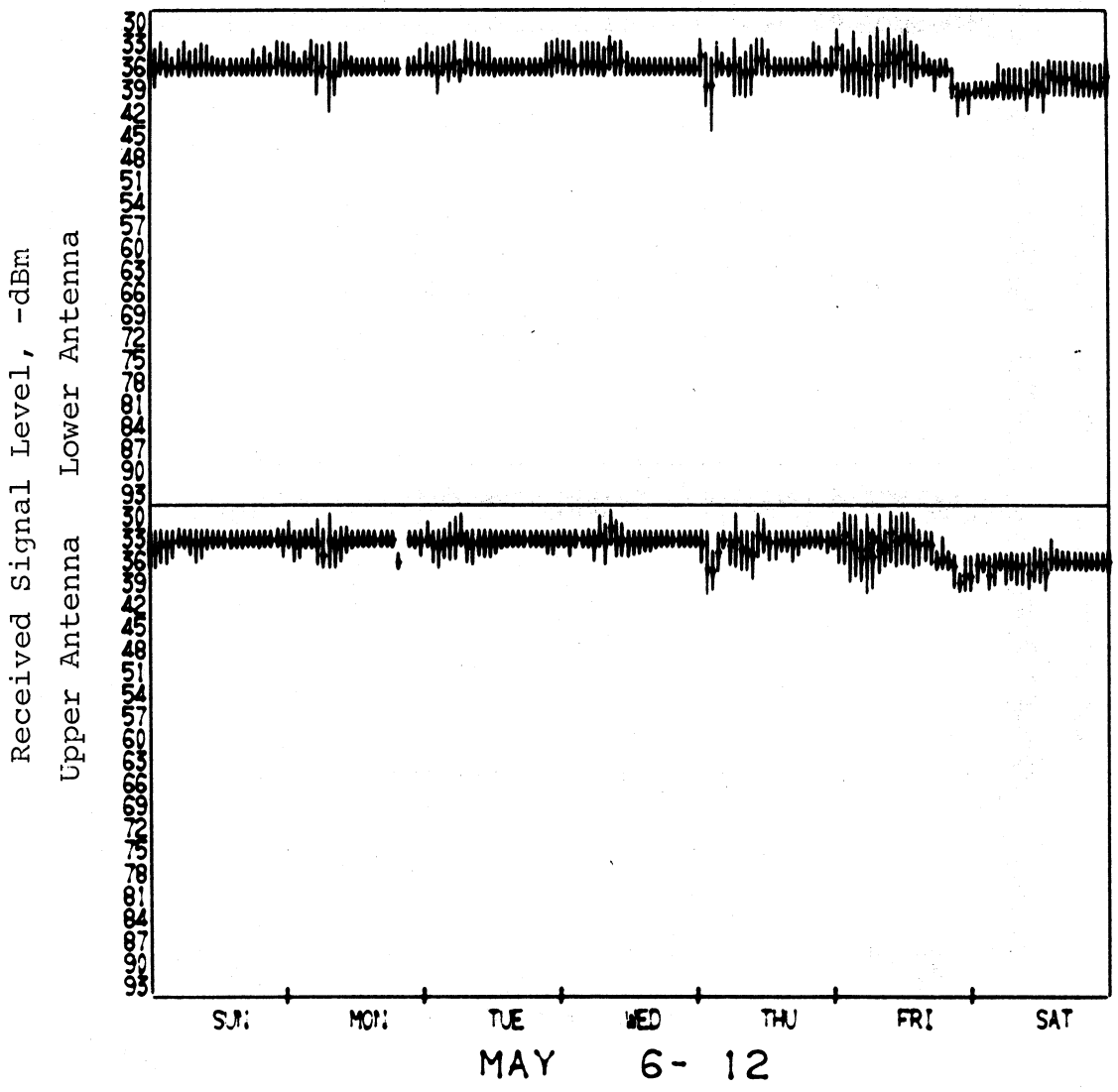

Figure A-54. Hourly histogram data, 1979.

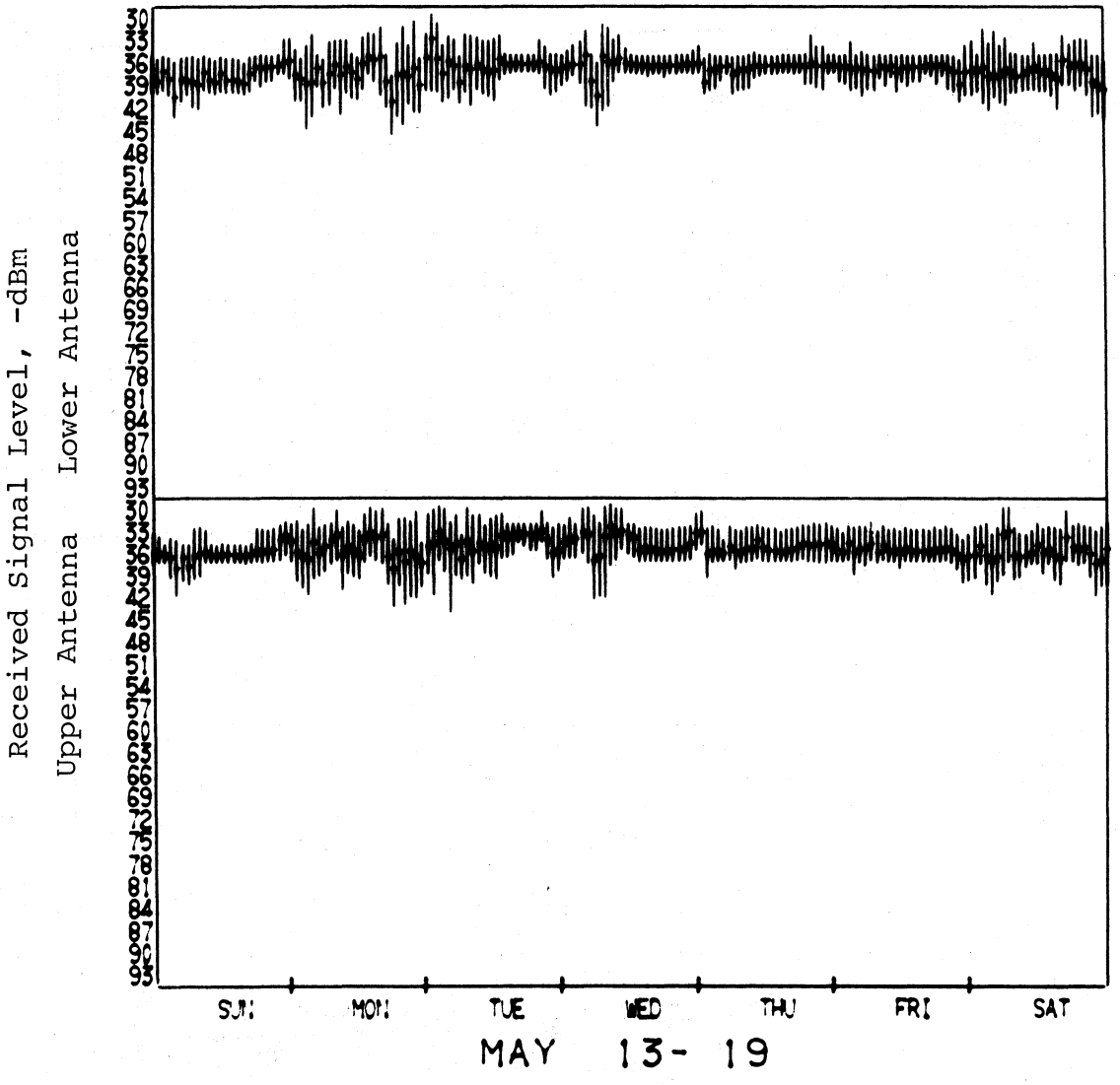

Figure A-55. Hourly histogram data, 1979.

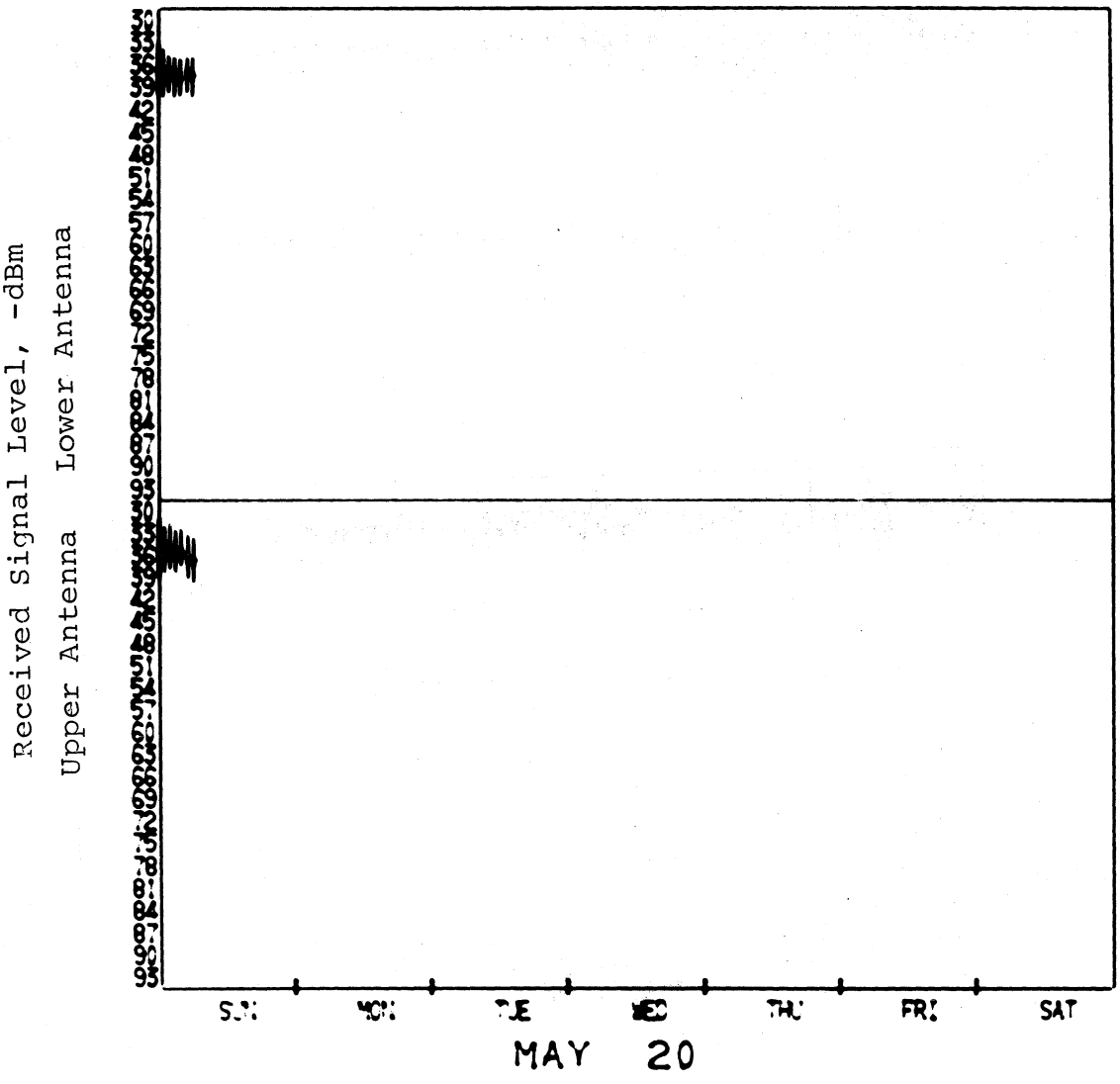

Figure A-56. Hourly histogram data, 1979.

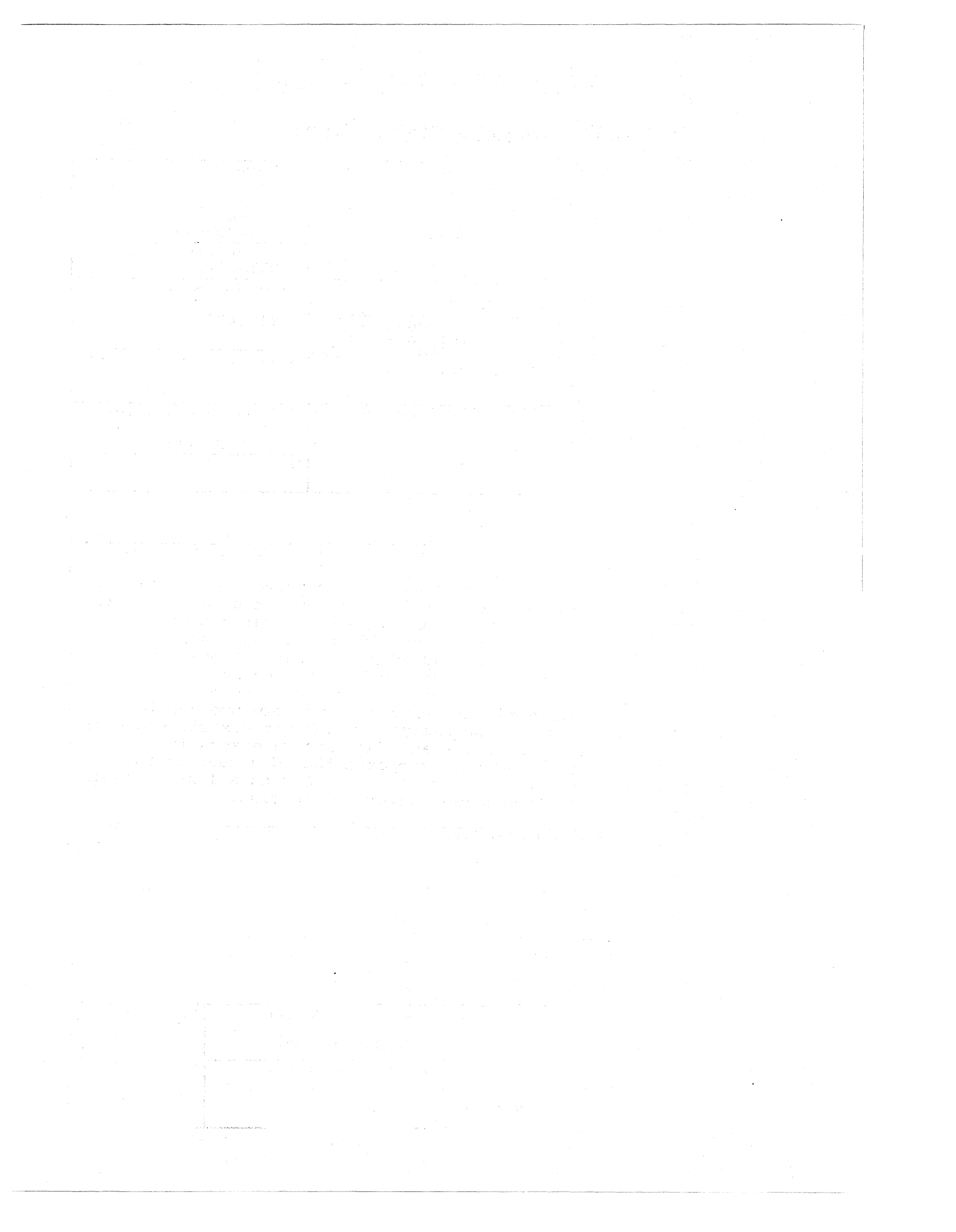

FORM OT-29
(3-73)

U.S. DEPARTMENT OF COMMERCE
OFFICE OF TELECOMMUNICATIONS

BIBLIOGRAPHIC DATA SHEET

	1. PUBLICATION OR REPORT NO. NTIA Report 79-31	2. Gov't Accession No.
		3. Recipient's Accession No.

4. TITLE AND SUBTITLE
PERFORMANCE OF A VERY LONG 8 GHz MICROWAVE LINK

5. Publication Date
November 1979

6. Performing Organization Code
NTIA/ITS

7. AUTHOR(S)
J.E. Farrow and R.E. Skerjanec

9. Project/Task/Work Unit No.
9103479

8. PERFORMING ORGANIZATION NAME AND ADDRESS U.S. Department of Commerce, National Telecommunications and Information Administration, Institute for Telecommunication Sciences, 325 Brdwy., Boulder, Colorado 80303

10. Contract/Grant No.

11. Sponsoring Organization Name and Address
Electronics System Division
Hanscom AFB

12. Type of Report and Period Covered
NTIA Report

13.

14. SUPPLEMENTARY NOTES

15. ABSTRACT *(A 200-word or less factual summary of most significant information. If document includes a significant bibliography or literature survey, mention it here.)*

This paper discusses measurement of signals received over a 160-km (100-mile) line-of-sight microwave radio link operating at 8.4 GHz. Signals were recorded at both ends of the path at various times over a period of about 18 months. The effects of macro-scale meteorological conditions are discussed particularly those which are peculiar to the central European location of the path. The data obtained from this measurement effort are presented both in terms of radio link availability and in terms of long-term propagation performance. The data were also analyzed to obtain distributions of fade duration for single receivers and for both receivers in a diversity configuration. The study supports the idea that it is possible to achieve reliable propagation at 8 GHz on a link as long as 160 km and with less than normal diversity spacing.

16. Key works *(Alphabetical order, separated by semicolons)*

17. AVAILABILITY STATEMENT [X] UNLIMITED. [ ] FOR OFFICIAL DISTRIBUTION.	18. Security Class *(This report)* Unclassified	20. Number of pages 106
	19. Security Class *(This page)* Unclassified	21. Price:

USCOMM-DC 29716-P73

☆ U. S. GOVERNMENT PRINTING OFFICE 1979 - 682-212/170 Reg. 8